THESIS ON NATURAL AND EXACT SCIENCES B193

Organocatalytic Asymmetric Addition to Unsaturated 1,4-Dicarbonyl Compounds

SERGEI ŽARI

TUT
PRESS

TALLINN UNIVERSITY OF TECHNOLOGY
Faculty of Science
Department of Chemistry

This dissertation was accepted for the defence of the degree of Doctor of Philosophy in Chemistry on August 24, 2015.

Supervisor: Prof. Tõnis Kanger, Department of Chemistry, Faculty of Science, Tallinn University of Technology, Estonia

Opponents: Ass. Prof. Jan H. van Maarseveen, University of Amsterdam, Van 't Hoff Institute For Molecular Sciences, The Netherlands

Ass. Prof. Uno Mäeorg, University of Tartu
Department of Chemistry, Estonia

Defence of the thesis: 16th of October 2015

Declaration:

Hereby I declare that this doctoral thesis, my original investigation and achievement, submitted for the doctoral degree at Tallinn University of Technology has not been submitted for any academic degree.

/Sergei Žari/

ISSN 1406-4723
ISBN 978-9949-23-840-8 (publication)
ISBN 978-9949-23-841-5 (PDF)

LOODUS- JA TÄPPISTEADUSED B193

Organokatalüütiline asümmeetriline liitumine küllastumata 1,4-dikarbonüülühenditele

SERGEI ŽARI

TTÜ
KIRJASTUS

Contents

List of Publications

I Žari, S.; Kailas, T.; Kudrjashova, M.; Öeren, M.; Järving, I.; Tamm, T.; Lopp, M.; Kanger, T. Organocatalytic Asymmetric Addition of Malonates to Unsaturated 1,4-Diketones. *Beilstein Journal of Organic Chemistry*, **2012**, *8*, 1452-1457.

II Žari, S.; Kudrjashova, M.; Pehk, T.; Lopp, M.; Kanger, T. Remote Activation of the Nucleophilicity of Isatin. *Organic Letters*, **2014**, *16*, 1740-1743.

III Žari, S.; Metsala, A.; Kudrjashova, M.; Kaabel, S.; Järving, I.; Kanger, T. Asymmetric Organocatalytic Aza-Michael Reactions of Isatin Derivatives. *Synthesis*, **2015**, *47*, 875-886.

Author's contribution

I-III. Planning and performing all the experiments, analysis of the obtained compounds, major role in the preparation of the manuscripts.

Used Abbreviations

1,2-DCE	1,2-dichloroethane
AcOH	acetic acid
aq	aqueous
Ar	aryl
BINOL	1,1'-Bi-2-naphthol
Bn	benzyl
Boc	*tert*-butyloxycarbonyl
cat.	catalyst
Cy	cyclohexyl
DCC	*N*,*N*′-dicyclohexylcarbodiimide
DCM	dichloromethane
DFT	density functional theory
DMSO	dimethyl sulfoxide
dr	diastereomeric ratio
ee	enantiomeric excess
EI	electron ionization
El	electrophile
ESI	electrospray ionization
equiv.	equivalent
Et	ethyl
EtOD	OH-deuterated ethanol
GS-MS	gas chromatography-mass spectrometry
h	hours
Hept	heptane
Hex	hexane
HPLC	high pressure liquid chromatography
HRMS	high resolution mass spectrometry
*i*Bu	isobutyl
*i*Pr	isopropyl
IR	infrared
LC-MS	liquid chromatography-mass spectrometry
Me	methyl
mp	melting point
NBO	natural bond orbital
*n*Bu	*n*-butyl
nd	not determined
NMR	nuclear magnetic resonance
Nu	nucleophile
Ph	phenyl
ppm	parts per million
Pr	propyl
*p*TsOH	*para*-toluenesulfonic acid

QTOF	quadrupole time of flight
rt	room temperature
S_N2	bimolecular nucleophilic substitution
*t*Bu	*tert*-butyl
THF	tetrahydrofuran
TLC	thin layer chromatography
Tol	tolyl
Ts	tosyl
VCD	vibrational circular dichroism

Introduction

In the case of chiral molecules, stereochemistry plays an important role in determining the bioactivity of compounds. Using racemic compounds as drugs often involves risks due to different activities of the enantiomers. The pharmacological effect of the "wrong" enantiomer depends on the particular compound and can vary from lower or no activity to nullifying the desired effect of the "right" enantiomer. In some cases, the "wrong" enantiomer can even have a harmful effect due to a better affinity towards some other receptor. This raises the need for efficient methods of accessing enantiomerically pure or at least highly enantioenriched molecules.

Several efficient strategies making it possible to achieve this goal have been developed, including starting from natural enantiopure chemical "building blocks", using chiral auxiliaries, resolving racemates and asymmetric catalysis. At first, stereoselective enzymatic transformations or organometallic (with chiral ligands) catalysis dominated this field of asymmetric catalysis. At the end of the 20^{th} century, organocatalysis using small natural enantiopure molecules became a new mainstream branch of this discipline. Organocatalysis can by divided in two main classes: covalent (the catalyst reversibly forms a reactive intermediate with the substrate) and H-bond-mediated catalysis (the catalyst coordinates and activates the substrates through H-bond interactions).

This thesis outlines the development of H-bond-mediated organocatalysis leading to highly potent bifunctional catalytic systems. The second main focal point was using unsaturated 1,4-dicarbonyl compounds as substrates for organocatalytic asymmetric reactions (mainly conjugated additions). In the course of the work, asymmetric desymmetrization of aromatic unsaturated 1,4-diketones using malonates and β-ketoesters was achieved (Publication **I**). Next, we studied the aza-Michael addition of isatin Schiff bases to different unsaturated 1,4-dicarbonyl compounds (Publications **II** and **III**). A lot of attention was focused on understanding the interactions between the catalysts and the substrates, as well as investigating the reaction mechanisms using different approaches.

1. Literature overview

1.1. H-bond-mediated asymmetric catalysis

Over the last two decades, activation via H-bonding has become one of the most important branches of asymmetric organocatalysis.[1] Hydrogen bonds can promote reactions both thermodynamically and kinetically. They provide thermodynamic assistance by stabilizing compounds or reactive intermediates, or kinetic assistance by activating the substrates that increase the reaction rate. In order to accelerate the reaction, the catalyst must interact with the activated complex in the transition state more strongly than with the starting materials, meaning that an H-bond donating catalyst is more effective if a partial or full negative charge is generated on the substrate during the reaction (for example, on a carbonyl oxygen during a 1,2- or 1,4-addition). In such a case, the H-donor will stabilize the intermediate or a transition state leading to it. The availability of various natural enantiopure small molecules, such as amino acids and alkaloids, possessing catalytic units in tandem with the possibility of combining them with H-bond-donating moieties, such as (thio)urea, squaramide and guanidine, resulted in the design of highly efficient multifunctional catalysts. The main success of this strategy comes from the catalyst's ability to simultaneously recognize, activate and coordinate the functional groups of nucleophiles and electrophiles participating in the reaction, while chiral elements of the catalysts create "chiral pockets", providing a high level of stereocontrol due to the assembly of a well-defined substrate A/substrate B/catalyst complex. There are a lot of enzymatic processes working on the same principle,[1a,2] and the H-bonding catalysts are often called small enzyme analogues or mimics. The milestones of the development of H-bond mediated asymmetric catalysis are presented in Figure 1. The ability of the diarylureas **1** to recognize and form co-crystals with different proton acceptors, such as cyclohexanone and THF, was first described by Etter in 1988,[3] and the possibility of using **2** as a catalyst for allylation[4] and Claisen rearrangement[5] was demonstrated some years later by Curran. However, the true potential of this moiety was revealed by Schreiner in 2002 by introducing the 3,5-bis(trifluoromethyl)phenyl fragment, making thiourea **3** a highly potent catalyst for Diels-Alder reactions.[6] One year later Takemoto designed the first chiral bifunctional thiourea catalyst **4** by replacing the 3,5-bis(trifluoromethyl)phenyl unit with a chiral tertiary amine serving as a base, and applying it for the addition of malonates to nitrostyrenes (yield up to 95%, *ee* up to 93%),[7] starting the new age of asymmetric H-bond-mediated organocatalysis. Recently, a significant number of bifunctional catalysts working through H-bond activation have been prepared and applied, while modern computational chemistry methods and analytical techniques make it possible to design the specific catalyst for a particular chemical transformation. On the practical level, this means moving from classic simple one-step aldol or Michael additions to multicomponent domino reactions, while the possibility of

immobilizing the catalysts creates an opportunity to use them in industry. Next, an overview of the types of catalysts working by H-bond formation is given.

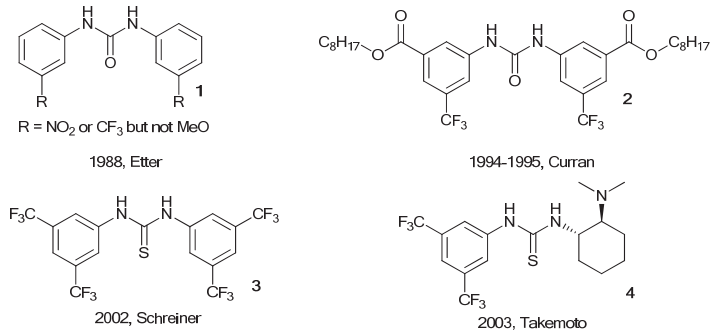

Figure 1. The development of bifunctional thiourea-mediated organocatalysis.

1.1.1. *Cinchona* alkaloid-based catalysts

The *Cinchona* alkaloids quinine **QN**, quinidine **QD**, cinchonine **CN** and cinchonidine **CD,** isolated from the roots of *Cinchona officinalis* in 1820,[8] form a well-known class of natural compounds, with quinine being most frequently mentioned (Figure 2). Apart from the use of quinine[9] as an effective antimalarial agent and food/beverage additive, these compounds have a long history of use in chemistry areas connected with chirality. Due to their possession of possible catalytic groups, together with stability, wide abundance and relatively low price, *Cinchona* alkaloids have become widely used as organocatalysts. As the compounds can simultaneously serve as H-bond donors via secondary alcohol and H-bond acceptors via the tertiary amine of the quinuclidine unit, *Cinchona* alkaloids can be considered bifunctional catalysts. Over the years there have been a large number of examples concerning asymmetric reactions promoted by *Cinchona* alkaloids or their derivatives,[10] with the first one dating back to 1912[11], decades before asymmetric organocatalysis became a topic of interest. Apart from asymmetric catalysis, they are used for the resolution of racemates (mainly acids due to their basic nature)[12], the preparation of chiral ligands[13], as chromatographic selectors[14] and NMR-discriminating agents.[15] When discussing *Cinchona* alkaloids, it is worth mentioning such 10,11-dihydro analogues as dihydroquinine **DQN,** a natural minor component of the *Cinchona* tree bark extract having a reduced vinyl group, unnatural 9-epi alkaloids (e.g. epiquinine ***epi*-QN**), with a reversed absolute configuration of the secondary alcohol, as well as cupreine **CPN** and cupreidine **CPD**: demethylated analogues of **QN** and **QD** (minor components of the natural extract), having phenolic OH, which is important as a strong H-bond donor, as well as a modification site (Figure 2). All of these modifications effect catalytic activity. The compounds have 5

stereogenic centers: N1, C3, C4, C8 and C9 (Figure 3), although three of them (N1, C3 and C4) are identical in all cases. As C8 and C9 are considered to play a major role in asymmetric induction, the pairs **QN**/**QD** and **CN**/**CD** are often called pseudoenantiomers when stereochemical issues are discussed. For example, if a reaction catalyzed by **QN** or its derivative yields an *R* product, switching to **QD** will most likely result in an *S* product with a close *ee* value, although this rule is not absolute. The difference in stereocontrol will be discussed later and there are reported examples where immobilized pairs of pseudoenantiomers yielded the same enantiomer in excess when used as catalysts.[16]

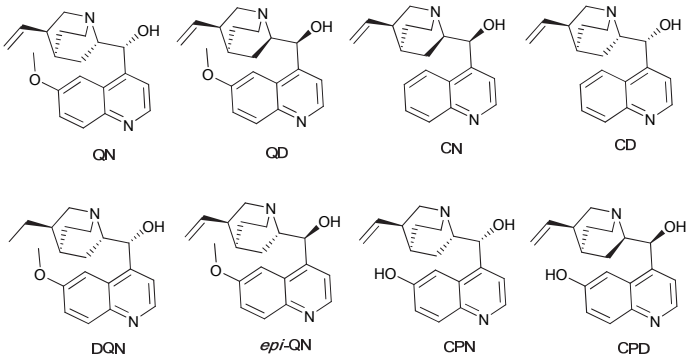

Figure 2. Natural *Cinchona* alkaloids and their closely related analogues.

Cinchona alkaloids are small yet complex molecules consisting of a quinuclidine fragment (a tertiary amine), a flat bulky quinolone unit (with a methoxy substituent in the case of **QN** and **QD**), secondary alcohol and a terminal olefin. This structural diversity has been successfully exploited in order to obtain a large number of derivatives, which in turn has resulted in a significant broadening of their application as catalysts. Figure 3 gives a short overview of the role of the fragments and the possibilities of the modification of *Cinchona* alkaloids.

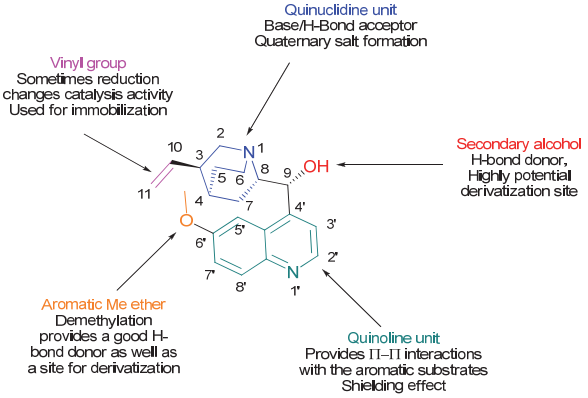

Figure 3. Numbering and catalytic units of *Cinchona* alkaloids.

All of the fragments play an important role in making the *Cinchona* alkaloids effective catalysts, while chemical reactivity allows for their derivatization, further increasing the catalytic properties, as well as tuning the catalysts for specific needs. The tertiary amine of the quinuclidine fragment serves as a base, playing an important role in the activation of the nucleophilic substrates. *Cinchona* alkaloids can be easily converted to quaternary salts, yielding the efficient phase-transfer catalysts used in many reactions.[17] All *Cinchona* alkaloids possess a vinyl group that is a convenient site for immobilization, making the catalysts reusable, while retaining their catalytic properties.[16,18] In some cases, the reduction of the double bond changes the catalytic activity of the discussed compounds. The demethylation of **QN** and **QD,** leading to additional reactive functionality, has not received much attention in the early studies of asymmetric catalysis promoted by *Cinchona* alkaloids. The main advantage of this modification is the newly created possibility for the functionalization of the secondary alcohol (C9 OH), thus tuning the catalytic properties, while phenolic OH serves as a H-bond donor.[19] The newly obtained phenolic OH is also used for further derivatization. The two main roles of the flat aromatic quinoline unit are to provide additional Π-Π interactions with aromatic substrates and to contribute to the stereoselectivity of the reaction by shielding. Moreover, sometimes an additional derivatization on this fragment results in higher efficiency in the catalyst. The 9-hydroxy group serves as an H-bond donor in the case of unmodified alkaloids. Its main importance is the possibility of giving a large number of derivatives varying from simple ether formation, resulting in conformational changes in the molecule to combining the alkaloids **5** with the H-bond-donating moieties, yielding highly potent bifunctional catalytic systems. The important step for this development is the S_N2 replacement of OH- with an NH_2-group. The obtained primary amine is both an efficient aminocatalyst and a precursor to bifunctional catalysts working through H-bond activation.

1.1.2. Thiourea, squaramide and other catalysts

Over the years several 9-NH_2 modified catalysts have been introduced (Figure 4): (thio)urea **6**, **7**[20], squaramide **8**[21], guanidine **9**[22], amide **10**[23], and sulfonamide **11**[24]. As the current work deals with thiourea- and squaramide-derived catalysts, they will be briefly discussed.

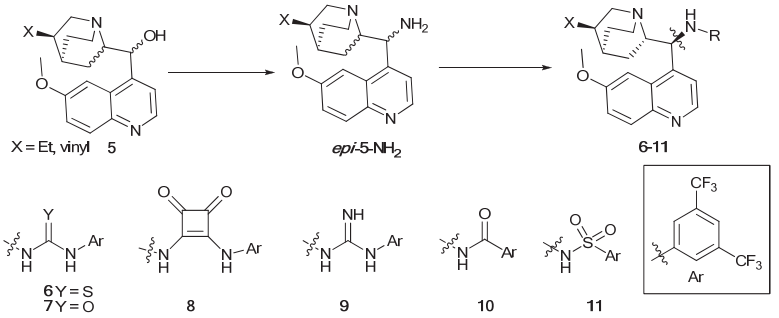

Figure 4. *Cinchona*-derived bifunctional catalysts.

The simplicity of the construction of both thiourea and squaramide scaffolds (Scheme 1) yields a large number of specific catalysts. The commercial availability of many isothiocyanates **12** (as well as many methods for their preparation) or dimethyl squarate **13** and primary amines (and their precursors) possessing the needed properties (for example, chiral, bulky, acidic and basic), explains the great structural diversity of these catalysts, which has now been demonstrated.

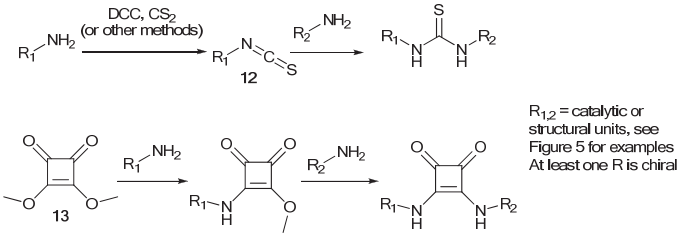

Scheme 1. General approach for the synthesis of chiral thioureas and squaramides.

Since the pioneering work of Takemoto (**4** and analogues)[25], a large number of chiral bifunctional (thio)urea/chiral tertiary amine catalysts (**4**, **6**, **14**-**17**) have been developed (Figure 5, **A**). Over the years, Jacobsen's group has prepared a number of chiral thioureas containing amino acid amide and chiral 1,2-diamine fragments[26] (the first example was a Schiff base containing catalyst **26**, used for a Strecker reaction in 1998).[27] Jacobsen's thiourea **14** containing Takemoto's tertiary amine fragment was first used for asymmetric cyanosilylation in 2005.[28] In the same year Soos, Dixon and Connon demonstrated that thiourea catalysts **6** derived from *Cinchona* alkaloids promote conjugate addition reactions in a highly asymmetric manner,[20a,29] and Wang applied a BINOL-derived diamine containing thiourea **15** for a Baylis-Hillman reaction.[30] Hiemstra et al. prepared and used another *Cinchona* thiourea **16** connected through the 6′ quinoline position for an effective asymmetric Henry reaction one year later.[31] A thiourea-mediated H-bond catalysis has been successfully combined with imine/enamine activation by preparation of a primary or secondary amine containing thioureas (**18**-**22**). Many of these catalysts are actually the analogues of the first examples

of tertiary amine-containing catalysts, but having unsubstituted amino groups (Figure 5, **B**).[32] The first example was demonstrated by Tsogoeva in 2006 (**18**, Michael addition to nitroolefins),[33] the same year Tang published the chiral secondary amine containing a thiourea **22-**mediated analogous reaction.[34] The availability of the building blocks and the simplicity of the preparation resulted in a great number of structurally diverse thioureas (Figure 5, **C, 23**-**28**). There have been plenty of examples of effective chiral thiourea catalysts bearing multiple hydrogen donors (**23**)[35], including bis-thioureas connected by chiral diamine linkers (**24**).[36] Recently, a review of terpene-derived thiourea catalysts (**25**) was published. These bulky chiral moieties have a strong rigidifying effect on the electrophilic activation profile of the catalysts.[37] In 2012 Pihko et al. designed new dual-activated catalysts containing two (thio)urea moieties (**27**).[38,39] The careful structure design resulted in one (thio)urea strengthening the H-donor properties of the other one, while allowing both substrates to enter the active site. The structure of thioureas allows for the combining of a chiral base (tertiary amine), H-bond donor activation (thiourea unit) and imine/enamine activation in one catalyst (**28**).[40]

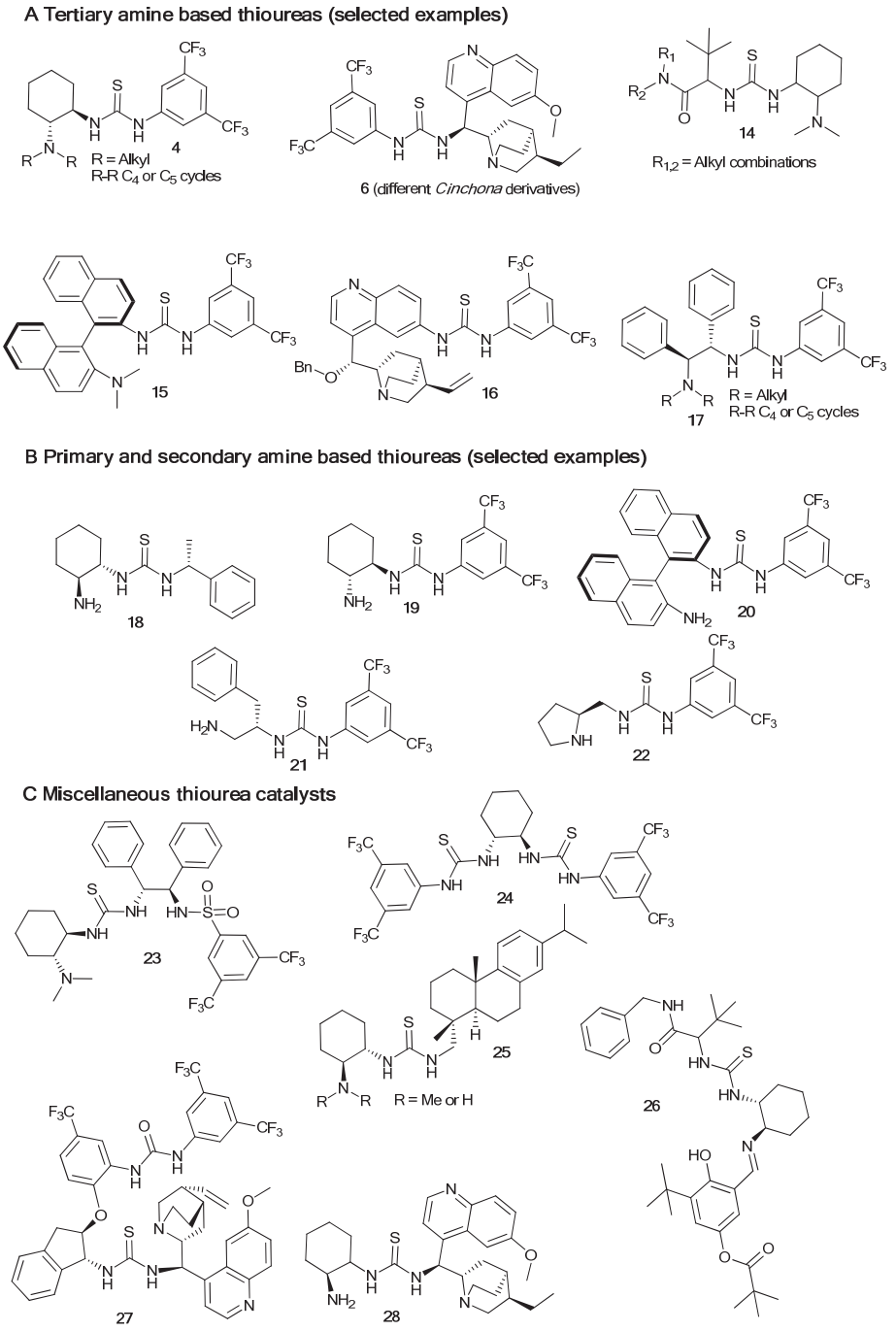

Figure 5. Representative examples of thiourea-based chiral bifunctional catalysts.

In 2008, Rawal et al. introduced bis-amides of squaric acid or squaramides as an alternative to a thiourea moiety.[21] As most of the squaramide catalysts resemble the thioureas presented in Figure 5, the structures of the analogues are not presented here. Instead, important new structural features are demonstrated in Figure 6. Rawal changed the aromatic 3,5-$(CF_3)_2$Ph unit with its methylene bridged analogue in his first chiral squaramide catalyst (Figure 6, **A**). Later, both units were successfully used in squaramide catalysts and, in many cases the catalysts differing only by this moiety showed different results in both reactivity and stereocontrol. This difference has not been discussed in review articles on squaramide-mediated catalysis or the importance of the 3,5-$(CF_3)_2$Ph moiety[41], but might be connected with sterical issues (the benzyl derivative is optimal). On the other hand, the 3,5-$(CF_3)_2$Ph moiety makes the squaramide NH protons more acidic, providing better activation. Moreover, NMR studies suggest that the *ortho* protons of this moiety are acidic enough to participate in activation.[42] The bifunctionality of thioureas and squaramides has an important negative feature connected with self-aggregation. The resulting dimers (and possible higher aggregates) act as distinct catalysts and influence the stereoselectivity of the reaction. As a result, higher catalyst loading, concentration or lower temperature, as well as using substrates that do not strongly bind to the catalysts, may result in a decrease in stereoselectivity. The self-aggregation phenomenon has been experimentally and analytically studied, proving its effect on stereoselectivity.[43] Song *et al.* have designed C2 symmetric squaramide catalysts **29** derived from *Cinchona* alkaloids (Figure 6, **B**). Due to the bulkiness of the alkaloidal units, self-association is not possible (and was not experimentally observed).[44]

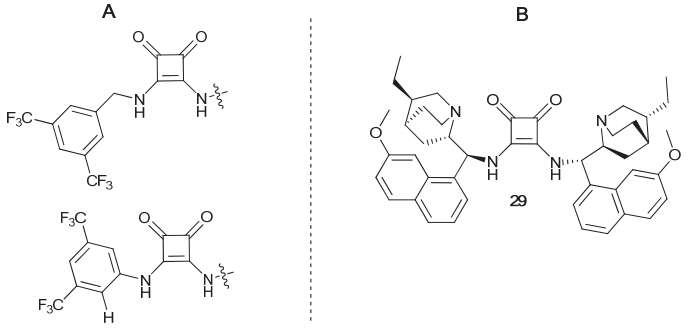

Figure 6. New features of the squaramide catalysts.

While working by the same principle, squaramide and thiourea scaffolds have important structural and electronic differences that affect the H-bond formation and activation of the substrates (Scheme 2).[45]

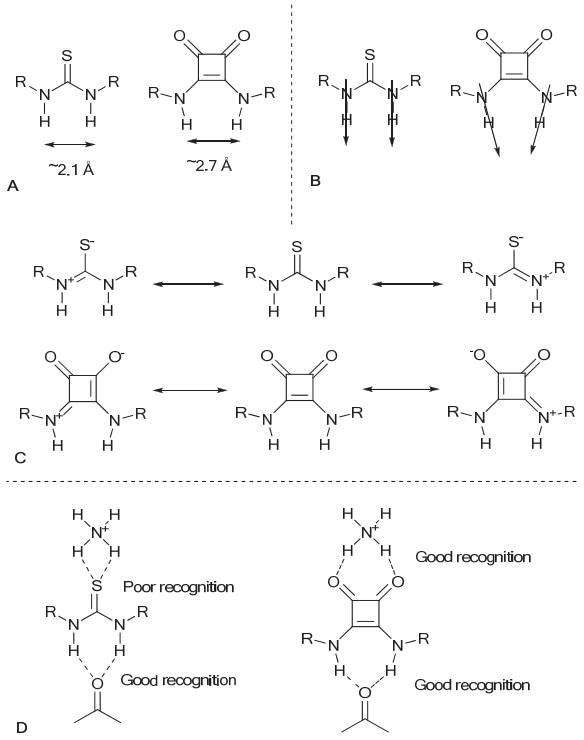

Scheme 2. The differences between thiourea and squaramide scaffolds.

First of all, calculations showed a significant difference in the relative distance and spacing between the NH groups of the moieties (Scheme 2, **A**). In addition, the structure of the cyclobutenedione ring induces a convergent orientation of the NH groups, canting both by ~6° (Scheme 2, **B**). While in both cases the electron pair from the nitrogen can be delocalized (Scheme 2, **C**), contributing to the rigidity of both scaffolds, the squaramide moiety provides further delocalization because of the partially aromatic cyclobutenedione system. This, in turn, results in squaramides being more acidic compared to their thiourea analogues, which has also been experimentally proved (Figure 7).[46] While lower pK_a values generally make squaramides better H-bond donors and more active catalysts, this does not mean that replacing a thiourea catalyst with its squaramide analogue will result in a higher reaction rate, yield and stereoselectivity in every case. Finally, squaramide carbonyl groups make the moiety dual in terms of ion recognition and H-bonding (Scheme 2, **D**): while both squaramides and thioureas are known for high affinity towards anions, the ability of thiourea to bind cations through a sulfur atom is quite limited. To sum up, the differences between the two classes result in a dissimilarity between the transition states for the same reaction, leading to the continuous development of both classes of catalysts.

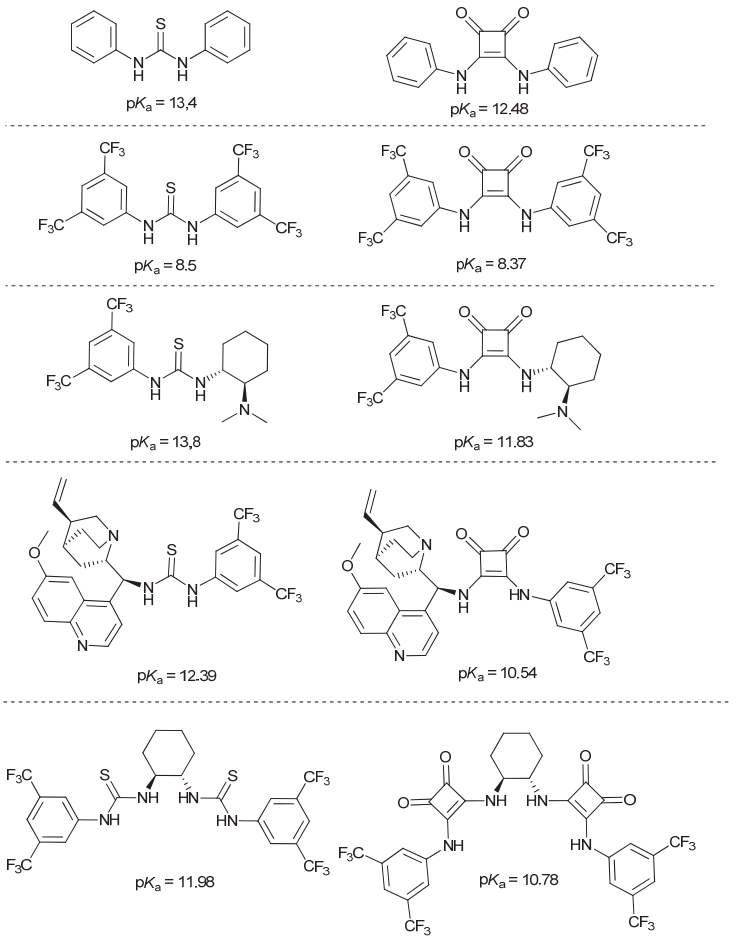

Figure 7. pK_a values of some thioureas and squaramides (in DMSO).

There are also differences in physical properties: squaramides have significantly lower solubilities compared to thioureas. Sometimes the catalysts even precipitate during their preparation, making purification easier, although this makes their use as catalysts more complicated.

Despite previously proposed transition states leading to products with experimentally observed stereochemistry, a full understanding of the activation mechanisms is still lacking. Recently, Soós et al. made a summary of previously reported activation mechanisms of bifunctional thioureas (Figure 8) and studied the activation mechanism of squaramide catalysts.[47] Takemoto postulated that an electrophile can be activated by hydrogen bonding from a thiourea moiety, while a tertiary amine activates the nucleophile (Figure 8, **A**).[48] Both experimental and computational studies confirm that a reaction can proceed through this transition state.[49] Soós's group proposed an alternative activation model with a thiourea unit binding the deprotonated nucleophile while the protonated amine activates

and coordinates the electrophile (Figure 8, **B**).[50] This possibility was also supported by experimental and computational studies.[49] The most recent transition state studies were carried out by Wang's group. It was suggested that a deprotonated nucleophile is simultaneously coordinated by the protonated amine and one NH group from the thiourea moiety, while the second thiourea NH interacts with the electrophile (Figure 8, **C**). This mechanism was supported by NMR and DFT calculations on the vinylogous Michael addition of α,β-unsaturated γ-butyrolactam to chalcone.[51] Based on experimental and computational studies on squaramide transition states, Soós et al. concluded that pathway B is the most plausible mechanism (for the addition of 1,3-dicarbonyl compounds to nitrostyrene); however, some of the reaction channels described in pathway A are also available, meaning that the reaction mechanism can't always be rationalized with only one transition state model.

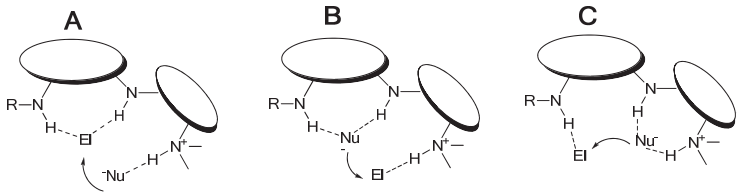

Figure 8. Different proposed bifunctional activation mechanisms.

In general, the structure and electronic nature of the substrates play an important role in the geometry of the transition state and this may explain why a small difference in the structure of the substrate can result in a drastic change in stereoselectivity or reactivity.
In the next chapter, examples of thiourea- and squaramide-promoted asymmetric catalysis will be briefly presented. Due to the very large number of articles published on the topic,[52] it is impossible to cover all the reactions and catalysts. As catalysts **33** and **29** gave the best results for the reactions studied in this thesis, the chosen examples depict their other uses in asymmetric synthesis. In addition, our lab's projects involving H-bond-mediated organocatalysis are described.

1.1.3. Examples of H-bond-mediated asymmetric organocatalysis

Alemán et al. have studied an enantioselective aza-Henry addition of nitroalkanes **31** to 2-aryl-3H-indol-3-ones **30** (Scheme 3).[53] Optimization of the reaction conditions revealed that a thiourea catalyst's **33** performance was the best among the different thioureas and squaramides tested. The reaction turned out to be very sensitive to the solvent, with *p*-xylene being the most efficient. The method works with different aryl substituents of **30** (mainly *para* derivatives have been studied) yielding the products **32a** in high yields (up to 95%) and good to excellent enantioselectivities (*ee* 70-96%). 2-Naphthyl and 4-biphenyl

derivatives were also tolerated, although the latter were less reactive, yielding the product in 37% yield, but still in high enantioselectivity (*ee* 84%). When nitromethane **31a** was replaced with nitroethane **31b**, the product **32b** (Ar = Ph) was obtained in excellent yield (97%) and high enantioselectivity (82/78%), but rather poor diastereoselectivity (dr = 3:1). An additional experiment revealed that the reason for low diastereoselectivity was epimerization, possibly induced by the basic unit of the catalyst. The authors proposed a transition state based on experimentally measured absolute configuration (by X-ray). The carbonyl group of **30** is coordinated by the H-bonds of the thiourea unit, while the nitronate is generated via deprotonation of nitroalkane **31** by a quiniclidine moiety. A *Si*-attack results in an aza-Henry product **32** with the same absolute configuration observed. An additional experiment with 2-nitropropane confirmed the proposed transition state, yielding the product in high yield but only in 17% *ee*. A Newman projection showed that the stability of the complex was not affected by R (H or Me), although it was drastically decreased if the R´ was not hydrogen.

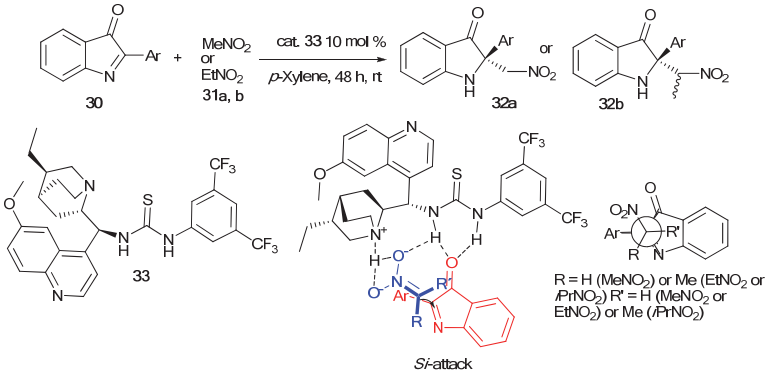

Scheme 3. Asymmetric aza-Henry addition to 2-aryl-3*H*-indol-3-ones **30**.

The same catalyst (**33**) proved to be optimal for the highly stereoselective Michael cyclization cascade reaction between 2-hydroxynaphthalene-1,4-diones **35** and isatylidene malononitriles **34** (Scheme 4).[54] While studying the substrate scope, attention was mainly focused on different aromatic substituents of **34**; in addition, the sensitivity to some *N*-protecting groups was investigated. It was found that the method can be used for a great number of substrates bearing electronically different substituents at positions 4, 5, 6 or 7. Although the yield and *ee* were excellent in most cases (both up to 99%), sometimes a larger amount of the catalyst was required to obtain the product **35** in a more reasonable time. Investigating the nitrogen substituents R_2 revealed that they did not have a serious influence on the outcome of the reaction. In addition, 7-Me-substituted dione **35** was also successfully used for this transformation (yield 88%, *ee* 97%). The reaction was also performed on a gram scale with no decrease in yield or enantioselectivity (R_1 = H, R_2 = allyl, R_3 = H). The authors proposed a transition state for the stereochemistry-determining step. A thiourea

fragment coordinates and activates the electrophilic alkylidene unit, while deprotonation by a tertiary amine results in the formation of a nucleophilic enolate intermediate. A *Re*-attack on the C3 position of the isatylidene malononitrile followed by an intramolecular cyanoaddition results in the formation of a spiro[benzo[g]chromene-oxindole] **36** with the same absolute configuration as was experimentally determined by X-ray.

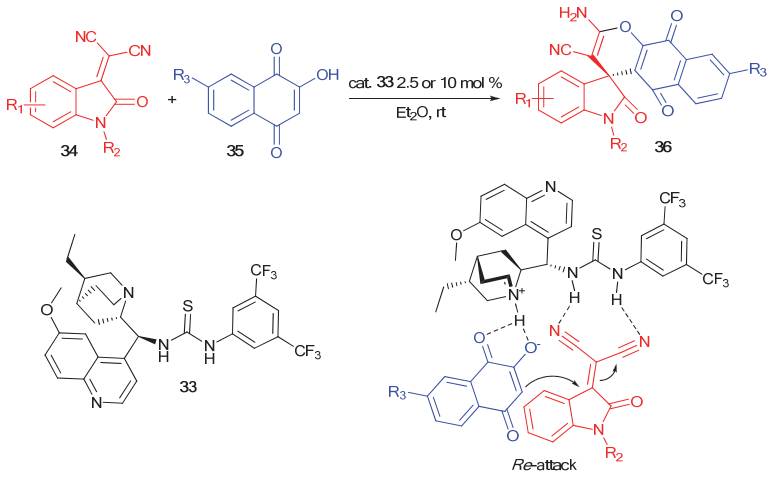

Scheme 4. Michael cyclization cascade reaction between 2-hydroxynaphthalene-1,4-diones **35** and isatylidene malononitriles **34**.

Zanardi et al. achieved a highly stereoselective direct vinylogous Michael addition of α-alkylidenepyrazolinones **37** to nitroolefins **38** (Scheme 5).[55] Based on previous studies of an analogous addition of alkylideneoxindoles[56], catalyst **33** and its pseudoenantiomer **33´**were used in this investigation. The method works well with different aryl-substituted nitroolefins **38**, yielding products **39** in high yields (73-93%) and excellent enantioselectivities (*ee* up to >99%) mainly as *Z* isomers (*Z*/*E* up to 20:1). Next, the authors investigated how different modifications of **37** influenced the reaction outcome. It was found that electronically different *N*-aryl-substituted substrates **37** could be used for the reaction with yields, *Z*/*E* ratio and enantioselectivity remaining at high levels. Changing the Me group at the C3 position (R_1) to Pr or Ph resulted in slightly lower yields (71-75%), although the *E*/*Z*- and enantioselectivities were excellent. In addition, prochiral symmetric and unsymmetric ylidene substrates (R_2 = Me, R_3 = Et and R_2 = Me, R_3 = Me instead of R_2 = H, R_3 = Me) were investigated. In both cases, the products were obtained in high yields, and excellent diastereo- and enantioselectivities as single *Z* isomers (*Z*/*E* >20:1). When catalyst **33** was replaced with a quinidine-derived pseudoenantiomer **33´**, the opposite enantiomeric products **39** were obtained with slightly reduced, but still high enantiomeric purities. Based on the observed (X-ray) absolute configuration, an organocatalytic cycle and transition state of the transformation was proposed.

The authors postulate that the nucleophile **37** undergoes γ-deprotonation by the quinuclidine unit, while the thiourea moiety coordinates and activates the nitroolefin **38** for a *Re*-attack. The dienolate intermediate has *s-cis* conformational preference, explaining why *Z*- and *anti*-isomers (if R_2 = Me) are preferred.

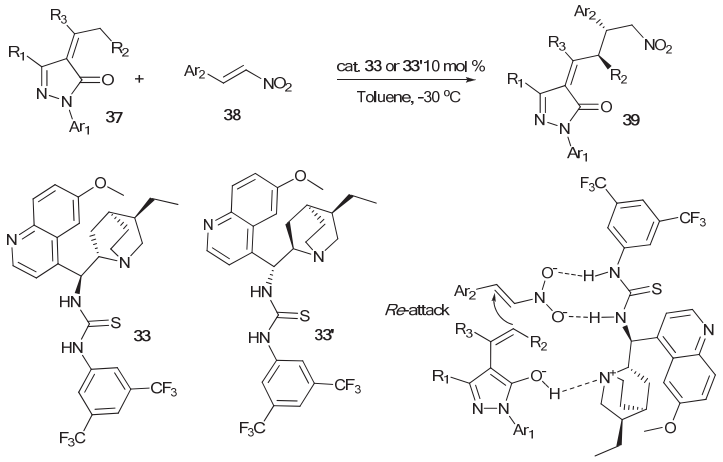

Scheme 5. Vinylogous Michael addition of α-alkylidenepyrazolinones **37** to nitroolefins **38** catalyzed by **33**/**33´**.

Song et al. used the self-association-free squaramide catalyst **29** for the preparation of α-deuterium labeled precursors of α-amino acids **41** via a dynamic kinetic resolution of racemic azlactones **40** using EtOD as a deuterium source (Scheme 6).[57] Under optimal conditions, the *N*-acylated esters **41** were obtained in high yields and enantioselectivities with up to 98% being deuterated. Single recrystallization led to an increase in *ee* to 99%. The method allows for broad variation in alkyl and aryl substituents R_1, providing access to deuterated natural and unnatural amino acid precursors. These compounds can be easily converted to amino acids **42** with no loss of *ee* or deuteration level. Interestingly, when a pseudoenantiomeric catalyst **29´** was used (R_1 = Me, Ar = Ph), the product was obtained in only 55% *ee*. The authors did not discuss the lactone-opening mechanism, although one was proposed by Berkessel for the same reaction catalyzed by a Takemoto thiourea **4**.[58] According to that mechanism, the thiourea unit coordinates the lactone, while the nucleophilicity of the alcohol is activated by the tertiary amine. Deracemization is possible due to the configurational lability of azlactones, while its acidic α-position[59] can be easily deuterated.

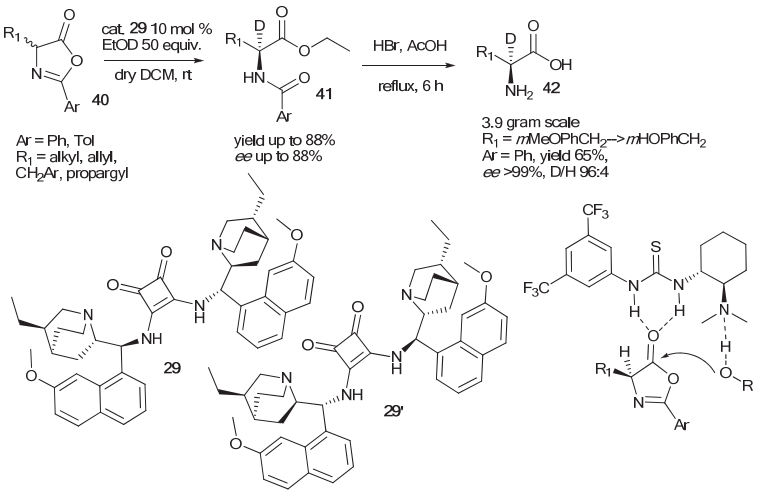

Scheme 6. Preparation of highly enantioenriched deuterated precursors of amino acids **41**.

The self-association-free squaramide **29** also showed good results for the addition of nitroalkanes **31b**,**c** to nitroalkenes **38**; however, in this case, the catalyst **43** with a non-reduced double bond performed slightly better than **29** (Scheme 7).[60] Under optimal conditions, a large number of 1,3-dinitro compounds **44** or **45** with two stereogenic centers were obtained in moderate to high yields (up to 98%), and good diastereo- (dr up to 95:5) and excellent enantioselectivities (*ee* up to 97%). It was found that the electronic properties of the Ar substituent of the nitroalkene **38** had only a limited impact on the outcome of the reaction; however, an aliphatic substrate was not suitable for the transformation due to very low yield. Nitroolefins **38** with heteroaromatic substituents could also be used, but the yields and dr were lower. Changing $EtNO_2$ (**31b**) to $PrNO_2$ (**31c**) resulted in lower, but acceptable yields and diastereoselectivities, while enantioselectivity did not drop. In order to broaden the substrate scope even more, an addition to nitrodienes was also investigated. Corresponding 1,4-addition products **46** were obtained, although in much lower yields and dr, compared to nitroolefins **38**. The method also worked on the gram scale.

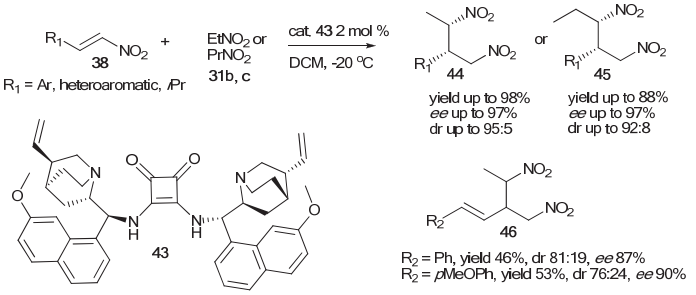

Scheme 7. Highly stereoselective addition of nitroalkanes **31b**, **c** to nitroolefins **38**.

Our laboratory is working in collaboration with Professor Malkov's group (Loughborough University, UK). While studying the [2+1] cycloaddition of 2-chloro-1,3-dicarbonyl compounds **47a-c** to unsaturated oxindole derivatives **48** (Scheme 8), our group has experienced problems with diastereoselectivity.[61] By replacing the 3,5-$(CF_3)_2$Ph moiety of the catalyst **33** with the less active and bulkier 2,6-(iPr)$_2$Ph (**50**), the problem was solved, (dr rose from 78:22 to 93:7 under the same conditions) providing access to highly substituted spiro-cyclopropyl oxindoles **51a-c** with two quaternary centers as one major stereoisomer out of eight. As the formed HCl deactivated the catalyst, 1 equivalent of $NaHCO_3$ was used to prevent this, and it was not strong enough to cause a significant background reaction. The optimized procedure was applied to different substituted oxindoles **48** and 1,3-dicarbonyl compounds **47**. In most cases, the reaction yielded spiro-cyclopropyl oxindoles **51** in excellent yields (up to 97%), enantio- and diastereoselectivities (98% and 99:1, respectively). In the case of dimethyl chloromalonate **47c**, the reaction took longer to finish, although this resulted in even better diastereoselectivity. Oxindoles **48** with strong electron-withdrawing groups R_1 in the 5th position showed lower diastereoselectivity with 3-chloroacetoacetone **47b**. Based on the importance of the isopropyl-substituted moiety of the catalyst **50,** the authors suggested the most likely transition state explaining the stereocontrol. Replacing the catalyst resulted in a significant increase in stereocontrol for the formation of the tertiary center during the first step of the cascade. As similar stereochemical outcomes for the addition of chiral ketoester **47a** and achiral **47b**,**c** were observed, this indicated that a high level of diastereocontrol was provided. Both **49** and **50** exclusively promoted the last stereocenter formation via a *Si*-attack for the major stereoisomer **51**. It was proposed that the thiourea moiety binds to the oxindole-Boc fragment, while the 1,3-dicarbonyl compound **47** is coordinated and activated by the tertiary amine. However, the authors believe that additional computational and mechanistic studies are required to present a precise activation model. After this work, several articles on asymmetric reactions with oxindole derivatives using H-bond activation catalysis[62-64] and aminocatalysis[65] were published by our group.

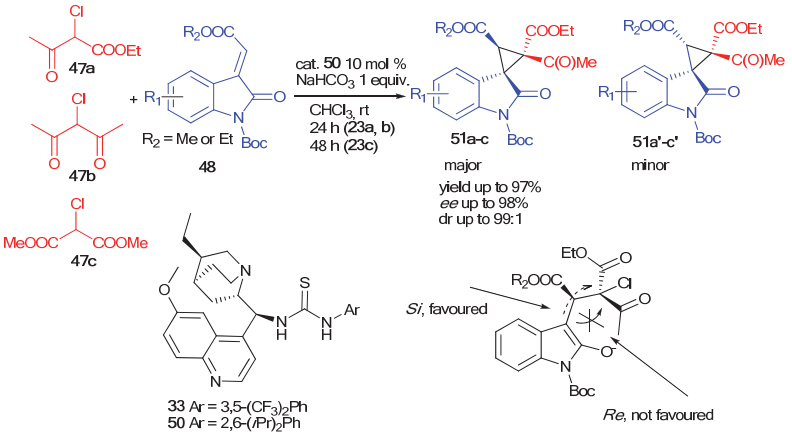

Scheme 8. A highly stereoselective formation of spiro-cyclopropyl oxindoles **51a-c**.

Another recent study from our lab involving H-bond-mediated organocatalysis is connected with using cyclic 1,2-diketones as Michael donors. After successful work on a highly enantioselective aminocatalyzed Mukaiyama-Michael addition of cyclopentane-1,2-dione *bis*-TBS enol ether to unsaturated aldehydes[66], our coworkers investigated the possibility of using non-protected cyclopentane-1,2-dione **51** as a nucleophile with nitrostyrenes **38** being the Michael acceptors (Scheme 9).[67] A DHQ-derived thiourea catalyst **33** showed the best result out of the different thioureas and squaramides screened. The method turned out to be moderately sensitive to the position and nature of the substituents of the aromatic ring of the nitroolefin **38** both in terms of yield (48-90%) and enantioselectivity (*ee* 56-76%). Heteroaromatic and Cy-substituted electrophiles were also efficient, although Cy-nitroalkene was less reactive than other substrates (reaction time 24 h *vs* 2-5 h).

Scheme 9. Using cyclopentane-1,2-dione **51** for the synthesis of Michael adducts **52**.

1.2. Chemistry of unsaturated 1,4-dicarbonyl compounds

The 1,4-enedione unit[68] can be found in many natural products and biologically active compounds (Figure 9).[69-73]

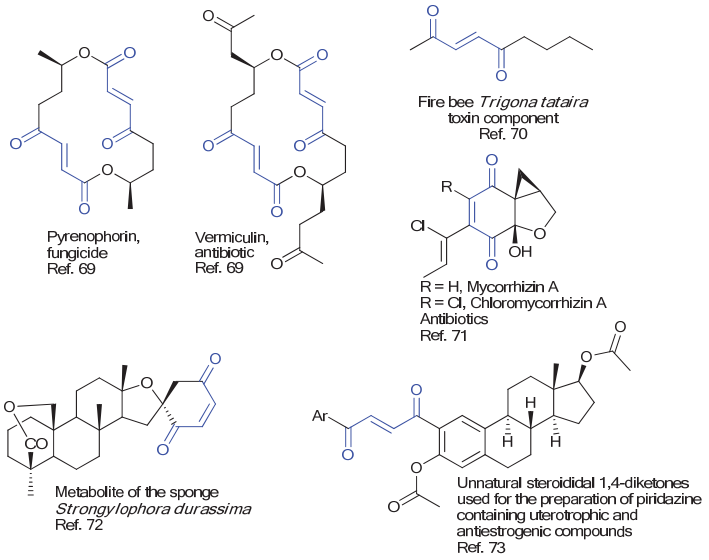

Figure 9. Natural compounds and their derivatives containing a 1,4-enedione unit.

Moreover, this multifunctional unit makes these compounds the perfect targets for further synthetic transformations. There have been multiple examples of the use of such compounds in asymmetric synthesis, some of which are discussed in the next chapter. A conjugated addition to unsaturated 1,4-dicarbonyl compounds makes it possible to insert a nucleophile at the α-position of the other carbonyl group, being an example of formal umpolung reactivity.

1.2.1. Methods of preparation

Over the years many strategies have been used to obtain the above-mentioned compounds. The chosen examples reveal different principles of 1,4-enedione unit formation, as well as different advantages or disadvantages, such as price or the hazardousness of the reagents, the ability to run the whole transformation in one pot and the scope of the methods.

Recently, two groups have published methods for the preparation of symmetric and non-symmetric unsaturated diaryl 1,4-diketones **54** by coupling reactions of acetophenones **53a** and **53b** (Scheme 10). Wang's group used a radical coupling/ copper-induced β-elimination strategy[74] to prepare the target compounds, while Kong used a base-mediated coupling between acetophenone-derived α-

sulphones (generated *in situ*) and α-halides.[75] Both methods make it possible to obtain the desired unsaturated 1,4-diketones **54** in good to very good yields and exclusively as *E*-isomers. Highly selective heterodimerization is possible due to the persistent-radical effect[76] that is achieved by using one starting compound in excess (for **A**) and by adding the reagents stepwise (for **B**). The commercial availability and cheapness of the starting compounds **53a, b,** along with good tolerance towards substituents of the substrates, make both methods attractive.

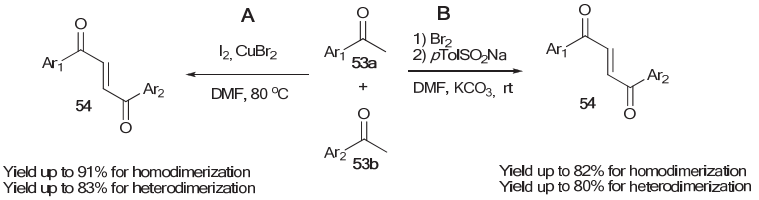

Scheme 10. Synthesis of unsaturated symmetric and non-symmetric diketones by the coupling of acetophenones **53**.

Nair and Bannister have developed a cross-metathesis/oxidation sequence for the synthesis of unsaturated 1,4-ketoesters **59** (Scheme 11).[77] The secondary alcohol **56** prepared by a Gringard reaction from the corresponding aldehyde **55** was coupled with acrylates **57,** affording the unsaturated 4-hydroxyester **58**, which was then oxidized by either a MnO_2 or Dess-Martin reagent depending on the substrate. To get a better result, Lipshutz's strategy was applied, by adding CuI as a co-catalyst for the metathesis step. The authors suggest that an iodide ion serves as a stabilizing ligand on ruthenium, thus prolonging the catalyst's lifetime while Cu(I) has phosphine-scavenging properties.[78] Structurally diverse substrates are suitable for this reaction, although the possibility of using benzaldehydes with different substituents has not been studied. As both substrates are type II olefins (their homodimerization is slow, while homodimers are sparingly consumable)[79], no significant homocoupling was observed. Additional studies showed that this method also works fine for large-scale reactions.

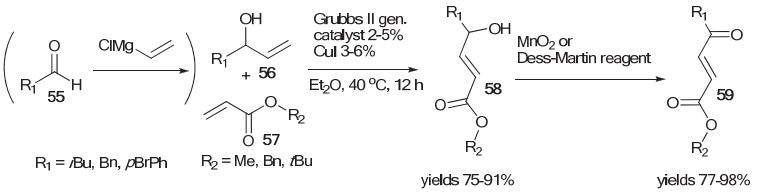

Scheme 11. Synthesis of unsaturated 1,4-ketoesters **59** by a cross-metathesis/oxidation sequence.

While a Wittig reaction is often used for the preparation of the discussed compounds, its application is sometimes limited due to the corresponding α-ketoaldehydes not being stable, creating such problems as hydration, aerial

oxidation, polymerization and limited options for isolation. Runchie and Taylor have developed a simple and effective procedure that exploits the high reactivity of the α-ketoaldehydes while avoiding the above-mentioned problems (Scheme 12).[80] The method involves a one-pot oxidation of the corresponding terminal α-hydroxyketones **60** to the corresponding α-ketoaldehydes with MnO_2 and a Wittig reaction. Due to high reactivity, the produced α-ketoaldehyde is immediately trapped by the Wittig reagent **61**. Both reagents can be varied, making it possible to prepare a great number of target compounds **62** (as a rule, exclusively *E* isomer), although in some cases the yields were moderate. The ease of obtaining a great variety of the starting compounds makes this method quite attractive.

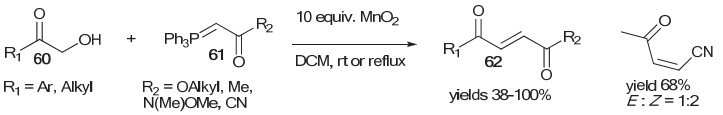

Scheme 12. Synthesis of the unsaturated 1,4-dicarbonyl compounds by a one-pot oxidation/Wittig reaction sequence.

Another oxidation-based method for the preparation of unsaturated 1,4-diketones was studied by Yu and Corey.[81] The method deals with the mild and highly selective oxidation of α,β-enones **62** to the corresponding diketones **63** (Scheme 13, the newly formed carbonyl group is shown in blue). This is a Pd(II)-catalyzed radical reaction with the carbonyl group forming during the base-promoted elimination of the peroxyether. The method works for systems of different structures, including cyclic ones, making it possible to obtain diketones, which are not accessible by using the coupling-based strategy. In order to prepare cyclic diketones with both carbonyls on the cycle, the starting compounds were first protected by ketal. These examples are particularly important as the corresponding products are not very stable and are hard to obtain. This method is also especially important because of the great structural diversity of the products.

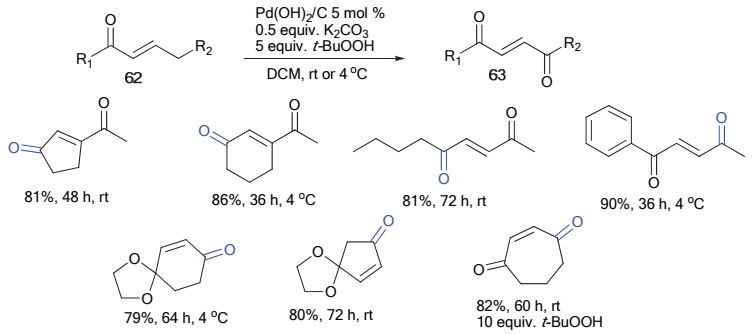

Scheme 13. Pd(II) and *t*BuOOH-promoted oxidation of α,β-enones **62** leading to 1,4-enediones **63**.

Bonete and Nájera have proposed a lithiation/acylation/β-elimination sequence for the synthesis of different unsaturated 1,4-dicarbonyl compounds **67** (Scheme 14).[82] By lithiation of the γ-acetal- or ketal-protected sulphones **65** (available from the corresponding unsaturated or γ-halo ketones or aldehydes **64**) and acylation of the corresponding lithium compounds, 1,4-dicarbonyl precursors **66** were obtained. Deprotection and β-elimination led to the formation of unsaturated 1,4-diketones, ketoaldehydes or ketoesters **67**. While the reaction sequence is quite long (4-5 steps with two compounds isolated by column chromatography), the yields for all steps are acceptable in most cases. The main advantage of the method is the ability to prepare different classes of unsaturated 1,4-dicarbonyl compounds having branched alkyl substituents (R_2) using relatively cheap reagents.

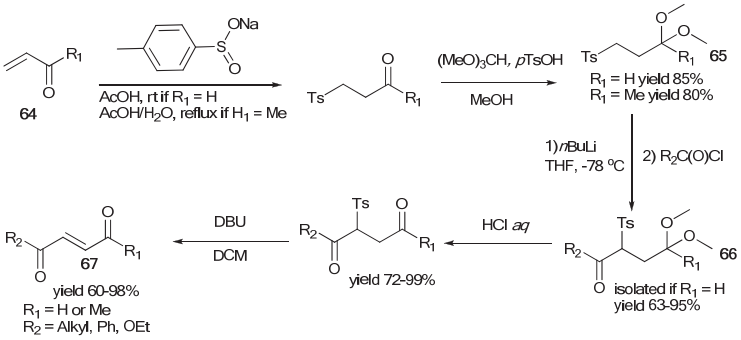

Scheme 14. Lithiation/acylation/β-elimination sequence leading to unsaturated 1,4-dicarbonyl compounds.

Ronsheim and Zercher have reported an efficient one-pot method for the preparation of unsaturated 1,4-ketoesters as well as diketones and ketoamides (single examples) **69** starting from 1,3-dicarbonyl compounds **68**.[83] The method involves a zinc carbenoid-mediated chain extension due to subsequent formation and the opening of the cyclopropane-containing intermediate **70** (Scheme 15).[84] The double bond is formed via base-mediated β-elimination (see Ref. 83 and 83 for full mechanism). The wide availability of the starting compounds, being able to run the whole sequence in one pot and the possibility of obtaining different classes of dicarbonyl compounds make the method efficient.

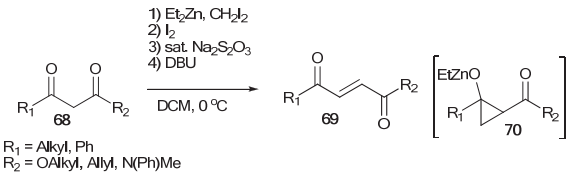

Scheme 15. Synthesis of unsaturated 1,4-dicarbonyl compounds using the Zn-mediated chain extension approach.

1.2.2. Unsaturated 1,4-dicarbonyl compounds in asymmetric synthesis

Unsaturated 1,4-dicarbonyl compounds are mainly used for cycloadditions or different types of conjugated additions. Examples involving various modes of asymmetric induction can be found in the literature, but in this work examples with different H-bonding catalysts were chosen.

Tan's group achieved a highly efficient asymmetric Michael addition of thiomalonate **71a,** aromatic β-ketothioesters **71b** and β-cyanothioester **71c** to 1,4-dicarbonyl compounds **72a-c** catalyzed by chiral guanidine **73** (Scheme 16).[85] The study was at first focused on the addition of thiomalonate **71a** to ketoamides **72a**. It was found that the reactivity of substrate **71a** greatly depended on the amide substituent R_2, with **f** being the most efficient. At the same time, a wide range of aromatic substituents of the ketone (R_1) were tolerated, although in some cases the reaction had to be performed at lower temperatures (up to -60 °C) to obtain the Michael products **74** in higher yield and enantioselectivity. Other sulfur-containing nucleophiles, **71b** (R_3 = Ar) and **71c** (R_3 = CN), also turned out to be applicable for the addition to **72a**, yielding the product **74** in high yield; however, in all cases a 1:1 mixture of diastereomers was formed. Both diastereomers were formed in very high enantioselectivity (up to 97% *ee*). The authors experienced a problem while trying to broaden the reaction scope to unsaturated 1,4-diketones **72b** and **72c**. Although the product **74** still formed in high yield and enantioselectivity, a significant amount of sulfa-Michael by-product **75** was obtained. The corresponding *S*-nucleophile was more likely to have been cleaved from the thiomalonate under the reaction conditions, although the mechanism was not proposed. The problem was solved by replacing the catalyst with its ammonium salt **76** (switching to phase transfer catalysis) and additional optimization. Under optimized conditions, both symmetric (**72b**) and non-symmetric (**72c**) diketones were successfully used and the products **74** were formed in excellent yields and enantioselectivities. Later the same group reported a Soós-type thiourea-promoted asymmetric sulfa-Michael addition of *tert*-butyl mercaptan to unsaturated 1,4-ketoamides and non-symmetric diketones.[86]

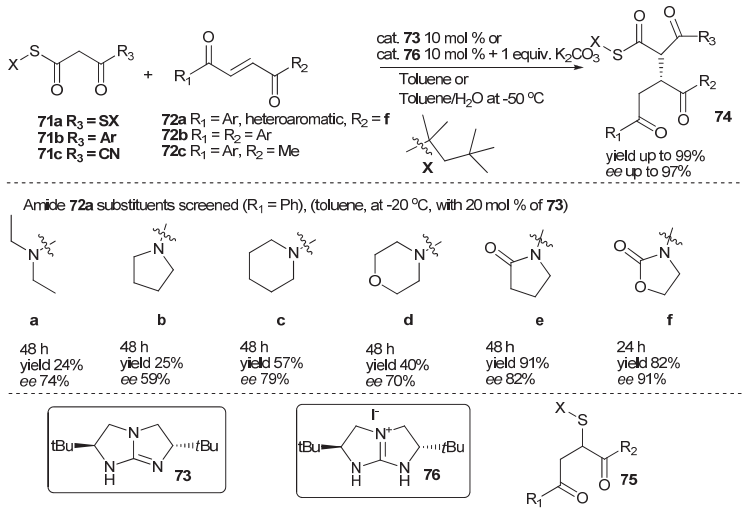

Scheme 16. Asymmetric conjugated addition of sulfur-containing nucleophiles **71a-c** to unsaturated 1,4-dicarbonyl compounds **72a-c**.

Lin et al. used aromatic unsaturated 1,4-ketoesters **77** and diketones **78** as starting compounds for a direct vinylogous Michael addition of γ-substituted butenolides **79** (Scheme 17).[87] The screening of different derivatives of the *Cinchona* alkaloids (including thioureas) revealed that cupreine (**CPN**) is the most efficient for this transformation. Studies of the substrate scope showed that dicarbonyl compounds with different aromatic substituents can be used, as well as different alkoxy groups R_1 (using bulky *i*Pr resulted in a lower yield). The substituent of the butenolide R_2 can also be varied. Ph was the most effective and Me and Bn were acceptable, although switching this substituent to Et resulted in a serious decrease in reactivity (yields for Me *vs* Et: 79 *vs* 35%). The diastereoselectivity of the products **80** and **81** was high in all cases. The authors believe that the phenolic OH of **CPN** activated the dicarbonyl compound, while the tertiary amine deprotonated the butenolide, with the activation of it as a nucleophile. The authors recently published a Soós-type thiourea-catalyzed addition reaction of *N*-protected α,β-unsaturated γ-butyrolactam instead of **79**.[88]

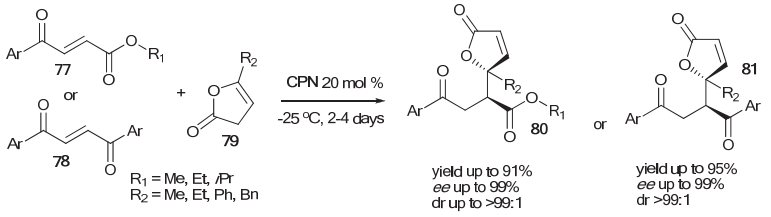

Scheme 17. Asymmetric direct vinylogous conjugated addition of γ-substituted butenolides **79** to unsaturated 1,4-dicarbonyl compounds **77** and **78**.

Yuan et al. have studied the organocatalytic asymmetric addition of 3-substituted oxindoles **82** to unsaturated aromatic diketones **83** (Scheme 18).[89] A detailed catalyst screening revealed that simple unsubstituted *Cinchona* alkaloid **CN** produced the best result. The optimized reaction conditions made it possible to use oxindoles **82** with different substituents both at C3 and C5´ positions, as well as different aromatic and heteroaromatic diketones **83**. No product **84** was obtained with an aliphatic diketone, probably due to its lower electrophilicity. One unsaturated 1,4-ketoester was also used, yielding the product in high yield and enantioselectivity, although the dr was only 3:1.

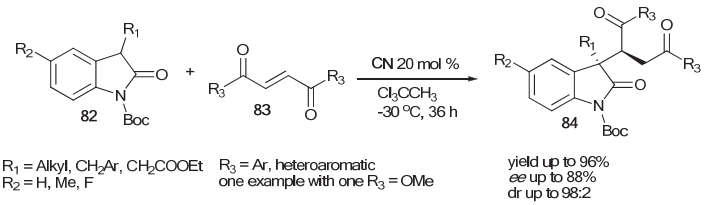

Scheme 18. Michael addition of C3-substituted oxindoles **82** to unsaturated diketones **83**.

As a part of a series of successful asymmetric organocatalytic reactions involving oxindole derivatives performed by our research group,[61-65] we studied a Michael-initiated ring closure cascade reaction between 3-chlorooxindole **85** and unsaturated 1,4-dicarbonyl compounds **86** (Scheme 19).[90] The thiourea catalyst **33** was the best for this reaction, yielding the spiro-product in an optimal yield/enantio-/diastereoselectivity combination. Protecting the chlorooxindole with Boc turned out to be crucial for a smooth transformation. $NaHCO_3$ was used as a mild base in order to trap the formed HCl. The investigation of the substrate scope started with symmetric and non-symmetric diketones. The spiro-oxindoles **87** were obtained in medium to high yields, and enantio- and diastereoselectivities. The diastereoselectivity was higher in the case of non-symmetric diketones. In all cases, crude mixtures contained uncyclized Michael adduct **88** (5-20%). There was no clear correlation between the electronic effect of the substituents and the outcome of the reaction. Using a bromo-substituted chlorooxindole (R_1 = Br) had a small negative effect on stereoselectivity. When unsaturated 1,4-ketoesters **89** were used, an inseparable 2:1 mixture of **88** and **87** was obtained, although only one diastereomer was detected by NMR.

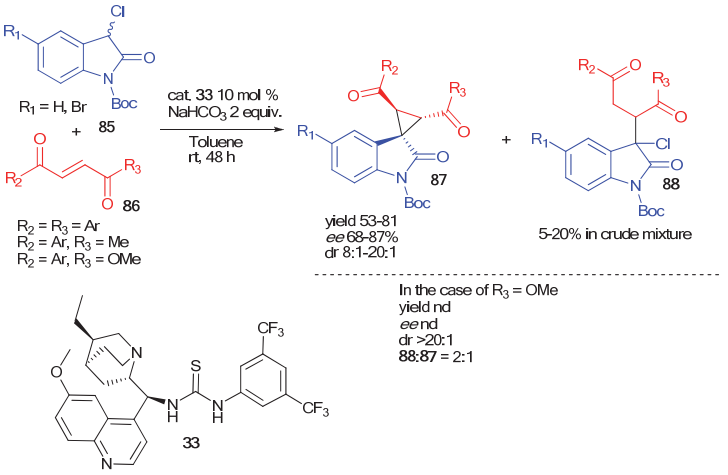

Scheme 19. A Michael-initiated ring closure reaction between 3-chlorooxindoles **85** and unsaturated 1,4-dicarbonyl compounds **86.**

1.3. Summary of literature overview

Outstanding achievements in the field of H-bond-mediated asymmetric organocatalysis have provided access to a great number of highly enantioenriched synthetically and pharmacologically useful compounds. This has mainly been achieved due to the possibility of combining and modifying catalytic units of such bifunctional catalysts as thioureas and squaramides. Because of this, one can find an optimal catalyst in order to perform the desired chemical transformation.

The multifunctionality of the unsaturated 1,4-dicarbonyl compounds, together with the possibility of efficiently activating them by using H-bond catalysis, resulted in their wide application in asymmetric synthesis. A wide range of synthetic methods allowing for the preparation of structurally diverse unsaturated 1,4-dicarbonyl compounds greatly contributes to this.

1.4. Aims of the current work

The multifunctionality of the unsaturated 1,4-dicarbonyl compounds makes them an important class of building blocks that can be used for the preparation of potentially biologically active compounds. In bioactivity, chirality plays an important role, making highly stereocontrolled transformations a high priority. Studying the interactions between the catalyst and substrates and the reaction mechanisms is important in order to improve reaction efficiency; moreover, it contributes to general research on organocatalysis. Investigation of the above-mentioned features was the general aim of the study. More specific aims were:

• Asymmetric desymmetrization of unsaturated 1,4-diketones.

• Expanding the scope of unsaturated 1,4-dicarbonyl compounds as bifunctional Michael acceptors to ketoesters, diesters and others.

• Developing new asymmetric reactions of the unsaturated 1,4-dicarbonyl compounds, leading to synthetically valuable products.

• Studying the mechanistic aspects of organocatalytic asymmetric reactions of unsaturated 1,4-dicarbonyl compounds by experimental, spectroscopic and computational methods.

2. Results and discussion

2.1. Preparation of unsaturated 1,4-dicarbonyl compounds

A literature review reveals many approaches to accessing the desired compounds. While the proposed methods are different, the key elements are formation of a double bond and 1,4-dione unit. Detailed study of the reaction scope often requires a series of analogous compounds with one varied element (e.g. substituents with different electronic effects, aromatic/aliphatic etc). Because of this, universal, cheap and fast methods for the preparation of the desired compounds were required. The literature provided good ideas to solve this problem. The methods chosen for the preparation of the unsaturated 1,4-dicarbonyl compounds used in this work are summarized in Scheme 20. All of the compounds can be obtained in one to two days involving only one or no purification by column chromatography and using mainly cheap reagents. Syntheses of the non-symmetric diketones **90a-i** were fully based on the literature one-pot oxidation/Wittig reaction procedure (Scheme 20, $\mathbf{A_1}$).[80] The same method was chosen for aliphatic symmetric diketone **89a**. As the chosen procedures for aromatic symmetric diketones **89b-f** and ketoesters **91b-f** include Friedel-Crafts acylation, another method was needed for nitro derivatives (Friedel-Crafts acylation is an aromatic electrophilic substitution reaction, and strong electron-withdrawing substituent makes nitrobenzene unreactive). Thus Wittig reactions were used for compounds **89g** and **91g** (Scheme 20, $\mathbf{A_2}$). Double Friedel-Crafts acylation was chosen to obtain symmetric diketones in one step (Scheme 20, **B**).[91] However, in the case of the MeO substituent, the procedure was inefficient due to the high reactivity of the substrate, and the corresponding diketone **89d** was obtained by an oxidation/Wittig sequence (Scheme 20, $\mathbf{A_1}$). The preparation of the ethyl analogue of the aliphatic ketoester **91a** by a bromination/β-elimination sequence (Scheme 20, **C**) has been reported in the literature[92], although the yield was low due to the side reaction (bromination of the methyl group). This method turned out to be highly effective for the preparation of aromatic unsaturated ketoesters **91b-f**, affording the products in high yields.

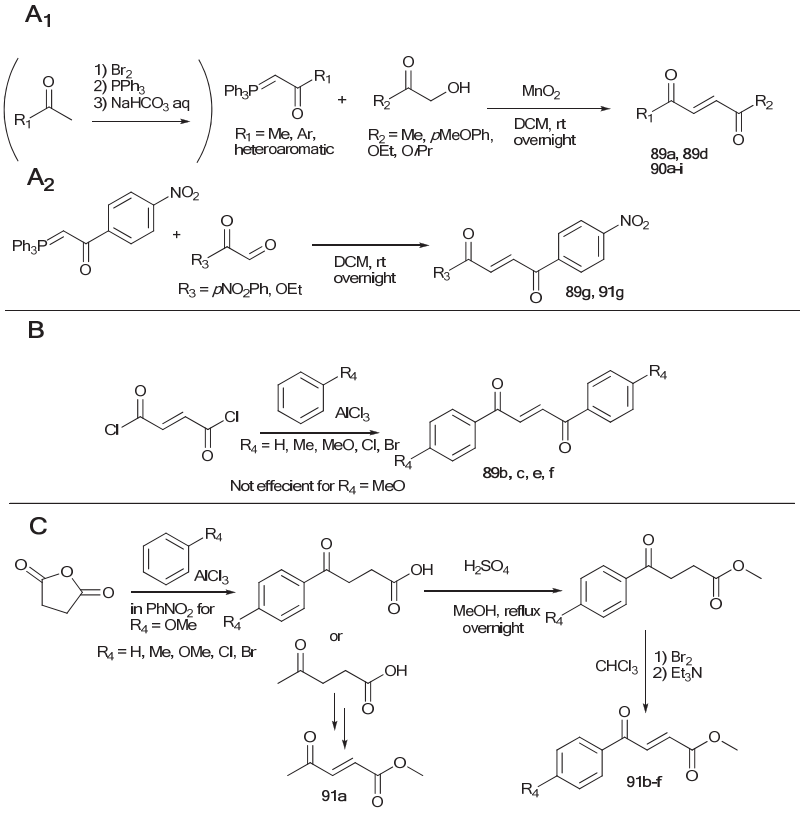

Scheme 20. Preparation of the unsaturated 1,4-dicarbonyl compounds **89-91** used in the current work.

2.2. Asymmetric conjugated addition of 1,3-dicarbonyl compounds to symmetric unsaturated 1,4-diketones

Symmetric unsaturated 1,4-diketones are attractive yet challenging targets for asymmetric conjugated additions. Because of the possibility of stereoselectively introducing a nucleophile into the α-position of the carbonyl group not participating in the conjugated addition, such a reaction can be called a formal umpolung (Scheme 21, **A**). In addition, having α- and β-carbonyl groups, as well as functional groups from the nucleophile, makes the Michael products useful intermediates for further transformations (Scheme 21, **B**). At the same time, a chiral center at the α-position of the carbonyl group may racemize under harsh conditions. Another interesting point is the desymmetrization step: *Si*-attack on different carbons of the double bond lead to the formation of opposite enantiomers (Scheme 21, **C**). This means, that both reaction partners must be well coordinated and activated in order to achieve high stereocontrol.

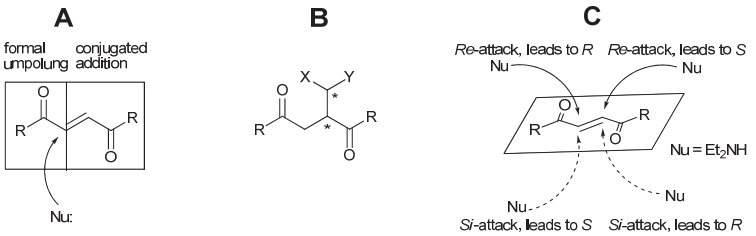

Scheme 21. Symmetric unsaturated 1,4-diketones as specific electrophiles.

2.2.1. Addition of malonates (Publication I)

We started our studies with the desymmetrization of the mentioned compounds with malonates, choosing unsubstituted diketone **89b** and diethylmalonate **94a** for the model reaction. These studies were partially inspired by previously published works by Padmavathi et al., who used the corresponding racemic Michael adducts for the preparation of biologically active compounds containing different heterocycles.[93] We began the catalyst screening with *Cinchona* alkaloids (**QN**, **QD**, **CN**, **CD** and **DHQ**). While all of them catalyzed the reaction, enantioselectivities were very low in all cases (Table 1, Entries 1-5). We observed a remarkable difference in the reaction rates between the catalysts: it took five to six times as long to convert all the diketone to the Michael adduct for **CN**/**CD** compared to **QN**/**QD**. This might be connected with the differences in the solubility. The reduction of the double bond of **QN** led to even lower enantioselectivity (Table 1, entry 2 *vs* 5). It is worth mentioning that the pseudoenantiomers **CN**/**CD** yielded the same enantiomer in excess (Table 1, entries 1 and 3). Next, we investigated the bifunctional thiourea and squaramide catalysts (Table 1, entries 6-9). Thioureas **33** and **92** derived from **DHQ** and **CN** yielded the product in excellent yield and good enantioselectivity. To our surprise, using these structurally different catalysts resulted in the same *ee* (74%). Squaramide **93** afforded the product in lower enantioselectivity compared to the thioureas, while C2 symmetric self-association-free squaramide was much less reactive (4 days *vs* 15 h) and yielded the product **95aa** in even lower *ee*. The modest result can be partially explained by the poor solubility of the catalyst **29**.

Table 1. Screening of the catalysts.

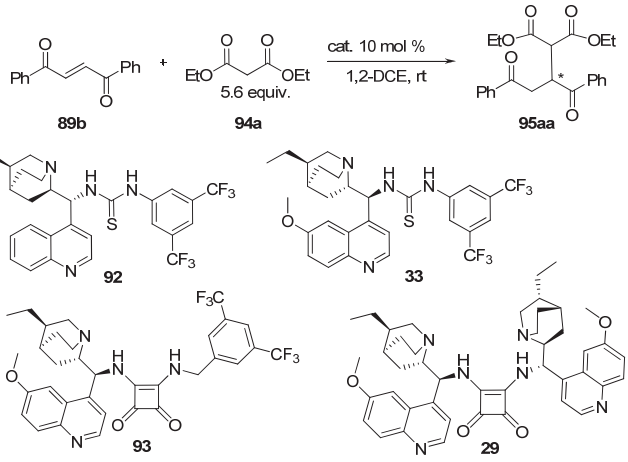

Entry	Catalyst	Time (h)	Yield[a] (%)	*ee*[b] (%)	Abs. conf.[c]
1	**CN**	120	97	13	*R*
2	**QN**	28	98	27	*R*
3	**CD**	168	88	10	*R*
4	**QD**	24	98	19	*S*
5	**DHQ**	20	98	18	*R*
6	**92**	24	98	74	*S*
7	**33**	19	98	74	*R*
8	**93**	15	96	60	*R*
9	**29**	96	96	39	*R*

[a] Isolated yield
[b] Determined by chiral HPLC
[c] Determined by comparison of the calculated and measured VCD spectra of **95aa**

The thiourea catalysts **33** and **92** performed with quite similar efficiencies, but **33** was chosen for further studies because it was slightly more efficient. Despite C2 symmetrical squaramide's **29** poor performance during the screening, it was also chosen in order to compare the obtained results with the catalyst **33**. The reaction was also performed in different solvents (toluene, 1,4-dioxane and *p*-xylene); however, it had only a minor effect on the stereoselectivity, with the initially used 1,2-DCE being slightly more efficient.

With the optimal conditions in hand, we studied the effect of the malonate substituent on the outcome of the reaction. While the ester moiety can be replaced with other functional groups, choosing an optimal substituent is important in order to obtain a higher *ee* value. When thiourea **33** was used as a catalyst, the Michael products **95aa**-**ag** were obtained in high yields and moderate to good enantioselectivities. Bulkier malonic esters resulted in lower

enantioselectivities (Table 2, entries 1 and 3 *vs* 5, 7, 11 and 13). When the same reactions were carried out in the presence of squaramide **29**, some interesting observations were made. Malonates with aromatic units (**94f** and **94g**) resulted in higher enantioselectivities than with thiourea **33** (Table 2, entries 11 and 13 *vs* 12 and 14). It is assumed that the difference in enantioselectivities was connected with the additional aromatic interactions between the aromatic part of the malonic ester and the catalyst. At the same time, there was no clear dependence between the bulkiness of the malonates and enantioselectivity. With dimethyl malonate **94b**, the product was obtained in the highest *ee* (Table 2, entry 4), although the ethyl-substituted substrate gave a significantly lower *ee* (Table 2, entry 2). Surprisingly, *i*Pr- and *t*Bu- malonates **94c** and **94d** were more efficient in terms of enantioselectivity than **94a** (Table 2, entries 6 and 8 *vs* 2). We could not find a satisfactory explanation for this. The reaction with the more sterically demanding *t*Bu malonate **94d** required heating, while Cy-malonate **94e** did not react even at elevated temperatures. Diphenyl malonate **94f** turned out to be less suitable for the reaction because of the formation of the by-products and low yields in both cases (Table 2, entries 11 and 12).

Table 2. Enantioselective addition of malonates to unsaturated 1,4-diketone **89b**.

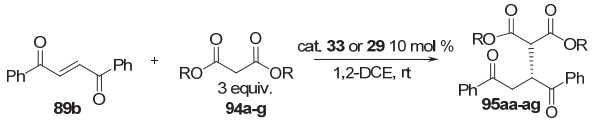

Entry	R	Cat.	Time (h)	Yield[c] (%)	*ee*[d] (%)
1	**a:** Et	**33**	19	99	74
2		**29**	96	96	39
3	**b:** Me	**33**	15	92	73
4		**29**	30	95	87
5	**c:** iPr	**33**	36	96	69
6		**29**	96	96	60
7[a]	**d:** *t*-Bu	**33**	75	70	59
8[a]		**29**	33	95	70
9[a]	**e**: Cy	**33**	48	-	-
10[a]		**29**	48	-	-
11[b]	**f:** Ph	**33**	3	44	37
12[b]		**29**	2	41	81
13	**g:** Bn	**33**	6	95	68
14		**29**	6	92	84

[a] Reaction at 80 °C, malonate: dione ratio 2:1
[b] Malonate: dione ratio 1:1
[c] Isolated yields
[d] Determined by chiral HPLC

Next, we investigated the electronic effect of the *para*-phenyl substituents of the 1,4-diketones **89b**-**d**, **f**, **g (**Table 3**)**. In the case of thiourea **33**, both electron-

donating (**89d**) and electron-withdrawing (**89f**, **89g**) substituents had a positive effect on enantioselectivity, although these reactions were slower than with **89b** (Table 3, entries 7, 10 and 13 *vs* 1). The Me-substituted substrate **89c** showed slightly lower enantiomeric excess compared to **89b** (Table 3, entry 4 *vs* 1). The reactions became sluggish and inefficient when thiourea **33** was replaced with squaramide **29**. At room temperature, the products **95** were obtained in low yields and in some cases poor enantioselectivities (Table 3, entries 2, 5, 8, 11 and 14). Surprisingly, the worst result was observed in the case of Me-substituted 1,4-diketone **89c** (Table 3, entry 5). In an attempt to obtain better results, we repeated the experiments with squaramide **29** at 80 °C. To our delight, this had a strong positive effect on the outcome of the reaction: as was expected, the reaction time and yield became acceptable (Table 3, entries 3, 6, 9, 12 and 15). Raising the temperature also significantly improved the enantioselectivity in some cases (Table 3, entries 3 and 6).

Table 3. Enantioselective addition of diethylmalonate **94a** to unsaturated 1,4-diketones **89b-d**, **f**, **g**.

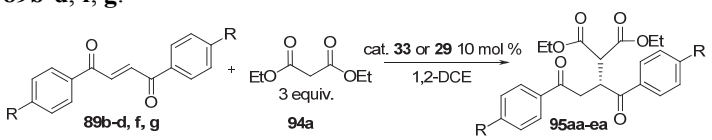

Entry	R	Catalyst	*T* (°C)	Time (h)	Yield[b] (%)	*ee*[c] (%)
1	**b:** H	**33**	rt	19	99	74
2		**29**	rt	96	97	39
3		**29**	80	10	97	82
4	**c:** Me	**33**	rt	18	96	69
5		**29**	rt	213	25	18
6		**29**	80	22	76	66
7	**d:** MeO	**33**	rt	88	90	79
8		**29**	rt	48	-	-
9		**29**	80	22	90	83
10[a]	**f:** Br	**33**	rt	48	83	81
11[a]		**29**	rt	123	20	93
12		**29**	80	6	86	91
13	**g:** NO_2	**33**	rt	54	66	81
14		**29**	rt	94	44	89
15		**29**	80	6	98	89

[a] Dione: malonate ratio 1.2:1
[b] Isolated yields
[c] Determined by chiral HPLC

We determined the absolute configuration of the products **95** by comparing measured and calculated VCD spectra of the compound **95aa**. The calculated (red) and measured (blue) IR spectra matched well, in the range 1500-1800 cm^{-1} (Figure 10, **A**). The assignment of the absolute configuration was based on the

most characteristic peaks of the VCD spectra from the same region. The calculated VCD spectrum of the *R*-enantiomer of **95aa** matched the spectrum of the compound obtained in the presence of catalyst **33 (**Figure 10, **B)**, allowing us to determine the absolute configuration as *R*.

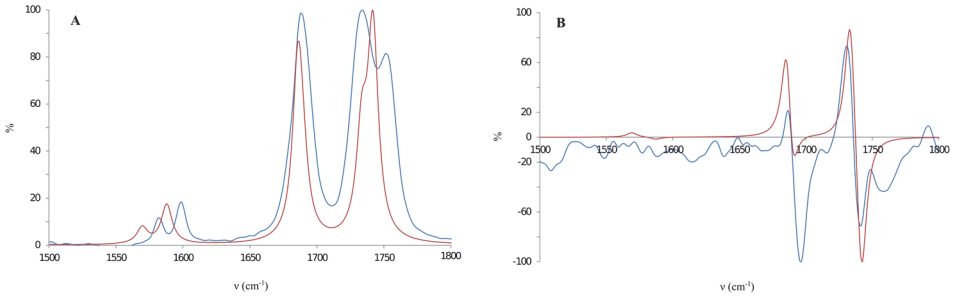

Figure 10. Calculated (red) and experimental (blue) IR (**A**) and VCD (**B**) spectra of the *R* enantiomer of **95aa**.

Having determined the absolute configuration, we proposed a transition state of the reaction catalyzed by squaramide **29** (Scheme 29). The squaramide moiety coordinated and activated the 1,4-diketone while the tertiary amine activated the malonate. As the used 1,4-diketones were symmetric, there was no regioselectivity problem. The substrates were coordinated for the *Si*-attack; moreover, the *Re*-face was shielded by the quinuclidine unit of the alkaloid fragment not participating in the activation. The *Si*-attack led to the formation of the *R*-enantiomer as was experimentally observed.

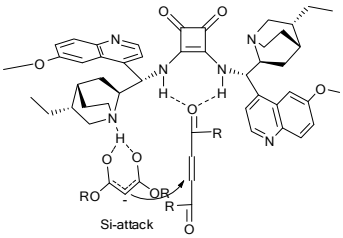

Scheme 29. Proposed transition state of the Michael addition of malonates **94** to symmetric unsaturated 1,4-diketones **89** catalyzed by **29**.

Recently, we also reported the asymmetric addition of dimethylmalonate **94b** to different electrophiles, including unsaturated 1,4-dicarbonyl compounds catalyzed by Ca^{2+} chiral complexes.[94]

2.2.2. Addition of β-ketoesters

Having obtained good results with malonates, we decided to broaden the scope of the desymmetrization of the unsaturated 1,4-diketones **89** by switching to β-ketoesters **96** (Table 4).

Table 4. Enantioselective addition of β-ketoesters **96a-d** to symmetric unsaturated 1,4-diketone **89b**.

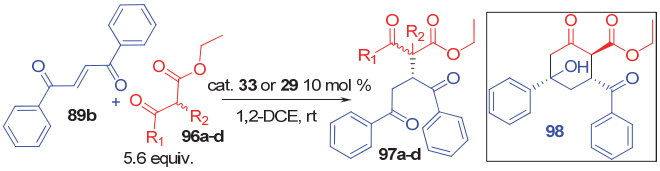

Entry	R_1	R_2	Catalyst	Time (h)	Yield of **97**[a] (%)	*ee*[b] (%)	dr[c]
1	a: Me	H	**33**	15	48% of **97a** 51% of **98**	78/79 79	64:36 nd[d]
2	a: Me	H	**29**	15	94	81/78	57:43
3	b: Ph	H	**33**	17	99	70/70	64:36
4	b: Ph	H	**29**	20	95	90/88	62:38
5	c: Me	F	**33**	0.5	74	80/63	66:34
6	c: Me	F	**29**	24	75	68/49	65:35
7	d: Me	Me	**33**	312	69	59/39	50:50
8	d: Me	Me	**29**	432	34	26/-25	82:18

[a] Isolated yield
[b] Determined by chiral HPLC
[c] Determined by NMR after column chromatography
[d] NMR showed **98** as one main isomer, however HPLC showed two pairs of enantiomers with a 2:1 ratio. This is probably connected with tautomerization

As with the malonates, we used both catalysts **33** and **29** and compared the obtained results. The reaction with ethyl acetoacetate **96a** afforded the product **97a** in similar good enantio- and poor diastereoselectivities with both catalysts (Table 4, entry 1 vs 2); however, the reaction mediated by thiourea **33** proceeded further and half of **97a** was converted to the Michael/aldol cascade reaction adduct **98**. Interestingly, using a squaramide catalyst made it possible to isolate the whole product as a simple Michael adduct. In the case of a Ph-group containing ethyl benzoylacetate **96b**, a similar observation as in the case of aromatic malonates was made: squaramide **29** gave significantly higher *ee* compared to thiourea **33**. Again, the diastereoselectivities remained low with both catalysts. Next, we investigated the possibility of using substituted ethyl acetoacetates. As expected, fluoro-substituted substrate **96c** was active and reacted smoothly, especially in the presence of the thiourea catalyst **33**, giving the product in good yield and enantioselectivity, but again in low diastereoselectivity (Table 4, entries 5 and 6). Methyl-substituted substrate **96d** turned out to be a poor nucleophile for this transformation probably due to additional sterical hindrance and deactivation due to the +I effect of the methyl group. The reactions with both catalysts were very sluggish and the products were obtained in low yields and enantiomeric purities. Unexpectingly, there was a remarkable difference in diastereoselectivity, but no definite conclusions can be reached from one experiment, as many factors may influence it. We also

performed an additional experiment to observe if it was possible to exclusively obtain the cascade product **98** in the reaction with ethyl acetoacetate **96a**. When all of the diketone **89b** was consumed, the temperature was risen to 80 °C; however, these conditions turned out to be too harsh and a mixture of cyclic products was obtained (concluded from the ^{1}H NMR spectrum of the isolated product). A literature search revealed that the Michael-aldol cascade reaction between 1,4-diketones and acetoacetate had already been reported, although $Ba(OH)_2$ had been used as a catalyst, yielding a racemic compound.[95] Although the Michael adduct **97a** had formed in low diastereoselectivity, only one diastereoisomer of the cyclic product was detected by NMR. This can be explained by tautomerization of the compound **98** to **98´** (Scheme 30).The same article demonstrates the possibility of further derivatisation. For example, dehydration and decarboethoxylation took place under acidic conditions, affording unsaturated cyclohexanone **99** with one stereogenic center. As a failed full cyclization attempt yielded a mixture of the cyclic compounds, we decided to apply these conditions in order to reach **99**. Indeed we managed to isolate **99** as a single product, although the yield was low and partial racemization occurred (the *ee* of **99** was 34%).

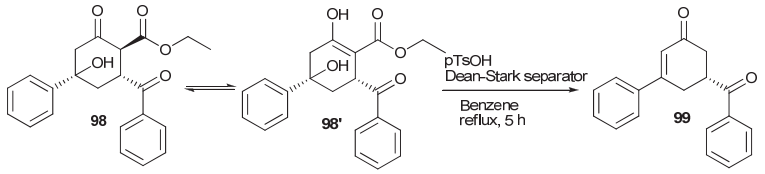

Scheme 30. Tautomerisation of **98** to **98´**and dehydration/decarboethoxylation product **99**.

2.3. Asymmetric aza-Michael addition of isatin Schiff Bases to unsaturated 1,4-dicarbonyl compounds (Publications II and III)

Isatin is a well-known natural compound.[96] In addition to being a core structure of many compounds possessing a wide range of biologically important properties, isatin has been an important research object for synthetic chemists. A combination of a phenyl ring and γ-lactam moiety and the carbonyl group in the molecule of isatin gives rise to a variety of chemical transformations. Indeed, reactions involving all of these functional groups have been well-described. The C3 carbonyl group has been the most popular target for stereoselective cascade reactions and the preparation of spiro-cyclic compounds useful for pharmacological research. Inspired by a highly stereoselective aldol reaction with a C3 carbonyl group of isatin,[97] we decided to improve this chemistry by using enolizable unsaturated ketoester **91a** for an aldol reaction followed by an oxa-Michael addition to the conjugated system, leading to the heterocyclic spiro-compound **102** (Scheme 31, **A**). After long optimization, we managed to find the conditions for a highly enantioselective aldol reaction, although all of the

attempts to cyclize the aldol adduct **101** failed (different bases and aminocatalysts were screened). After this failure, we switched to an isatin aniline Schiff base **103a** for the analogous Mannich/aza-Michael sequence, hoping that the Mannich product would undergo cyclization to spiro-compound **104** more easily. Knowing that Pihko's dual-activated thioureas, such as **27** and **105,** performed well for the Mannich addition of 1,3-dicarbonyl compounds to *N*-Boc aldimines,[38,39] we started our investigations with this type of catalysts. To our great surprise, an aza-Michael product **106aa** was formed in excellent yield and enantioselectivity. The product can be easily hydrolyzed to *N*-substituted isatin **107aa** with no loss of yield or enantiomeric excess (Scheme 31, **B**).

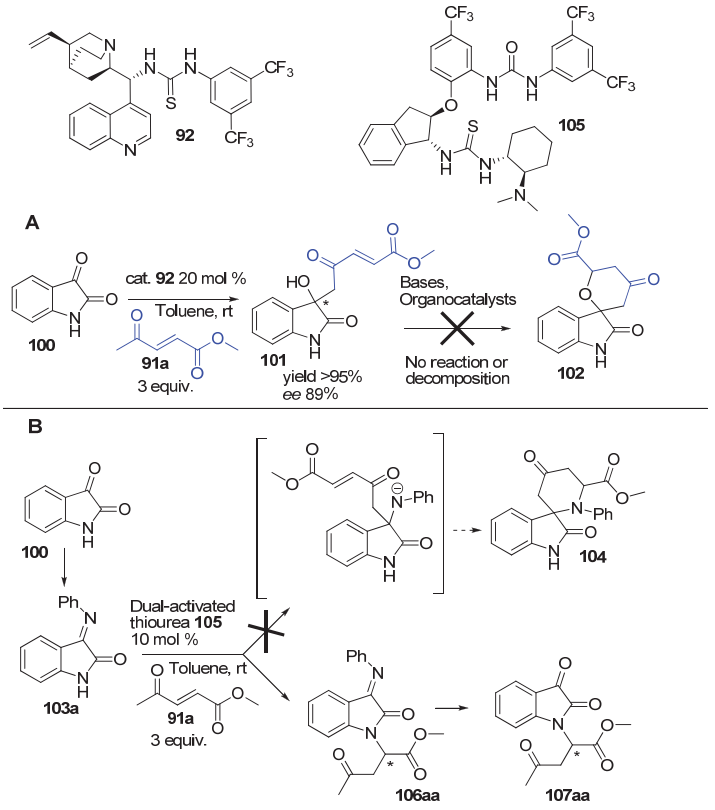

Scheme 31. The pathway to a highly stereoselective aza-Michael addition of isatin Schiff bases **103** to unsaturated 1,4-dicarbonyl compounds.

The nucleophilicity of the nitrogen atom of isatin is often used for simple reactions, such as alkylation and acylation, which are mainly done to avoid side reactions while performing other transformations. To the best of our knowledge, there have only been a few examples of asymmetric aza-Michael additions of isatin. Shi et al. reported the allylic amination of Morita–Baylis–Hillman carbonates with isatin promoted by *Cinchona* alkaloids.[98] Another example is

the prolinol-catalyzed conjugated addition of acetal-protected isatins to unsaturated aldehydes, which was recently published by Lu et al.[99] Moreover, there have been many examples of biologically active isatins differently substituted on the nitrogen (Figure 11).[100-102] These two points encouraged us to start research on an asymmetric aza-Michael addition of isatin Schiff bases to unsaturated 1,4-dicarbonyl compounds, which will be discussed in the next chapters.

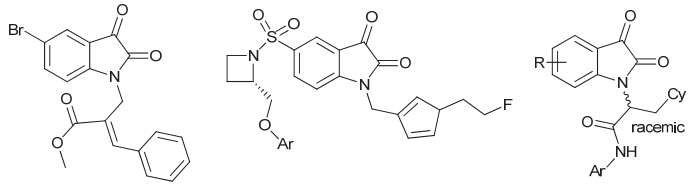

Figure 11. Examples of biologically active *N*-substituted isatins.

2.3.1. Scope of the reaction

2.3.1.1. Addition to 1,4-ketoesters (Publication II)

After the first successful experiments with the aliphatic ketoester **91a,** we screened for the optimal conditions using the above-mentioned isatin aniline Schiff base **103a** addition to unsaturated ketoester as a model reaction. A 10 mol % catalyst loading was optimal to complete the reaction in a reasonable time while not wasting the catalyst (Table 5, entries 1-3). Pihko's dual activated thioureas and their simple analogues were also used for screening (Figure 12).

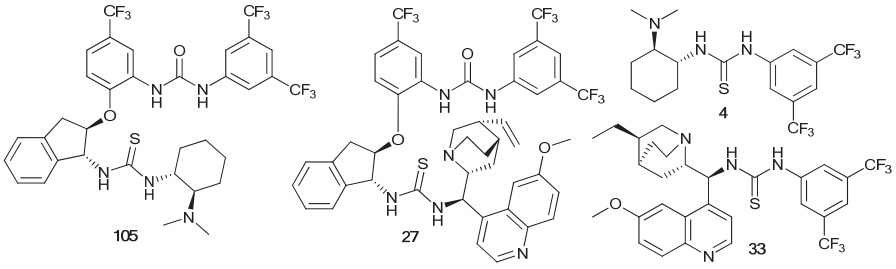

Figure 12. Screened catalysts.

All four catalysts exclusively gave the aza-Michael product **106aa** in excellent enantiomeric excess (Table 5, entries 2, 4-6), although the reaction rate strongly depended on the catalyst structure. Catalysts **105** and **33** showed good results, affording the product in high yields and selectivities in reasonable times. It should be noted that catalyst **105,** being a dual-activated analogue of **4,** was more efficient than **4** (Table 5, entry 2 *vs* 4), while **33** was superior to its dual-

activated analogue **27** (Table 5, entry 6 *vs* 5). As catalyst **33** is cheaper and easily obtainable it was chosen for further investigations. Screening typical solvents revealed that toluene was the most efficient for this reaction (Table 5, entries 6-8).

Table 5. Screening for the optimal conditions for 1,4-ketoesters

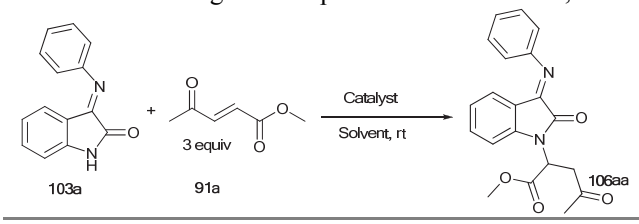

Entry	Catalyst (mol %)	Solvent	Time (h)	Yield[a] (%)	*ee*[b] (%)	Abs. conf.
1	**105** (20)	Toluene	48	97	95	*R*
2	**105** (10)	Toluene	96	95	98	*R*
3	**105** (5)	Toluene	216	51	99	*R*
4	**4** (10)	Toluene	72	46	97	*R*
5	**27** (10)	Toluene	72	29	97	*R*
6	**33** (10)	Toluene	72	95	96	*S*
7	**33** (10)	DCM	72	77	96	*S*
8	**33** (10)	THF	72	51	95	*S*

[a] Isolated yield
[b] Determined by chiral HPLC

With the optimal conditions in hand, we investigated the scope of this reaction by using different *para*-substituted aromatic ketoesters **91b-g**. The aza-Michael products **106** were hydrolyzed to substituted isatins **107.** Their purification and analyses were easier than relatively unstable imines. All of the aromatic ketoesters studied were more reactive than aliphatic **91a**. As expected, the substrates with the electron-withdrawing substituents were more reactive (Table 6, entries 5 and 7), although for some reason the reaction with the bromo-substituted substrate **91f** did not proceed to completion (Table 6, entry 6). In all cases, the products were obtained in excellent yields and *ee*-s. Next, we studied the effect of different aromatic substituents R_1 of the indolinone ring of the Schiff base **103** (Table 6, entries 2, 8-11). Electron-withdrawing substituents increased the acidity of the N-H proton, activating the substrates **103d**, **e** (Table 6, entries 10 and 11), while the substrates possessing electron-donating substituents (**103 b**, **c**) were less reactive compared to unsubstituted **103a** (Table 6, entries 8 and 9 *vs* 2). Again, all of the products were obtained in excellent enantioselectivities.

Table 6. The scope of the aza-Michael addition of isatin Schiff bases **103** to 1,4-ketoesters **91**.

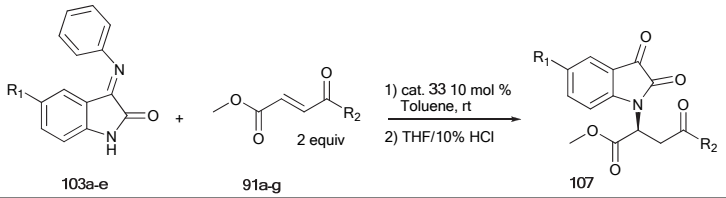

103a-e 91a-g 107

Entry	**103** R_1	**91** R_2	**107**	Time (h)	Yield (%)[b]	*ee* (%)[c,d]
1	**a** H	**a** Me	**107aa**	72	80	97
2	**a** H	**b** Ph	**107ab**	18	95	94
3	**a** H	**c** *p*MePh	**107ac**	16	97	95
4	**a** H	**d** *p*MeOPh	**107ad**	16	95	96
5	**a** H	**e** *p*ClPh	**107ae**	5	95	93
6	**a** H	**f** *p*BrPh	**107af**	24	82	96
7[a]	**a** H	**g** *p*NO_2Ph	**107ag**	4	73	88
8	**b** Me	**b** Ph	**107bb**	20	83	90
9	**c** MeO	**b** Ph	**107cb**	96	75	95
10	**d** Br	**b** Ph	**107db**	3.5	91	91
11	**e** NO_2	**b** Ph	**107eb**	2.5	96	95

[a] Ethyl ester was used
[b] Isolated yield
[c] Determined by chiral HPLC
[d] The absolute configuration (*S*) was determined by an X-ray structure analysis of **107ae** and was assumed to be the same with the other substrates

Recently, in collaboration with the Saint Petersburg State Institute of Technology, we started studying the bioactivity of the obtained chiral *N*-substituted isatins as Caspase 3[103] inhibitors.[104] The preliminary results revealed that one racemic compound possessed inhibitory activity that was much stronger than the *S* isomer of the same compound (*ee* 93%). In order to continue these studies, as well as to better understand the possibilities of obtaining the *R* enantiomer in excess and checking the influence of the ester substituent, additional experiments were conducted. To our delight, switching to a thiourea catalyst prepared from cinchonine (**92**) had no negative effect on the enantioselectivity, making the *R* enantiomer available in even slightly better enantioselectivity. In addition, changing Me ester to Et or *i*Pr had no negative effect.

2.3.1.2. Addition to non-symmetric 1,4-diketones (Publication III)

Having obtained good results with the 1,4-ketoesters, we investigated the possibility of using non-symmetric diketones for the same reaction. When a reaction with 1,4-diketone **90a** was performed under the optimal conditions used

for 1,4-ketoesters, the product was obtained in excellent yield and high selectivity, although it was a bit lower than in the case of the unsubstituted ketoester **91b**. We experienced a problem of regioselectivity: regioisomers were derived from either attack on the α-position of an aliphatic (**108a**, major product) or aromatic carbonyl (**109a**, minor product). Thus, we had to optimize the reaction conditions for these new substrates. First, different thiourea catalysts were evaluated (thiourea catalysts from Table 1, Figure 12, catalyst **50**).

Table 7. Screening for the optimal conditions for non-symmetric 1,4-diketones.

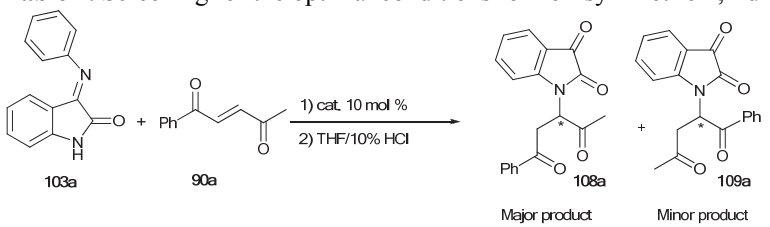

Entry	Cat.	Solvent	*T* (°C)	Time (h)	Yield (%)[a]	Ratio of **108a**:**109a**[b]	**108a** *ee* (%)[c]	Abs. conf.[d]
1	**33**	toluene	rt	4	91	8:1	85	*S*
2	**33**	THF	rt	20	85	6.5:1	88	*S*
3	**33**	1,2-DCE	rt	3.5	>95	5:1	87	*S*
4	**33**	toluene	2	20	>95	9.5:1	86	*S*
5	**33**	toluene	-25	72	>95	12:1	92	*S*
6	**92**	toluene	rt	7	>95	6:1	83	*R*
7	**50**	toluene	rt	48	95	6:1	86	*S*
8	**4**	toluene	rt	20	95	11.5:1	80	*R*
9	**105**	toluene	rt	20	95	3.3:1	67	*R*
10	**27**	toluene	rt	60	94	2.1:1	35	*R*

[a] Isolated yield
[b] Determined by ^{1}H NMR after column chromatography
[c] Determined by chiral HPLC
[d] The absolute configuration was determined by an X-ray structure analysis of compound **110b**

Cinchona-derived thioureas (**33**, **92** and **50**) exhibited an analogous stereoselectivity pattern in toluene (Table 7, entries 1, 6 and 7), affording the product **108a** in high yield and enantioselectivity, and the ratio of regioisomers varied from 8:1 to 6:1. Dual-activated thioureas **105** and **27** turned out to be unsuitable for this reaction due to low regioselectivity (Table 9, entries 9 and 10). Although Takemoto catalyst **4** provided the product in the highest regioselectivity, the reaction was significantly slower than in the case of **33** (Table 7, entry 8 *vs* 1); moreover, it had a slight negative impact on enantioselectivity. Based on these results, we varied other parameters while using catalyst **33**. Changing toluene to 1,2-DCE led to a slightly faster reaction

and better enantioselectivity, combined with lower regioselectivity (Table 7, entry 2). Performing the reaction in THF resulted in both a slower reaction and lower regioselectivity (Table 7, entry 3). Finally, we studied the effect of temperature (Table 7, entries 1, 4 and 5). The high catalytic activity of **33** made it possible to perform the reaction at -25 °C. This led to a significantly slower reaction compared to room temperature, although the product was obtained in the best enantio- and regioselectivity.

Having determined the optimal conditions, we started exploring the reaction scope with non-symmetric methyl aryl diketones **90** (Table 8). Decreasing the temperature to 2 ^{o}C or -25 ^{o}C (if possible) allowed us to obtain most of the aza-Michael products in excellent yields, and high enantio- and regioselectivities.[105] As was expected, the reaction outcome greatly depended on the substituent of the diketone **90**. Electron-withdrawing groups of the phenyl ring (**90d**, **e** and **f**) promoted the formation of the major regioisomer **108** and increased the reaction rates, while the electron-donating MeO-group (**90c**) resulted in very low regioselectivity (Table 8, entries 4-6 vs 3). There was no significant difference when the phenyl ring was replaced with a naphthyl ring (Table 8, entry 1 *vs* 2). Reactions with the heteroaromatic substrates (**90g** and **90h**) afforded the products in moderate enantioselectivities (Table 8, entries 7 and 8), while using 2-pyrrolyl-substituted diketone **90i** resulted in a racemate that was obtained in low yield and regioselectivity (Table 8, entry 9).

Table 8. The scope of the aza-Michael addition of isatin Schiff base **103a** to non-symmetric 1,4-diketones **90**.

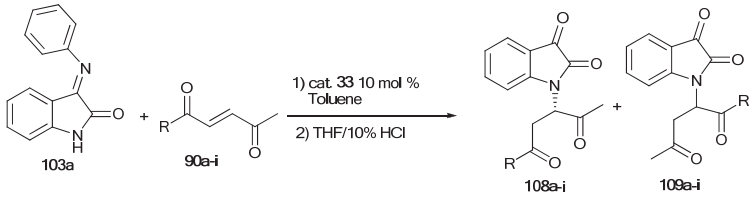

Entry	R (**90**)	*T* (°C)	Time (h)	Ratio of **108**:**109**[a]	Yield (%)[b]	*ee* of **108** (%)[c]
1	**a**, Ph	-25	72	12:1	>95	92
2	**b**, 2-naphthyl	2	24	8.5:1	>95	90
3	**c**, *p*MeOPh	2	24	4.5:1	>95	93
4	**d**, *p*ClPh	-25	72	15.5:1	>95	90
5	**e**, *p*BrPh	-25	72	15:1	>95	92
6	**f**, *p*NO_2Ph	2	24	16.5:1	85	89
7	**g**, 2-thiophenyl	2	72	4:1	76	66
8	**h**, 2-furanyl	2	60	19.5:1	>95	74
9	**i**, 2-pyrrolyl	rt	72	4:1	10	rac

[a] Determined by ^{1}H NMR after column chromatography
[b] Isolated yield
[c] Determined by chiral HPLC

2.3.1.3. Addition to symmetric 1,4-diketones (Publication III)

As symmetric 1,4-diketones **89** are similar to **90**, we did not perform full screening of the reaction conditions for these substrates and performed the reaction in toluene in the presence of thiourea catalyst **33**. The first obtained results were rather modest, as most of the products were obtained in moderate yields and enantioselectivities in the course of sluggish reactions.[106] Our previous studies showed that 1,2-DCE had a positive effect on both reaction rate and enantioselectivity when screening for non-symmetric diketones **90** was performed; however, it could not be used for that reaction due to a drop in regioselectivity (Table 7, entry 3). The results of the aza-Michael addition of isatin Schiff base **103a** to symmetric 1,4-diketones **89** obtained in 1,2-DCE are presented in Table 9.

Table 9. The scope of the aza-Michael addition of isatin Schiff base **103a** to symmetric 1,4-diketones **89**.

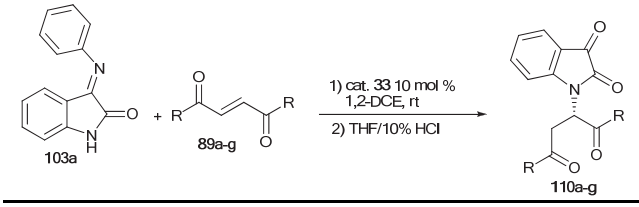

Entry	R (**89**)	Time (h)	Yield (%)	*ee* (%)[c]
1[a]	**a**, Me	36	93	83
2	**b**, Ph	2	>95	95
3	**c**, *p*MePh	3.5	>95	95
4	**d**, *p*MeOPh	36	>95	84
5	**e**, *p*ClPh	30	>95	87
6[b]	**f**, *p*BrPh	228	72	64
7	**g**, *p*NO_2Ph	4.5	74	nd[d]

[a] The reaction was performed in toluene in the presence of 10 mol % of catalyst **4**
[b] The reaction was carried out under more diluted conditions (0.2 M)
[c] Determined by chiral HPLC
[d] We were unable to resolve the enantiomers

Unsubstituted and Me-substituted substrates **89b** and **c** were the most efficient, affording the products in excellent yields and enantioselectivities in only 2-3.5 hours (Table 9, entries 2 and 3). Using MeO-substituted inactivated substrate **89d** also resulted in high yield and enantioselectivity, although it took much longer for the reaction to complete (Table 9, entry 4). There was a significant difference in the reactivity of Cl- and Br-substituted diketones **89e** and **89f**: while the *p*ClPh substrate afforded the product **110e** in excellent yield and high *ee*, the reaction with its bromo-analogue did not proceed to the end, even after more than a week (Table 9, entry 5 *vs* 6). The product **110f** was obtained in

moderate yield and enantioselectivity. NO_2-substrate **89g** reacted swiftly, yielding the product **110g** in good yield (Table 9, entry 7). In order to obtain good results with the aliphatic diketone **89a,** additional optimization had to be made. The corresponding product **110a** could be obtained in high yield and *ee* if the reaction was performed in toluene in the presence of the Takemoto catalyst **4** (Table 9, entry 1).

2.3.1.4. Addition to other electrophiles (Publication III)

With the promising results with different unsaturated 1,4-dicarbonyl compounds in hand, we decided to check if it was possible to use other electrophiles for this reaction. Unfortunately, it turned out that the method was relatively limited and additional studies were required in order to perform efficient aza-Michael additions of isatin Schiff bases to different electrophiles. Scheme 32 shows the obtained results. Reactions with chalcone and its aliphatic analogue afforded the aza-Michael products **111** and **112** in high enantioselectivities; however, probably because of the sterical hindrance near the prochiral carbon, chalcone was significantly less reactive. The symmetric unsaturated dibenzyl fumarate afforded the product **113**, but in much lower yield and enantioselectivity compared to the more reactive 1,4-dicarbonyl compounds. In order to obtain the addition product from alkylidenemalonate, a more reactive nitro-substituted isatin Schiff base **103e** was needed. Still, the yield and *ee* of the product **114** were very low. We also used α,β-unsaturated γ-nitroester and 1,4-ketosulphone, but only traces of the corresponding products **115** and **116** were detected. To sum up, at the moment the efficient application of the discussed methodology is limited to unsaturated 1,4-ketoesters and diketones. Of the other electrophiles, chalcone analogues and fumarates are the most promising types of electrophiles, although additional optimization is required in order to obtain decent results.

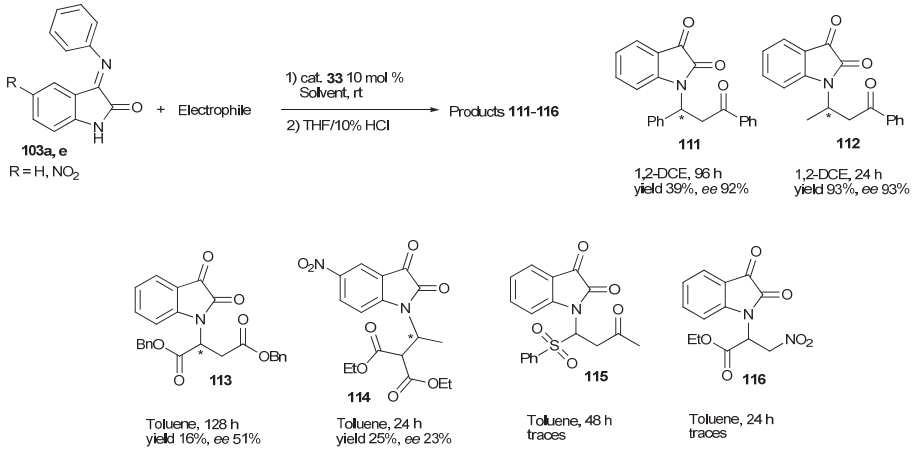

Scheme 32. Performing the aza-Michael addition of isatin Schiff bases **103** to other electrophiles.

2.3.2. Studying the interactions between thiourea catalysts and isatin Schiff bases

During the exploration of the reaction scope of aza-Michael additions of isatin imines **103** to unsaturated 1,4-dicarbonyl compounds, we performed additional research focused on explaining why the derivatization of isatin turns it into a highly potent nucleophile. In order to answer this question, a combination of synthetic, spectroscopic and computational methods was used. The next three chapters deal with the different approaches used to explain the activation mechanism, followed by a summary.

2.3.2.1. Synthetic studies (Publication II)

The fastest and easiest way to get insight into the activation mechanism was to prepare a number of structurally diverse isatin Schiff bases and use them for the same reaction (Table 10). The chosen substituents confirmed some of the assumptions we had made at the beginning of the mechanistic studies.

Table 10. The effect of different imine **103** substituents on the outcome of the aza-Michael reaction.

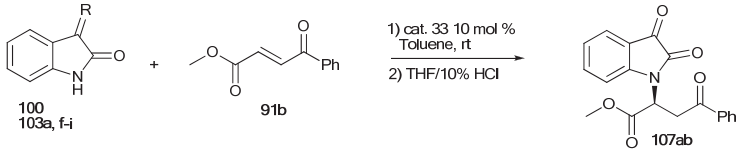

Entry	R	Time (h)	Yield (%)[b]	*ee* (%)[c]
1[a]	**100** O (isatin)	48	59	62
2	**103a** N-Ph	18	97	94
3	**103f** N-H	144	12	75
4	**103g** N-*i*Pr	128	30	88
5	**103h** N-*p*-MeOPh	72	62	98
6	**103i** N-*p*-NO_2Ph	72	21	90

[a] 3 equiv. of ketoester **91b** used
[b] Isolated yield
[c] Determined by chiral HPLC

At the beginning of our studies of the asymmetric aza-Michael addition, we wanted to use underivatized isatin **100** as a nucleophile. It soon became clear that in this case the product could only be obtained in moderate yield and enantioselectivity. Having proposed that changing the carbonyl group to an imino group would influence the electron density of the nucleophilic nitrogen, we synthesized the unsubstituted Schiff base **103f**. While this compound turned out to be less reactive, the product was obtained in higher *ee* compared to

unsubstituted isatin (Table 10, entry 3 *vs* 1). Next, we speculated that the imine substituent R would provide additional interactions with the catalysts, improving the reaction efficiency. An *i*Pr-substituted Schiff base was more reactive than **103f**, but the yield was much lower compared with **103a** (Table 10, Entry 4). Having obtained these results, we speculated that the reason for the activation might be the aromatic interactions between isatin's imine phenyl ring and the quinoline unit of the *Cinchona*-derived catalyst. As aromatic donor-acceptor interactions[107] would be stronger, we decided to prepare analogs of **103a** having good electron-donating and electron-withdrawing groups. We speculated that compound **103i** would provide stronger interactions than **103h** because of the electron-withdrawing nitro-group (as the quinoline fragment of the catalyst is electron rich, **103i** would be much more efficient for aromatic donor-acceptor interactions). Unfortunately, this did not work as planned: using **103h** resulted in slightly higher *ee* compared to **103a**, while in the case of **103i** *ee* was lower than for **103a** (Table 10, entries 5 *vs* 6 *vs* 2). Because of the poor solubility of **103g** and **103h,** no clear conclusions concerning the reaction rates could be reached.

2.3.2.2. NMR studies (Publication II)

Having obtained some information from the synthetic studies, we switched to NMR in order to detect some changes on the spectra when the thiourea catalyst **33** was added to a solution of Ph- or *i*Pr-substituted imine (**103a** or **103g**). Table 11 summarizes the most important differences in the chemical shifts when an imine/catalyst mixture was measured. In the presence of the catalyst **33**, the most significant differences occurred in the five-membered ring of isatin. The biggest difference was observed for the α-carbon to the nitrogen (0.5 ppm for ^{13}C). All signals of the protons of the imine substituents were shifted to higher field (lower chemical shifts) indicating the association with the aromatic ring(s) of the catalyst. In the case of *i*Pr-imine **103g**, two CH_3 doublets (3H) from the isopropyl group were clearly seen, which seemed to indicate that imine was placed in an anisotropic environment, most likely due to binding to the catalyst.

Table 11. Important changes of the chemical shifts of isatin Schiff bases in the presence of thiourea **33** (30 mol %). For full table see Supporting Information of Publication **II**.

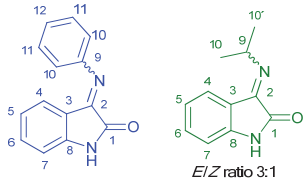

Atom	1-C	2-C	3-C	8-C	9-C	10-H	10-C	10´-H	10´-C
E	166.18	152.67	116.63	145.11	53.34	1.44	23.09		
E [a]	+0.12	+0.16	-0.03	+0.20	-0.07	-0.04	-0.12	-0.07[b]	-0.04[b]
Z	160.42	151.12	122.42	142.75	50.78	1.31	23.94		
Z [a]	+0.12	+0.11	0	+0.15	-0.05	-0.03	-0.06	-0.04[b]	-0.07[b]

Atom	1-C	2-C	3-C	8-C	9-C	10-H	10-C	11-H	11-C
E	165.61	154.76	116.15	145.80	150.07	7.05	117.87	7.45	129.41
E [a]	+0.14	+0.44	-0.17	+0.52	-0.35	-0.13	-0.08	-0.08	-0.06

[a] Chemical shift changes in ppm of the substrates in mixture with 30 mol % of the organocatalyst **33**

[b] Diastereotopic methyls from isopropyl groups

In addition to the difference in chemical shifts, important changes in the shapes of the peaks can be observed (Figure 13). Without the catalyst, the peaks of the Ph-imine **103a** (blue, left) are sharp. When the spectrum is measured in the presence of 30 mol % of Takemoto catalyst **4** (green, left), some of the peaks are much broader. When **103a** is mixed with the same amount of *Cinchona* thiourea **33**, some of the peaks even turn into broad singlets (red, left). The broadening of peaks is connected with the loss of free rotation, which in turn indicates interactions with the catalyst. The observed changes are in correspondence with the experiments (during the screenings, catalyst **33** was more effective than **4**). On the right, the splitting of the *i*Pr doublet of **103g** is shown. In the presence of **4,** the effect is seen only for the *E* isomer, while with **33** both isomers are involved, indicating a significant difference in imine/catalyst interactions.

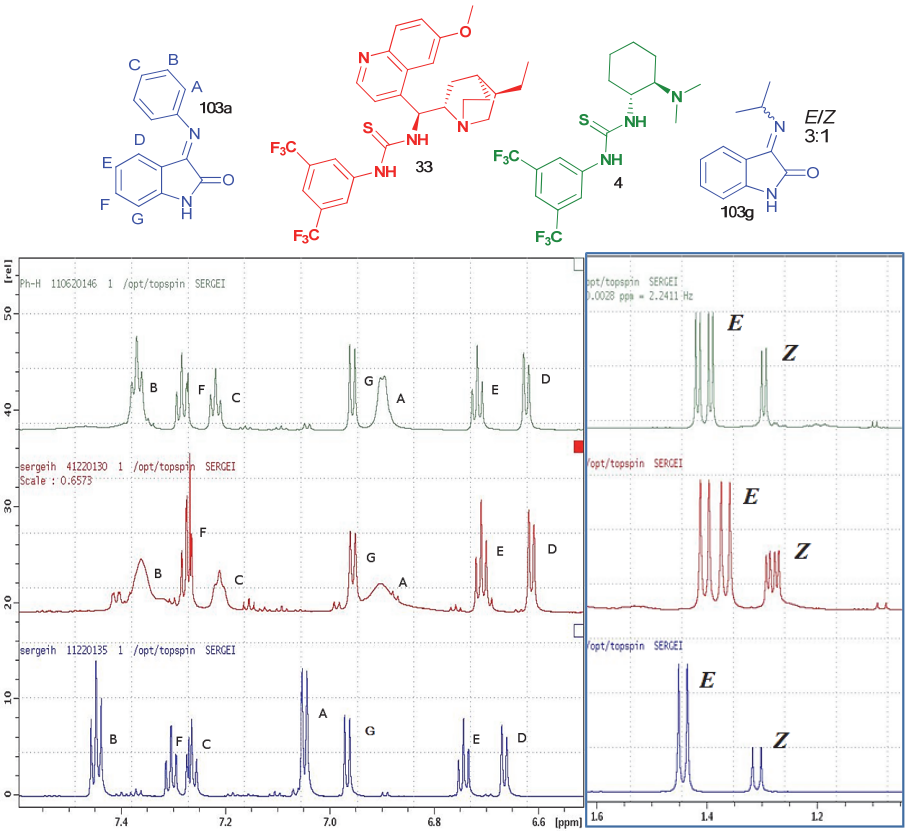

Figure 13. The changes in the shapes of the peaks of **103a** (left) and **g** (right) in the presence of thiourea catalysts: blue – imines without the catalyst, red – imines with 30 mol % of the catalyst **33**, green – imines with 30 mol % of the catalyst **4**.

2.3.2.3. Computational studies (Publication III)

Computational studies were performed by Prof. Toomas Tamm and Dr. Andrus Metsala (both from TUT). We determined if there was any difference between the nitrogen charges of unsubstituted isatin **100** and Schiff base **103a**.[108] After DFT calculations, the resulting charge densities were analyzed with NBO[109] and Mulliken[110] methods. Although the methods yielded different charges, both showed that the atomic charges for both compounds were virtually identical (Table 12).

Table 12. Calculated atomic charges of the nucleophilic nitrogens of **100** and **103a**.

Method	Isatin **100** N charge	Imine **103a** N charge
NBO	-0.5518	-0.5474
Mulliken	-0.2087	-0.2056

Later, we used molecular dynamics simulations in order to rationalize the remote activation of isatin by comparing the H-bond formation of **100** and **103a** with the catalyst **33**. The calculations were performed using an AMBER99 force field. The results of the simulation revealed that imine **103a** was more involved in the hydrogen bonding network. The prevailing number of H-bonds along the molecular dynamic trajectory for imine ranged from two to three, while in the case of isatin this number was one (Table 13).

Table 13. Comparison of the population of H-bonds between catalyst **33** and the substrates **103a** and **100** during 270 ns of simulation.

Compound	Probability of number of H-bonds (%)					
	0	1	2	3	>3	∑
Imine **103a**	5.90	14.66	37.57	41.87	0.00	100
Isatin **100**	2.46	97.47	0.06	0.00	0.00	100

In the case of the imine **103a,** thiourea moiety formed two hydrogen bonds with the lactamic oxygen. At the same time, the N-H group from the imine interacted with the tertiary amine of the quinuclidine unit (Figure 14, **A**). Surprisingly, for isatin **100** only one H-bond was formed between the sulfur atom of the thiourea unit and the N-H of the imine (Figure 14, **B**).

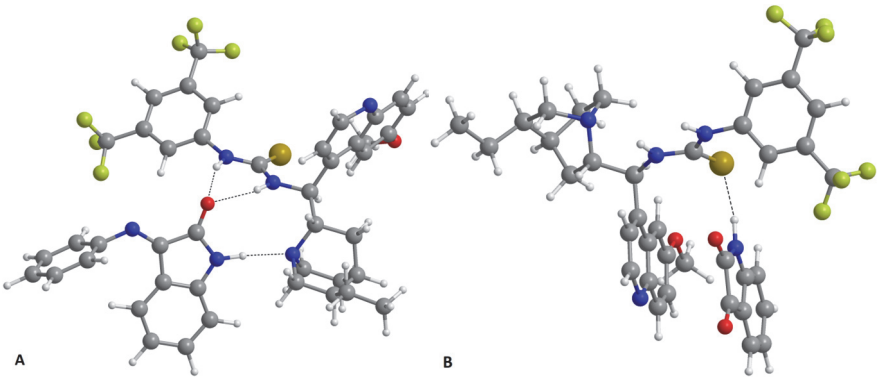

Figure 14. Two-component complexes between catalyst **33** and imine **103a** (**A**) and isatin **100** (**B**).

Next, we investigated the three-component mixture by "adding" aliphatic ketoester **91a**. In the case of isatin, this resulted in the disappearance of the S-H-N hydrogen bond; however, a lot of different lowly populated H-bonded complexes appeared, making these states very diverse. In the case of imine **103a**, the lowest energy complexes were nonreactive. However, the complex with the increased nucleophilicity of the nitrogen atom (having three H-bonds similar to the ones that were observed in the two-component complex, Figure 15) was also present.

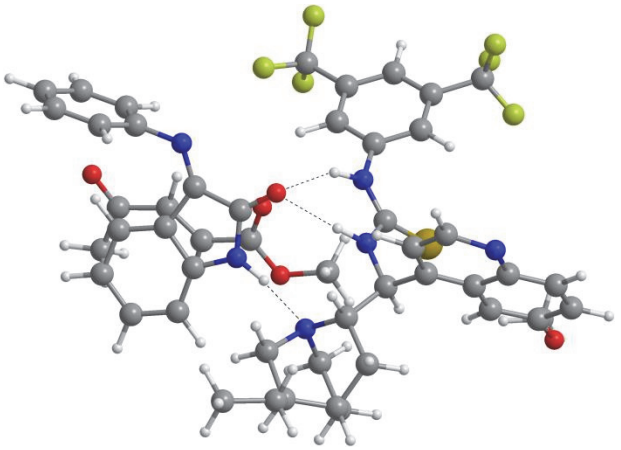

Figure 15. Three-component complex between catalyst **33**, imine **103a** and ketoester **91a**.

Additional *ab initio* calculations are underway to rationalize the obtained results.

In summary, by combining the synthetic, spectroscopic and computational results, it can be concluded that the remote activation of isatin by derivatization to an aniline Schiff base **103a** comes from the additional interactions between the catalyst and the phenyl ring. This results in a significant change in the geometry of the catalyst-substrate complex, leading to higher reactivity and increased stereocontrol, which is confirmed by the experimental work involving highly stereoselective aza-Michael additions of the above-mentioned imine to different unsaturated 1,4-dicarbonyl compounds. More sophisticated calculations are underway to demonstrate the possible Π–Π stacking interactions.

Conclusions

- A series of unsaturated 1,4-ketoesters, symmetric and non-symmetric diketones were synthesized by using cheap and fast methods.

- Highly enantioselective desymmetrization of unsaturated aromatic diketones was achieved via the addition of malonates in the presence of thiourea or squaramide catalyst (*ee* up to 93%).

- The catalytic activities of thiourea **33** and squaramide **29** were compared in the abovementioned reaction. It was found that catalyst **29** was more efficient in reactions with nucleophiles possessing aromatic substituents. In general, the reactions were more sluggish in the presence of catalyst **29**, although raising the temperature to 80 °C not only improved the reaction rates and yields, but also resulted in higher enantioselectivities (in some cases).

- An elegant method for the preparation of highly enantioenriched *N*-substituted isatins was developed by using unsaturated 1,4-dicarbonyl compounds as nucleophiles. The nucleophilicity of isatin *N*-atom can be increased by remote control via formation of aromatic imine moiety.

- The mechanism of the remote activation of isatin was combinatively studied by applying synthetic, spectroscopic and computational techniques. It was proposed that complex via H-bonds between the catalyst and reagents was formed in the transition state. Close proximity of reagents and preferred conformation of the transition state are responsible for the remote activation of isatin derivative and high enantioselectivity of the reaction.

- The performed work has the potential to be broadened to biological research and further computational chemistry studies.

3. Experimental

Full assignment of ^{1}H and ^{13}C chemical shifts is based on the 1D and 2D FT NMR spectra measured on a 400 MHz instrument. Residual solvent signals were used [$CDCl_3$ δ = 7.26 (^{1}H NMR), 77.16 (^{13}C NMR), DMSO-d_6 δ = 2.54 (^{1}H NMR), 40.45 (^{13}C NMR)] as internal standards. The ^{1}H NMR peaks are reported as follows: s = singlet, bs = broad singlet, d = doublet, t = triplet, q = quartet, hept = heptaplet, m = multiplet. High resolution mass spectra were recorded on QTOF LC/MS spectrometer using ESI ionization. MS spectra were measured on GC-MS spectrometer (70 eV EI). Chiral HPLC was performed using Chiralpak AD-H (250 x 4.6 mm) or Chiralcel OJ-H (250 x 4.6 mm) column. Precoated silica gel 60 F254 plates were used for TLC. Silica gel was used for column chromatography. The measured melting points are uncorrected. Commercial reagents were used as received. The solvents were freshly distilled using standard methods (DCM and ethyl acetate over phosphorous pentoxide, toluene over sodium). Commercial 1,2-DCE used for asymmetric reactions was distilled over CaH_2. The reactions were performed under air atmosphere without additional moisture elimination unless stated otherwise.

*Characterization of symmetric diketones **89a-g***

(*E*)-Hex-3-ene-2,5-dione (89a). The compound was prepared by the procedure used for non-symmetric diketones (see below). The product was purified by column chromatography on silica gel, eluent Hex/EtOAc 4:1. Isolated yield 207 mg; 74%. Colorless needles. Mp 76-78 °C .^{1}H NMR (400 MHz, $CDCl_3$) δ 6.76 (s, 2H), 2.35 (s, 6H). ^{13}C NMR δ 198.60, 137.92, 28.08. IR (KBr) *v*: 3043, 1673, 1636, 1419, 1359, 1126, 1000, 588 cm^{-1}. MS (70 eV) *m/z*: 112 [M^{+}], 97, 69, 43. HRMS (ESI-QTOF): compound is not suitable for this analysis.

(*E*)-1,4-Diphenylbut-2-ene-1,4-dione (89b). Dry $AlCl_3$ (4.1 g; 30.7 mmol) was mechanically suspended in dry benzene (15 mL). The mixture was cooled to 5 °C and fumaryl chloride (1.5 mL; 13.5 mmol) was added dropwise. The mixture was allowed to warm to rt and was heated to 80 °C. After 2 h the mixture was cooled to rt and poured into ice. The product was extracted with DCM, washed with $NaHCO_3$ solution, dried with Na_2SO_4, concentrated and recrystallized from heptane/*i*PrOH. The obtained orange solid was boiled in *i*PrOH with charcoal and filtered through Celite to remove minor colored impurities. Isolated yield 2.4 g; 76%. Bright yellow crystalline solid. Mp 104-106 °C. ^{1}H NMR (400 MHz, $CDCl_3$) δ 8.10 – 8.03 (m, 4H), 8.01 (s, 2H), 7.67 – 7.60 (m, 2H), 7.57 – 7.49 (m, 4H). ^{13}C NMR δ (101 MHz, $CDCl_3$) δ 189.9, 137.0, 135.2, 134.0, 129.03, 129.02. IR (KBr) *v*: 1649, 1593, 1578, 1446, 1323, 1294, 1193, 1018, 704, 634 cm^{-1}. MS (70 eV) *m/z*: 236 [M+], 208, 131, 105, 77, 51. HRMS (ESI-QTOF): calculated for $C_{16}H_{12}O_2$ $[M + H]^{+}$ 237.0910, found 237.0914.

(*E*)-1,4-Di-*p*-tolylbut-2-ene-1,4-dione 89c. Obtained by the analogous procedure as for **89b** in toluene (15 mL). After the addition of fumaryl chloride, the mixuture was stirred overnight at rt, followed by 3 h at 60 °C. The reaction was quenched and the product isolated in the same manner. Isolated yield 1.8 g; 51%. Bright yellow crystalline solid. Mp 145-147 °C. ^{1}H NMR (400 MHz, $CDCl_3$) δ 8.00 (s, 2H), 7.97 (d, *J* = 8.2 Hz, 4H), 7.32 (d, *J* = 8.0 Hz, 4H), 2.44 (s, 6H). ^{13}C NMR (101 MHz, $CDCl_3$) δ 189.5, 145.0, 135.1, 134.6, 129.7, 129.2, 21.9. IR (KBr) *v*: 1647, 1601, 1568, 1410, 1324, 1300, 1190, 1036, 837, 746 cm^{-1}. MS (70 eV) *m/z*: 264 [M+], 236, 221, 145, 119, 91, 65. HRMS (ESI-QTOF): calculated for $C_{18}H_{16}O_2$ $[M + H]^+$ 265.1223, found 265.1227.

(*E*)-1,4-Bis(4-methoxyphenyl)but-2-ene-1,4-dione 89d. 1-(4-methoxyphenyl)-2-(triphenyl-λ^5-phosphanylidene)ethan-1-one (2.2 g; 5.4 mmol) was dissolved in DCM (30 mL) followed by the addition of 2-hydroxy-1-(4-methoxyphenyl)ethan-1-one[111] (0.9 g; 5.4 mmol) and 58% MnO_2 (4.7 g; 54 mmol). The reaction was followed by ^{1}H NMR (the disappearance of the ylide CH doublet). The mixture was stirred overnight at room temperature, filtered through Celite and concentrated. The product was separated from triphenylphosphine oxide by stirring in hot Hept/*i*PrOH solution followed by cooling, filtration and washing with cold *i*PrOH. Isolated yield 1.0 g; 63%. Bright yellow crystalline solid. Mp 163-165 °C. ^{1}H NMR (400 MHz, $CDCl_3$) δ 8.09 – 8.02 (m, 4H), 8.00 (s, 2H), 7.03 – 6.94 (m, 4H), 3.89 (s, 6H). ^{13}C NMR (101 MHz, $CDCl_3$) δ 188.2, 164.3, 134.7, 131.5, 130.2, 114.2, 55.7. IR (KBr) *v*: 2967, 1642, 1597, 1421, 1318, 1253, 1179, 1010, 852, 599 cm^{-1}. MS (70 eV) *m/z*: 296 [M$^+$], 268, 161, 135, 107, 92, 77, 64. HRMS (ESI-QTOF): calculated for $C_{18}H_{16}O_4$ $[M + H]^+$ 297.1121, found 297.1122.

(*E*)-1,4-Bis(4-chlorophenyl)but-2-ene-1,4-dione 89e. Dry $AlCl_3$ (7.4 g; 55.2 mmol) was mechanically suspended in dry chlorobenzene (5.6 mL; 55.2 mmol) and DCE (20 mL). The mixture was cooled to 5 °C and fumaryl chloride (1.5 mL; 13.5 mmol) was added dropwise. The mixture was allowed to warm to room temperature, stirred for 1 h and heated to 40 °C. The mixture was poured into ice. The product was extracted with DCM, washed with $NaHCO_3$ solution, dried with Na_2SO_4, concentrated and recrystallized from acetone/$CHCl_3$. The obtained rose solid was boiled in $CHCl_3$ with charcoal and filtered through Celite to remove minor colored impurities. Isolated yield 1.3 g; 34%. Pale yellow crystalline solid. Mp 172-174 °C. ^{1}H NMR (400 MHz, $CDCl_3$) δ 8.02 – 7.98 (m, 4H), 7.97 (s, 2H), 7.55 – 7.44 (m, 4H).^{13}C NMR δ (101 MHz, $CDCl_3$) δ 188.5, 140.7, 135.2, 135.0, 130.4, 129.5. IR (KBr) *v*: 1652, 1586, 1400, 1321, 1290, 1197, 1090, 1008, 842, 754 cm^{-1}. MS (70 eV) *m/z*: 304 [M$^+$], 269, 241, 207, 139, 111, 75. HRMS (ESI-QTOF): calculated for $C_{16}H_{10}Cl_2O_2$ $[M + H]^+$ 305.0131, found 305.0131.

(*E*)-1,4-Bis(4-bromophenyl)but-2-ene-1,4-dione 89f. Dry $AlCl_3$ (3.7 g; 27.7 mmol) was mechanically suspended in dry bromobenzene (3.3 mL; 31.4 mmol) and DCE (15 mL). The mixture was cooled to 5 °C and fumaryl chloride (1.5 mL; 13.5 mmol) was added dropwise. The mixture was allowed to warm to rt, stirred overnight and heated to 40 °C. After 5 h the mixture was poured into ice. The product was extracted with DCM, washed with $NaHCO_3$ solution, dried with Na_2SO_4, concentrated and recrystallized from acetone/$CHCl_3$. The obtained reddish solid was boiled in $CHCl_3$ with charcoal and filtered through Celite to remove minor colored impurities. Isolated yield 2.5 g; 46%. Orange crystalline solid. Mp 185-187 °C. ^{1}H NMR (400 MHz, $CDCl_3$) δ 7.97 (s, 2H), 7.95 – 7.90 (m, 4H), 7.70 – 7.64 (m, 4H). ^{13}C NMR (101 MHz, $CDCl_3$) δ 188.7, 135.6, 135.0, 132.5, 130.5, 129.6. IR (KBr) *v*: 1650, 1586, 1322, 1201, 1072, 1008, 845, 753 cm^{-1}. MS (70 eV) *m/z*: 394, 392 [M^+], 315, 313, 287, 285, 211, 209, 185, 183, 157, 155, 102, 76, 74. HRMS (ESI-QTOF): calculated for $C_{16}H_{10}Br_2O_2$ $[M + H]^+$ 392.9120, found 392.9105.

(*E*)-1,4-Bis(4-nitrophenyl)but-2-ene-1,4-dione 89g. 1-(4-nitrophenyl)-2-(triphenyl-λ^5-phosphanylidene)ethan-1-one (970 mg; 2.3 mmol) was dissolved in dry DCM (10 mL) and 2-(4-nitrophenyl)-2-oxoacetaldehyde[112] DCM solution (410 mg; 2.3 mmol/8 mL) was added dropwise. During the addition a yellow solid started to precipitate. The mixture was left to stir overnight at room temperature. The precipitated product was filtered and washed with cold DCM. Isolated yield 520 mg; 69%. Bright yellow crystalline solid. Mp 210-212 °C. ^{1}H NMR (400 MHz, DMSO-d_6) δ 8.41 – 8.37 (m, 4H), 8.34 – 8.29 (m, 4H), 7.94 (s, 2H).^{13}C NMR (101 MHz, DMSO-d_6) δ 189.3, 150.3, 140.9, 135.8, 130.4, 124.1. IR (KBr) *v*: 1659, 1601, 1521, 1345, 1314, 1199, 1032, 858, 721 cm^{-1}. MS (70 eV) *m/z*: 326 [M^+], 309, 298, 204, 176, 150, 120, 104, 92, 76. HRMS (ESI-QTOF): calculated for $C_{16}H_{10}N_2O_6$ $[M + Na]^+$ 349.0431, found 349.0435.

*Characterization of non-symmetric unsaturated 1,4-diketones **90a-i***

In the typical experiment, the correspoding ylide (2.5 mmol; 1 equiv) was dissolved in DCM (25 mL; 0.1 M), followed by the addition of 58% MnO_2 (2.2 g; 10 equiv) and hydroxyacetone (520 μL; 7.5 mmol; 3 equiv). The reaction mixture was left to stir for 24 h at room temperature, filtered through Celite, concentrated under reduced pressure and purified by column chromatography on silica gel using heptane/EtOAc mixtures as eluent.

(*E*)-1-Phenylpent-2-ene-2,4-dione 90a. Purified by column chromatography on silica gel, eluent Hept/EtOAc 8:1. Isolated yield 383 mg; 88%. Bright yellow crystalline solid. Mp 44-46 °C. ^{1}H NMR (400 MHz, $CDCl_3$) δ 8.01 – 7.95 (m, 2H), 7.69 (d, *J* = 15.8 Hz, 1H), 7.65 – 7.59 (m, 1H), 7.54 – 7.47 (m, 2H), 7.08 (d, *J* = 15.8 Hz, 1H), 2.43 (s, 3H). ^{13}C NMR (101 MHz, $CDCl_3$) δ 198.0, 190.4, 138.5, 136.8, 134.1, 134.0, 129.0, 128.9, 29.1. IR (KBr) *v*: 1664, 1614, 1594,

1578, 1451, 1271, 1252, 976, 772, 697 cm^{-1}. MS (70 eV) *m/z*: 174 [M^+], 159, 131, 105, 77, 51, 43. HRMS (ESI-QTOF): calculated for $C_{11}H_{10}O_2$ [M + H]$^+$ 175.0754, found 175.0754.

(*E*)-1-(Naphthalen-2-yl)pent-2-ene-2,4-dione 90b. Purified by column chromatography on silica gel, eluent Hept/EtOAc 6:1. Isolated yield 476 mg; 85%. Bright yellow crystalline solid. Mp 84-85 °C. ^{1}H NMR (400 MHz, $CDCl_3$) δ 8.49 (s, 1H), 8.04 (dd, *J* = 8.6, 1.5 Hz, 1H), 7.97 (d, *J* = 8.0 Hz, 1H), 7.92 (d, *J* = 8.7 Hz, 1H), 7.90 – 7.80 (m, 2H), 7.66 – 7.60 (m, 1H), 7.60 – 7.52 (m, 1H), 7.15 (d, *J* = 15.6 Hz, 1H), 2.46 (s, 3H). ^{13}C NMR (101 MHz, $CDCl_3$) δ 198.0, 190.0, 138.3, 136.0, 134.2, 134.0, 132.5, 131.1, 129.8, 129.2, 129.1, 128.0, 127.2, 124.1, 29.3. IR (KBr) *v*: 1702, 1654, 1626, 1596, 1575, 1469, 1359, 1303, 1124, 1012, 828, 760 cm^{-1}. MS (70 eV) *m/z*: 224 [M^+], 181, 155, 127, 77, 63, 43. HRMS (ESI-QTOF): calculated for $C_{15}H_{12}O_2$ [M + H]$^+$ 225.0910, found 225.0908.

(*E*)-1-(4-Methoxyphenyl)pent-2-ene-2,4-dione 90c. Purified by column chromatography on silica gel, eluent Hept/EtOAc 6:1. Isolated yield 382 mg; 75%. Bright yellow crystalline solid, turned reddish. Mp 60-62 °C. ^{1}H NMR (400 MHz, $CDCl_3$) δ 8.02 – 7.95 (m, 2H), 7.70 (d, *J* = 15.7 Hz, 1H), 7.07 (d, *J* = 15.7 Hz, 1H), 7.00 – 6.94 (m, 2H), 3.89 (s, 3H), 2.42 (s, 3H).^{13}C NMR (101 MHz, $CDCl_3$) δ 198.1, 188.5, 164.4, 137.8, 134.2, 131.4, 129.9, 114.3, 55.7, 29.2. IR (KBr) *v*: 1698, 1649, 1590, 1512, 1341, 1295, 1261, 1171, 1018, 980, 829, 676, 589 cm^{-1}. MS (70 eV) *m/z*: 204 [M^+], 189, 161, 135, 107, 92, 77, 43. HRMS (ESI-QTOF): calculated for $C_{12}H_{12}O_3$ [M + H]$^+$ 205.0859, found 205.0860.

(*E*)-1-(4-Chlorophenyl)pent-2-ene-2,4-dione 90d. Purified by column chromatography on silica gel, eluent Hept/EtOAc 6:1. Isolated yield 484 mg; 93%. Bright yellow crystalline solid. Mp 70-71 °C. ^{1}H NMR (400 MHz, $CDCl_3$) δ 7.96 – 7.90 (m, 2H), 7.65 (d, *J* = 15.7 Hz, 1H), 7.51 – 7.46 (m, 2H), 7.09 (d, *J* = 15.7 Hz, 1H), 2.43 (s, 3H).^{13}C NMR (101 MHz, $CDCl_3$) δ 197.8, 189.1, 140.7, 138.8, 135.1, 133.4, 130.3, 129.4, 29.3. IR (KBr) *v*: 1696, 1654, 1591, 1490, 1354, 1308, 1295, 1092, 826, 727, 529 cm^{-1}. MS (70 eV) *m/z*: 208 [M^+], 193, 165, 139, 111, 92, 75, 43. HRMS (ESI-QTOF): calculated for $C_{11}H_9ClO_2$ [M + H]$^+$ 209.0364, found 209.0365.

(*E*)-1-(4-Bromophenyl)pent-2-ene-2,4-dione 90e. Purified by column chromatography on silica gel, eluent Hept/EtOAc 6:1. Isolated yield 428 mg; 68%. Bright yellow needles. Mp 74-75 °C. ^{1}H NMR (400 MHz, $CDCl_3$) δ 7.87 – 7.81 (m, 2H), 7.68 – 7.63 (m, 2H), 7.63 (d, *J* = 15.7 Hz, 1H), 7.09 (d, *J* = 15.7 Hz, 1H), 2.42 (s, 3H). ^{13}C NMR (101 MHz, $CDCl_3$) δ 197.7, 189.3, 138.8, 135.5, 133.4, 132.4, 130.4, 129.4, 29.3. IR (KBr) *v*: 1699, 1653, 1584, 1487, 1397, 1294, 1069, 1019, 843, 725, 598 cm^{-1}. MS (70 eV) *m/z*: 254, 252 [M^+], 239, 237,

211, 209, 185, 183, 157, 155, 131, 102, 76, 74, 92, 43. HRMS (ESI-QTOF): calculated for $C_{11}H_9BrO_2$ $[M + H]^+$ 252.9859, found 252.9861.

(*E*)-1-(4-Nitrophenyl)pent-2-ene-2,4-dione 90f. Purified by column chromatography on silica gel, eluent Hept/EtOAc 5:1. Isolated yield 427 mg; 78%. Bright yellow needles. Mp 103-103 °C. ^{1}H NMR (400 MHz, $CDCl_3$) δ 8.40 – 8.33 (m, 2H), 8.17 – 8.10 (m, 2H), 7.66 (d, *J* = 15.7 Hz, 1H), 7.14 (d, *J* = 15.7 Hz, 1H), 2.45 (s, 3H). ^{13}C NMR (101 MHz, $CDCl_3$) δ 197.4, 189.0, 150.8, 141.3, 139.7, 132.7, 129.9, 124.2, 29.5. IR (KBr) *v*: 1697, 1656, 1600, 1514, 1350, 1308, 1022, 853, 701, 598 cm^{-1}. MS (70 eV) *m/z*: 219 [M^+], 204, 177, 150, 130, 104, 76, 43. HRMS (ESI-QTOF): calculated for $C_{11}H_9NO_4$ $[M + H]^+$ 220.0604, found 220.0605.

(*E*)-1-(Thiophen-2-yl)pent-2-ene-2,4-dione 90g. Purified by column chromatography on silica gel, eluent Hept/EtOAc 5:1. Isolated yield 338 mg; 75%. Yellow crystalline solid. Decomposes at >94 °C. ^{1}H NMR (400 MHz, $CDCl_3$) δ 7.85 (dd, *J* = 3.8, 0.9 Hz, 1H), 7.76 (dd, *J* = 4.9, 0.9 Hz, 1H), 7.57 (d, *J* = 15.6 Hz, 1H), 7.20 (dd, *J* = 4.9, 3.9 Hz, 1H), 7.15 (d, *J* = 15.6 Hz, 1H), 2.42 (s, 3H). ^{13}C NMR (101 MHz, $CDCl_3$) δ 197.8, 181.8, 144.5, 137.8, 135.8, 133.6, 133.5, 128.7, 29.4. IR (KBr) *v*: 1668, 1647, 1604, 1511, 1411, 1359, 1308, 1273, 1250, 974, 753, 550 cm^{-1}. MS (70 eV) *m/z*: 180 [M^+], 165, 137, 111, 83, 57, 43. HRMS (ESI-QTOF): calculated for $C_9H_8O_2S$ $[M + H]^+$ 181.0318, found 181.0317.

(*E*)-1-(Furan-2-yl)pent-2-ene-2,4-dione 90h. Purified by column chromatography on silica gel, eluent Hept/EtOAc 3:1. Isolated yield 308 mg; 75%. Pale yellow crystalline solid. Decomposes at >82 °C. ^{1}H NMR (400 MHz, $CDCl_3$) δ 7.69 (dd, *J* = 1.6, 0.6 Hz, 1H), 7.56 (d, *J* = 15.8 Hz, 1H), 7.37 (dd, *J* = 3.6, 0.6 Hz, 1H), 7.17 (d, *J* = 15.8 Hz, 1H), 6.62 (dd, *J* = 3.6, 1.7 Hz, 1H), 2.42 (s, 3H). ^{13}C NMR (101 MHz, $CDCl_3$) δ 197.9, 177.3, 153.1, 147.9, 138.0, 133.1, 119.6, 113.1, 29.2. IR (KBr) *v*: 1656, 1611, 1556, 1467, 1397, 1258, 1007, 978, 793, 593 cm^{-1}. MS (70 eV) *m/z*: 164 [M^+], 149, 121, 95, 65, 43. HRMS (ESI-QTOF): calculated for $C_9H_8O_3$ $[M + H]^+$ 165.0546, found 165.0542.

(*E*)-1-(1*H*-Pyrrol-2-yl)pent-2-ene-2,4-dione 90i. As the corresponding ylide[113] is pourly soluble in DCM, increasing the reaction time may improve the yield. Purified by column chromatography on silica gel, eluent Hept/EtOAc 3:1 to 2:1. Isolated yield 269 mg; 66%. Yellow crystalline solid. Decomposes at >105 °C. ^{1}H NMR (400 MHz, $CDCl_3$) δ 9.99 (bs, 1H), 7.52 (d, *J* = 15.7 Hz, 1H), 7.19 (s, 1H), 7.15 (d, *J* = 15.7 Hz, 1H), 7.11 (s, 1H), 6.42 – 6.33 (m, 1H), 2.42 (s, 3H). ^{13}C NMR (101 MHz, $CDCl_3$) δ 198.2, 177.8, 136.8, 134.2, 132.9, 127.4, 118.7, 111.8, 29.2. IR (KBr) *v*: 3271, 1670, 1642, 1592, 1543, 1405, 1253, 1145, 991, 765, 603, 567, 520 cm^{-1}. MS (70 eV) *m/z*: 163 [M^+], 148, 120, 94, 66, 43. HRMS (ESI-QTOF): calculated for $C_9H_9NO_2$ $[M + H]^+$ 164.0706, found 164.0706.

The reactions with β-ketoesters **96** were carried out under the same conditions as for the malonates **94** (see SE in Publication **I**) with 5.6 equiv. of the ketoester. The products **97** obtained with the optimal catalyst are described.

Ethyl 2-acetyl-3-benzoyl-5-oxo-5-phenylpentanoate 97a. Catalyst **29** was used. Isolated by column chromatography (Hept/EtOAc 6:1). Yield 94%. Colorless solid. *ee* = 81/78 (Chiralcel AD-H colomn, 1 ml/min, Hex:*i*PrOH 8:2, 254 nm), dr 57:43. First diastereoisomer: Major enantiomer t_r= 16.12 min, minor enantiomer t_r = 18.22 min. Second diastereoisomer: Major enantiomer t_r = 28.13 min, minor enantiomer t_r = 23.46 min. IR (KBr) ν = 2983, 1738, 1716, 1682, 1251, 1158, 1028, 754, 690 cm^{-1}. MS *m/z* 366 $(M)^+$, 348, 303, 261, 236, 171, 105, 77. HRMS (ESI-QTOF): calculated for $C_{22}H_{22}O_5$ $[M + Na]^+$ 389.1359, found 389.1361. ^{1}H NMR (400 MHz, $CDCl_3$) δ 8.06 – 7.98 (m, 3.5H, d.1+d.2), 7.90 – 7.84 (m, 3.5H, d.1+d.2), 7.59 – 7.51 (m, 3.5H, d.1+d.2), 7.50 – 7.37 (m, 7H, d.1+d.2), 4.91 (dt, *J* = 8.7, 5.9 Hz, 1H, d.1), 4.86 (dt, *J* = 8.6, 6.0 Hz, 0.75 H, d.2), 4.22 – 4.00 (m, 5.3H, d.1+d.2), 3.54 (dd, *J* = 7.6, 5.9 Hz, 0.75 H, d.2), 3.49 (dd, *J* = 7.7, 5.9 Hz, 1H, d.1), 3.34 (t, *J* = 6.0 Hz, 1H, d.1), 3.30 (t, *J* = 6.1 Hz, 0.75H, d.2), 2.31 (s, 2.3H, d.2), 2.28 (s, 3H, d.1), 1.19 (t, *J* = 7.1 Hz, 3H, d.1), 1.13 (t, *J* = 7.1 Hz, 2.3H, d.2). ^{13}C NMR (101 MHz, $CDCl_3$) δ 202.61 (d.2), 201.5 (d.1), 201.0 (d.1), 200.9 (d.2), 197.2 (d.2), 196.7 (d.1), 168.7 (d.1), 168.6 (d.2), 136.32 (d.1), 136.28 (d.2), 136.0 (d.2), 135.8 (d.1), 133.6 (d.2), 133.5 (d.1), 133.46 (d.2), 133.42 (d.1), 128.90-128.75 6C (d1.+d.2), 128.27 (d.2), 128.22 (d.1), 62.1 (d.1), 62.0 (d.2), 60.4 (d.2), 60.3 (d.1), 41.0 (d.1), 40.6 (d.2), 39.1 (d.2), 38.8 (d.1), 30.1 (d.2), 29.9 (d.1), 14.0 (d.1), 13.9 (d.2).

Ethyl 2,3-dibenzoyl-5-oxo-5-phenylpentanoate 97b. Catalyst **29** was used. Isolated by column chromatography (Hept/EtOAc 5:1 to 3:1).Yield 95%. Colorless solid. *ee* = 90/88 (Chiralcel AD-H colomn, 1 mL/min, Hex:*i*PrOH 9:1, 254 nm), dr 62/38. First diastereoisomer: major enantiomer t_r = 39.89 min, minor enantiomer t_r= 90.70 min. Second diastereoisomer: major enantiomer t_r = 70.01 min, minor enantiomer t_r = 80.90 min. IR (KBr) ν = 2982, 1733, 1682, 1597, 1448, 1284, 1227, 1002, 753, 706, 689 cm^{-1}. MS *m/z* 410 $[M\text{-}H_2O]^+$, 337, 323, 306, 277, 236, 105, 77. HRMS (ESI-QTOF): calculated for $C_{27}H_{24}O_5$ $[M + Na]^+$ 451.1516, found 451.1531. ^{1}H NMR (400 MHz, $CDCl_3$) δ 8.13 – 8.08 (m, 1.2H, d.2), 8.07 – 8.03 (m, 2H, d.1), 8.03 – 7.98 (m, 1.2H, d.2), 7.98 – 7.93 (m, 2H, d.1), 7.93 – 7.87 (m, 2H, d.1), 7.84 – 7.78 (m, 1.2H, d.2), 7.62 – 7.40 (m, 13.3H, d.1+d.2), 7.40 – 7.33 (m, 1.2H, d.2), 5.22 – 5.12 (m, 1H, d.1), 5.04 (ddd, *J* = 8.6, 7.7, 5.0 Hz, 0.6H, d.2), 4.93 (d, *J* = 9.4 Hz, 1H, d.1), 4.92 (d, *J* = 8.8 Hz, 0.6H, d.2), 4.10 – 3.93 (m, 2H, d.1), 3.86 (qd, *J* = 7.1, 1.9 Hz, 1.2H, d.2), 3.66 (dd, *J* = 18.1, 6.3 Hz, 1H, d.1), 3.54 (dd, *J* = 17.7, 5.0 Hz, 0.6H, d.2), 3.46 (dd, *J* = 17.7, 7.7 Hz, 0.6H, d.2), 3.35 (dd, *J* = 18.1, 5.3 Hz, 1H, d.1), 1.05 (t, *J* = 7.1 Hz, 3H, d.1), 0.95 (t, *J* = 7.1 Hz, 1.8H, d.2). ^{13}C NMR (101 MHz, $CDCl_3$) δ 201.6 (d.2), 200.9 (d.1), 197.4 (d.2), 196.5 (d.1), 194.1 (d.2), 193.6 (d.1), 169.0 (d.1), 168.3

(d.2), 136.6 (d.2), 136.5 (d.2), 136.4 (d.1), 136.2 (d.2), 136.1 (d.1), 135.7 (d.1), 134.0 (d.2), 133.7 (d.1), 133.5 (d.1), 133.4 (d.1+d.2), 133.3 (d.2), 129.0 (d.2), 128.96 (d.1), 128.94 (d.2), 128.90 (d.2), 128.82 (d.1), 128.79 (d.1), 128.75 (d.1), 128.69 (d.2), 128.62 (d.2), 128.61 (d.1), 128.2 (d.1+d.2), 62.1 (d.1), 62.0 (d.2), 56.2 (d.1), 55.2 (d.2), 41.3 (d.2), 41.0 (d.1), 39.9 (d.2), 39.1 (d.1), 13.8 (d.1), 13.7 (d.2).

Ethyl 2-acetyl-3-benzoyl-2-fluoro-5-oxo-5-phenylpentanoate 97c. Catalyst **33** was used. Isolated by column chromatography (Hept/EtOAc 10:1 to 8:1).Yield 74%. Yellow solid. *ee* = 80/63 (Chiralcel AD-H colomn, 1 mL/min, Hex:EtOH 95:5, 254 nm), dr 66/34. First diastereoisomer: Major enantiomer t_r = 28.61 min, minor enantiomer t_r = 26.69 min. Second diastereoisomer: Major enantiomer t_r = 31.56 min, minor enantiomer t_r = 33.73 min. IR (KBr) ν = 2984, 1755, 1737, 1683, 1597, 1449, 1357, 1231, 1002, 748, 690 cm^{-1}. MS *m/z* 341, 276, 237, 189, 105, 77. HRMS (ESI-QTOF): calculated for $C_{22}H_{21}FO_5$ $[M + H]^+$ 385.1446, found 385.1450. ^1H NMR (400 MHz, $CDCl_3$) δ 8.07 – 8.01 (m, 1.1H, d.2), 7.99 – 7.89 (m, 5.1H, d.1+d.2), 7.62 – 7.51 (m, 3.1H) (d.1+d.2), 7.52– 7.37 (m, 6.2H) (d.1+d.2), 5.33 (ddd, J_{H-F} = 23.5 Hz, J_{H-H}= 6.4, 4.9 Hz, 1H, d.1), 5.20 (ddd, J_{H-F}= 19.4 Hz, J_{H-H} = 7.4, 4.9 Hz, 0.6 H) (d.2), 4.23 (qd, J_{H-H} = 7.1 Hz, J_{H-F} = 2.5 Hz, 2H, d.1), 4.02 (dq, J_{H-F} = 10.8, J_{H-H} = 7.1 Hz, 0.6H, d.2), 3.90 (dq, J_{H-F} = 10.8 Hz, J_{H-H} = 7.2 Hz, 0.6H, d.2), 3.79 (dd, J = 18.8, 6.4 Hz, 1H, d.1), 3.72 (dd, J = 18.5, 4.9 Hz, 0.6H, d.2), 3.57 (ddd, J_{H-H} = 18.5, 7.4 Hz, J_{H-F} = 0.9 Hz, 0.6H, d.2), 3.36 (ddd, J_{H-H} = 18.7, 4.9 Hz, J_{H-F} = 0.5 Hz, 1H, d.1), 2.36 (d, J_{H-F} = 5.2 Hz, 1.5H, d.2), 2.36 (d, J_{H-F} = 5.1 Hz, 3H, d.1), 1.29 (t, J = 7.1 Hz, 3H, d.1), 1.10 (t, J = 7.2 Hz, 1.5H, d.2).^{13}C NMR (101 MHz, $CDCl_3$) δ 201.8 (d, J_{C-F} = 29.0 Hz, d.1), 201.68 (d, J_{C-F} = 28.7 Hz, d.2), 198.4 (d.2), 198.3 (d.1), 196.6 (d.2), 195.9 (d.1), 165.4 (d, J_{C-F} = 25.7 Hz, d.1), 165.2 (d, J_{C-F} = 25.4 Hz, d.2), 136.4 (d.2), 135.9 (d.1+d.2), 135.5 (d.1), 133.8 (d.1), 133.77 (d.1), 133.76 (d.2) 133.67 (d.2), 129.1 (d.2), 128.94 (d.1), 128,93 (d.1) 128,85 (d.1), 128.81 (d.2), 128.80 (d.2), 128.4 (d.2), 128.3 (d.1), 99.0 (d, J_{C-F} = 207.0 Hz, d.1), 98.5 (d, J_{C-F} = 204.5 Hz, d.2), 63.3 (d.1), 63.1 (d.2), 46.4 (d, J_{C-F} = 19.1 Hz, d.1), 45.9 (d, J_{C-F} = 20.7 Hz, d.2), 37.3 (d, J_{C-F} = 5.4 Hz, d.2), 36.5 (d, J_{C-F} = 5.2 Hz, d.1), 26.48 (d.2), 26.33 (d.1), 13.99 (d.1), 13.72 (d.2).

Ethyl 2-acetyl-3-benzoyl-2-methyl-5-oxo-5-phenylpentanoate 97d. Catalyst **33** was used. Isolated by column chromatography (Hept/EtOAc 75:10), diastereomers separated.Yield 69%. Colorless viscous oil. *ee* = 59/39 (Chiralcel OJ-H colomn, 1 mL/min, Hex:*i*PrOH 8:2, 254 nm), dr 1:1. First diastereoisomer: major enantiomer t_r = 42.69 min, minor enantiomer t_r = 18.96 min. Second diastereoisomer: major enantiomer t_r = 86.61, minor enantiomer t_r = 28.79. First diastereomer $[\alpha]_D^{25}$ = +39.1 (*c* 0.25; MeOH). Second diastereomer $[\alpha]_D^{25}$ = +54.3 (*c* 0.25; MeOH). IR (KBr) ν = 2984, 1713, 1681, 1448, 1226, 1111, 1002, 747, 689 cm^{-1}. MS *m/z* 320, 247, 185, 105, 77. HRMS (ESI-QTOF): calculated for $C_{23}H_{24}O_5$ $[M – H_2O + H]^+$ 363.1591, found 363.1602.

First diastereomer: ^{1}H NMR (400 MHz, $CDCl_3$) δ 8.11 – 8.07 (m, 2H), 7.93 – 7.89 (m, 2H), 7.58 – 7.50 (m, 2H), 7.50 – 7.39 (m, 4H), 4.92 (dd, *J* = 7.8, 4.5 Hz, 1H), 4.28 (qd, *J* = 7.1, 2.4 Hz, 2H), 3.66 – 3.51 (m, 2H), 2.16 (s, 3H), 1.41 (s, 3H), 1.33 (t, *J* = 7.1 Hz, 3H). ^{13}C NMR (101 MHz, $CDCl_3$) δ 204.8, 201.8, 197.8, 171.5, 137.9, 136.3, 133.3, 133.0, 128.9, 128.6, 128.6, 128.1, 61.9, 61.5, 44.5, 39.3, 27.0, 19.3, 14.1.
Second diastereomer: ^{1}H NMR (400 MHz, $CDCl_3$) δ 8.09 – 8.03 (m, 2H), 7.94 – 7.88 (m, 2H), 7.57 – 7.50 (m, 2H), 7.48 – 7.40 (m, 4H), 4.98 (dd, *J* = 8.8, 3.7 Hz, 1H), 3.73 (dq, *J* = 10.8, 7.1 Hz, 1H), 3.62 – 3.38 (m, 3H), 2.20 (s, 3H), 1.55 (s, 3H), 1.02 (t, *J* = 7.2 Hz, 3H). ^{13}C NMR (101 MHz, $CDCl_3$) δ 204.0, 201.8, 197.9, 171.2, 137.8, 136.4, 133.5, 133.0, 129.1, 128.7, 128.5, 128.3, 61.8, 60.7, 43.3, 38.6, 26.7, 16.2, 13.7.

Ethyl (2*R*,4*R*)-2-benzoyl-4-hydroxy-6-oxo-4-phenylcyclohexane-1-carboxylate 98. (Catalyst **33** was used). Isolated by column chromatography (Hept/EtOAc 55:10). The compound was obtained in 59% yield during the synthesis of **97a**. IR (KBr) *v* = 3432, 2963, 1740, 1719, 1681, 1448, 1261, 758, 704 cm^{-1}. MS *m/z* 171, 153, 128, 115, 105, 77, 51. HRMS (ESI-QTOF): calculated for $C_{22}H_{22}O_5$ $[M + Na]^+$ 389.1359, found 389.1364. ^{1}H NMR (400 MHz, $CDCl_3$) δ 8.06 – 8.00 (m, 2H), 7.60 – 7.53 (m, 1H), 7.50 – 7.41 (m, 4H), 7.39 – 7.32 (m, 2H), 7.31 – 7.26 (m, 1H), 4.82 (td, *J* = 12.7, 3.7 Hz, 1H), 4.26 – 4.08 (m, 3H), 3.10 (d, *J* = 13.7 Hz, 1H), 2.72 (dd, *J* = 13.9, 2.5 Hz, 1H), 2.36 (dt, *J* = 14.0, 3.5 Hz, 1H), 2.15 (t, *J* = 13.4 Hz, 1H), 1.22 (t, *J* = 7.1 Hz, 3H). ^{13}C NMR (101 MHz, $CDCl_3$) δ 204.3, 200.4, 169.1, 145.4, 135.2, 133.8, 129.0, 128.88 (2C), 128.85, 128.1, 124.3, 61.6, 58.1, 54.1, 44.4, 41.5, 14.2.

Methyl (*E*)-5-(3-hydroxy-2-oxoindolin-3-yl)-4-oxopent-2-enoate 101.
Isatin (14.7 mg; 0.1 mmol), thiourea **92** (11.3 mg; 20 mol %), and ketoester **91a** (38 mg; 0.3 mmol) were suspended in dry toluene (300 μL) and left to stir for 24 h. The orange heterogenous mixture became colorless. The product was suspended in DCM and isolated by column chromatography (Hept/EtOAc 4:3) yielding a white amorphous solid. Yield 27 mg, >95%. *ee* = 91% (Chiralpak AD-H column, Hex/*i*PrOH 8:2, 1 mL/min, 254 nm), major enantiomer t_r = 27.06 min, minor enantiomer t_r = 16.69 min. $[\alpha]_D^{25}$ = +45.0 (*c* 0,125; $CHCl_3$). IR (KBr) *v* = 3348, 2959, 2930, 1725, 1668, 1620, 1472, 1313, 1268, 1175, 1001, 791, 719 cm^{-1}. MS *m/z* 167, 149, 113, 84, 71, 57. ^{1}H NMR (400 MHz, DMSO-d_6) δ 10.28 (s, 1H), 7.24 (d, *J* = 7.3 Hz, 1H), 7.17 (td, *J* = 7.7, 1.2 Hz, 1H), 6.95 (d, *J* = 16.0 Hz, 1H), 6.90 (td, *J* = 7.6, 0.8 Hz, 1H), 6.78 (d, *J* = 7.7 Hz, 1H), 6.61 (d, *J* = 16.0 Hz, 1H), 6.12 (s, 1H), 3.73 (s, 3H), 3.58 (d, *J* = 16.6 Hz, 1H), 3.21 (d, *J* = 16.6 Hz, 1H). ^{13}C NMR (101 MHz, DMSO-d_6) δ 196.6, 177.9, 165.5, 142.4, 139.5, 131.2, 129.9, 129.2, 123.9, 121.3, 109.5, 73.0, 52.2, 48.4.

Preparation, spectral data or references concerning the compounds discussed in the thesis but not presented in Experimental part can be found in the corresponding publications.

Entry	Compound number in thesis	Compound number in publication		
		I	**II**	**III**
Catalysts				
1	**4**		**II**	**IV**
2	**27**		**III**	**VI**
3	**29**	**IX**		
4	**33**	**VII**	**IV**	**I**
5	**50**			**III**
6	**92**	**VI**		**II**
7	**93**	**VIII**		
8	**105**		**I**	**V**
Malonates				
9	**94b**	**2b**		
10	**94c**	**2c**		
11	**94d**	**2d**		
12	**94f**	**2e**		
13	**94g**	**2f**		
Malonate/1,4-diketone Michael products				
14	**95aa**	**3a**		
15	**95ab**	**3b**		
16	**95ac**	**3c**		
17	**95ad**	**3d**		
18	**95af**	**3e**		
19	**95ag**	**3f**		
20	**95ba**	**3g**		
21	**95ca**	**3h**		
22	**95da**	**3i**		
23	**95ea**	**3j**		
Unsaturated 1,4-ketoesters				
24	**91a**		**3a**	
25	**91b**		**3b**	
26	**91c**		**3c**	
27	**91d**		**3d**	
28	**91e**		**3e**	
29	**91f**		**3f**	
30	**91g**		**3g**	
Isatin Schiff bases (imines)				
31	**103a**		**2a**	
32	**103b**		**2b**	
33	**103c**		**2c**	

34	**103d**		**2d**	
35	**103e**		**2e**	
36	**103f**		**2f**	
37	**103g**		**2g**	
38	**103h**		**2h**	
39	**103i**		**2i**	
Aza-Michael products (imines/unsaturated 1,4-ketoesters)				
40	**106aa**		**4aa**	
41	**107aa**		**5aa**	
42	**107ab**		**5ab**	
43	**107ac**		**5ac**	
44	**107ad**		**5ad**	
45	**107ae**		**5ae**	
46	**107af**		**5af**	
47	**107ag**		**5ag**	
48	**107bb**		**5bb**	
49	**107cb**		**5cb**	
50	**107db**		**5db**	
51	**107eb**		**5eb**	
Aza-Michael products (imines/non-symmetric unsaturated 1,4-diketones)				
52	**108a**			**7a**
53	**108b**			**7b**
54	**108c**			**7c**
55	**108d**			**7d**
56	**108e**			**7e**
57	**108f**			**7f**
58	**108g**			**7g**
59	**108h**			**7h**
60	**108i**			**7i**
Aza-Michael products (imines/symmetric unsaturated 1,4-diketones)				
61	**110a**			**9a**
62	**110b**			**9b**
63	**110c**			**9c**
64	**110d**			**9d**
65	**110e**			**9e**
66	**110f**			**9f**
67	**110g**			**9g**
Aza-Michael products (imines/miscellaneous electrophiles)				
68	**111**			**10**
69	**112**			**11**
70	**113**			**12**
71	**114**			**13**
72	**115**			**14**
73	**116**			**15**

List of References

[1] (a) *Hydrogen Bonding in Organic Synthesis;* Pihko, P. M., Ed.; Wiley-VCH Verlag GmbH & Co. KGaA, Weinheim, Germany, **2009**. (b) Marqués-López, E; Herrera, R. P. *Organocatalysis* in *Total Synthesis*, in *Comprehensive Enantioselective Organocatalysis: Catalysts, Reactions, and Applications*; Dalko, P. I., Ed.; Wiley-VCH Verlag GmbH & Co. KGaA, Weinheim, Germany, **2013**.
[2] Machajewski, T. D.; Wong, C.-H. *Angew. Chem. Int. Ed.* **2000**, *39*, 1352.
[3] Etter, M. C.; Panunto, T. W. *J. Am. Chem. Soc.* **1988**, *110*, 5896.
[4] Curran, D. P.; Kuo, L. H. *J. Org. Chem.* **1994**, *59*, 3259.
[5] Curran, D. P.; Kuo, L. H. *Tetrahedron Lett.* **1995**, *36*, 6647.
[6] Schreiner, P. M.; Wittkopp, A. *Org. Lett.* **2002**, *4*, 217.
[7] Okino, T.; Hoashi, Y.; Takemoto, Y. *J. Am. Chem. Soc.* **2003**, *125*, 12672.
[8] As stated in [10d] the first reference concerning the isolation is: Pelletier, J.; Caventon, J. B. *Ann. Chim. Phys.* **1820**, *14*, 69.
[9] Verpoorte, R.; Schripsema, J.; Van der Leer, T. In The *Alkaloids. Chemistry and Pharmacology*, Vol. 34; Brossi, A., Ed.; Academic Press: New York, **1988**.
[10] Reviews on using *Cinchona* alkaloids as catalysts starting from the oldest one: (a) Pracejus, H. *Fortschr. Chem. Forsch.* **1967**, *8*, 493. (b) Morrison, J. D.; Mosher, H. S. *Asymmetric Organic Reactions*. Prentice-Hall, Englewood Clifts, N.J, **1971**. (c) Wynberg, H. *Top. Stereochem.* **1986**, *16*, 87. (d) Kacprzak, K.; Gawroński, J. *Synthesis* **2001**, *7*, 961. (e) Marcelli, T.; Hiemstra, H. *Synthesis* **2010**, *8*, 1229.
[11] Song, C. E. *An Overview of Cinchona Alkaloids in Chemistry*, in *Cinchona Alkaloids in Synthesis and Catalysis: Ligands, Immobilization and Organocatalysis*; Song, C. E., Ed. Wiley-VCH Verlag GmbH & Co. KGaA, Weinheim, Germany, **2009**. states that the first example is: Bredig, G.; Fiske, W. S. *Biochem. Z.* **1912**, 7.
[12] Toda, F.; Tanaka, K.; Stein, Z.; Goldberg, I. *J. Org. Chem.* **1994**, *59*, 5748.
[13] Kolb, H. C.; van Nieuwenhze, M. S.; Sharpless, K. B. *Chem. Rev.* **1994**, *94*, 2483.
[14] (a) Lämmerhofer, M.; Peters, E. C.; Yu, C.; Svec, F.; Fréchet, J. M. J.; Lindner, W. *Anal. Chem.* **2000**, *72*, 4614. (b) Lämmerhofer, M.; Svec, F.; Fréchet, J. M. J.; Lindner, W. *Anal. Chem.* **2000**, *72*, 4623.
[15] Salvadori, P.; Pini, D.; Rosini, C.; Bertucci, C.; Uccell-Barrett, G. *Chirality* **1992**, *4*, 43.
[16] (a) Kobayashi, N.; Iwai, K. Tetrahedron Lett. 1980, 21, 2167. (b) Alvarez, R.; Hourdin, M.-A.; Cavé, C.; d'Angelo, J.; Chaminade, P. *Tetrahedron Lett.* **1999**, *40*, 7091. (c) Salvadori, P.; Pini, D.; Petri, A. *J. Am. Chem. Soc.* **1997**, *119*, 6929.
[17] Ooi, T.; Maruoka, K. *Angew. Chem. Int. Ed.* **2007**, *46*, 4222.
[18] (a) Campos, C. H.; Torres, C.; Fierro, J. L. G.; Reyes, P. *Appl. Catal., A.* **2013**, *466*, 198. (b) Kacprzak, K. M.; Maier, N. M.; Lindner, W. *Tetrahedron Lett.* **2006**, *47*, 8721.
[19] Marcelli, T.; van Maarseveen, J. H.; Hiemstra, H. *Angew. Chem. Int. Ed.* **2006**, *45*, 7496.
[20] (a) Vakulya, B.; Varga, S.; Csámpai, A.; Soós, T. *Org. Lett.* **2005**, *7*, 1967 (thiourea). (b) Rana, N. K.; Selvakumar, S.; Singh, V. K. *J. Org. Chem.* **2010**, *75*, 2089 (urea).
[21] Malerich, J. P.; Hagihara, K.; Rawal, V. H. *J. Am. Chem. Soc.* **2008**, *130*, 14416.
[22] Han, X.; Zhong, F.; Lu, Y. *Adv. Synth. Catal.* **2010**, *352*, 2778.

[23] Shao, Q.; Chen, J.; Tu, M.; Piotrowski, D. W.; Huang, Y. *Chem. Commun.* **2013**, *49*, 11098.
[24] Oh, S. H.; Rho, H. S.; Lee, J. W.; Lee, J. E.; Youk, S. H.; Chin, J.; Song, C. E. *Angew. Chem. Int. Ed.* **2008**, *47*, 7872.
[25] For the research made by Takemoto's group see: Takemoto, Y. *Chem. Pharm. Bull.* **2010**, *58*, 593.
[26] For more information on Jacobsen's catalysts not shown in Figure 4 see: Doyle, A. G.; Jacobsen, E. N. *Chem. Rev.* **2007**, *107*, 5713.
[27] Sigman, M. S.; Jacobsen, E. N. *J. Am. Chem. Soc.* **1998**, *120*, 4901.
[28] Jacobsen has introduced the first chiral thiourea catalyst **26** in 1998 (with a Schiff base fragment), while Takemoto's thiourea catalyst **4** is the first one having a tertiary amine, thus both works can be considered pioneering.
[29] (a) Ye, J.; Dixon, D. J.; Hynes, P. S. *Chem. Commun.* **2005**, 4481. (b) McCooey, S. H.; Connon, S. J. *Angew. Chem. Int. Ed.* **2005**, *44*, 6367.
[30] Wang, J.; Li, H.; Yu, X.; Zu, L.; Wang, W. *Org. Lett.* **2005**, *7*, 4293.
[31] Marcelli, T.; van der Haas, R. N. S.; van Maarseveen, J. H.; Hiemstra, H. *Angew. Chem. Int. Ed.* **2006**, *45*, 929.
[32] Serdyuk, O. V.; Heckel, C. M.; Tsogoeva, S. *Org. Biomol. Chem.* **2013**, *11*, 7051.
[33] (a) Tsogoeva, S. B.; Wei, S. *Chem. Commun.* **2006**, 1451. (b) Yalalov, D.A.; Tsogoeva, S. B.; Schmatz, S. *Adv. Synth. Catal.* **2006**, *348*, 826.
[34] Cao, C.-L.; Ye, M.-C.; Sun, X.-L.; Tang, Y. *Org. Lett.* **2006**, *8*, 2901.
[35] Fang, X.; Wang, C.-J. *Chem. Commun.* **2015**, *51*, 1185.
[36] Sohtome, Y.; Tanatani, A.; Hashimoto, Y. Nagasawa, K. *Tetrahedron Lett.* **2014**, *45*, 5589.
[37] Narayanaperumal, S.; Rivera, D. G.; Silva, R. C.; Piaxão, M. W. *ChemCatChem* **2013**, *5*, 2756.
[38] Probst, N.; Madarász, Á.; Valkonen, A.; Pápai, I.; Rissanen, K.; Neuvonen, A.; Pihko, P. M. *Angew. Chem. Int. Ed.* **2012**, *51*, 8495.
[39] Neuvonen, A. J.; Pihko, P. M. *Org. Lett.* **2014**, *16*, 5152.
[40] J.-R. Chen, Y.-Q. Zou, L. Fu, F. Ren, F. Tan and W.-J. Xiao, *Tetrahedron*, **2010**, *66*, 5367.
[41] Zhang, Z.; Bao, Z.; Xing, H. *Org. Biomol. Chem.* **2014**, *12*, 3151.
[42] Lippert, K. M.; Hof, K.; Gerbig, D.; Ley, D.; Hausmann, H.; Guenther, S.; Schreiner, P. R. *Eur. J. Org. Chem.* **2012**, 5919.
[43] (a) Tárkányi, G.; Király, P.; Varga, S.; Vakulya, B.; Soós, T. *Chem. Eur. J.* **2008**, *14*, 6078. (b) Rho, H. S.; Oh, S. H.; Lee, J. W.; Lee, J. Y.; Chin, J.; Song, C. E. *Chem. Commun.* **2008**, 1208.
[44] Lee, J. W.; Ryu, T. H.; Oh, J. S.; Bae, H. Y.; Jang. H. B.; Song, C. E. *Chem. Commun.* **2009**, 7224.
[45] Alemán, J.; Parra, A.; Jiang, H.; Jørgensen, K. A. *Chem. Eur. J.* **2011**, *17*, 6890.
[46] Ni, X.; Li, X.; Wang, Z.; Cheng, J.-P. *Org. Lett.* **2014**, *16*, 1786.
[47] Kótai, B.; Kardos, G.; Hamza, A.; Farkas, V.; Pápai, I.; Soós, T. *Chem. Eur. J.* **2014**, *20*, 5631.
[48] Okino, T.; Hoashi, Y.; Furukawa, T.; Xu, X.; Takemoto, Y. *J. Am. Chem. Soc.* **2005**, *127*, 119.
[49] See [47] for references.
[50] Hamza, A.; Schubert, G.; Soós, T.; Pápai, I. *J. Am. Chem. Soc.* **2006**, *128*, 13151.
[51] Zhu, J.-L.; Zhang, Y.; Liu, C.; Zheng, A.-M.; Wang, W. *J. Org. Chem.* **2012**, *77*, 9813.

[52] For the recent reviews on H-bond mediated catalysis see: Chauhan, P.; Mahajan, S.; Kaya, U.; Hack, D.; Enders, D. *Adv. Synth. Catal.* **2015**, *357*, 253 and refernces therein.
[53] Parra, A.; Alfaro, R.; Marzo, L.; Moreno-Carrasco, A.; García Ruano, J. L.; Alemán, J. *Chem. Commun.* **2012**, *48*, 9759.
[54] Pan, F.-F.; Yu, W.; Qi, Z.-H.; Qiao, C.; Wang, X.-W. *Synthesis* **2014**, *46*, 1143.
[55] Rassu, G.; Zambrano, V.; Pinna, L.; Curti, C.; Battistini, L.; Sartori, A.; Pelosi, G.; Casiraghi, G.; Zanardi, F. *Adv. Synth. Catal.* **2014**, *356*, 2330.
[56] Rassu, G.; Zambrano, V.; Pinna, L.; Curti, C.; Battistini, L.; Sartori, A.; Pelosi, G.; Zanardi, F.; Casiraghi, G. *Adv. Synth. Catal.* **2013**, *355*, 1881.
[57] Oh, J.-S.; Kim, K. I.; Song, C. E. *Org. Biomol. Chem.* **2011**, *9*, 7983.
[58] Berkessel, A.; Mukherjee, S.; Müller, T. N.; Cleemann, F.; Roland, K.; Brandenburg, M.; Neudörfl, J.-M.; Lex, J. *Org. Biomol. Chem.* **2006**, *4*, 4319.
[59] De Jersey, J.; Zerner, B. *Biochemistry* **1969**, *8*, 1967.
[60] Yang, W.; Du, D.-M. *Chem. Commun.* **2011**, *47*, 12706.
[61] Noole, A.; Sucman, N. S.; Kabeshov, N. A.; Kanger, T.; Macaev, F. Z.; Malkov, A. V. *Chem. Eur. J.* **2012**, *18*, 14929.
[62] Noole, A.; Järving, I.; Werner, F.; Lopp, M.; Malkov, A.; Kanger, T. *Org. Lett.* **2012**, *14*, 4922.
[63] Noole, A.; Malkov, A. V.; Kanger, T. *Synthesis* **2013**, *45*, 2520.
[64] Noole, A.; Ilmarinen, K.; Järving, I.; Lopp, M.; Kanger, T. *J. Org. Chem.* **2013**, *78*, 8117.
[65] Noole, A.; Ošeka, M.; Pehk, T.; Öeren, M.; Järving, I.; Elsegood, M. R. J.; Malkov, A. V.; Lopp, M.; Kanger, T. *Adv. Synth. Catal.* **2013**, *355*, 829.
[66] Reile, I.; Paju, A.; Kanger, T.; Järving, I.; Lopp, M. *Tetrahedron Lett.* **2012**, *53*, 1476.
[67] Preegel, G.; Noole, A.; Ilmarinen, K.; Järving, I.; Kanger, T.; Pehk, T.; Lopp, M. *Synthesis* **2014**, *46*, 2595.
[68] While formally „1,4-enedione“ and „1,4-dicarbonyl compounds“ should mean 1,4-diketones, in current work other analogous compounds like 1,4-ketoesters or 1,4-diesters are also called the same way for simplicity.
[69] Seebach, D.; Seuring, B.; Kalinowski, H. O.; Lubosch, W.; Renger, B. *Angew. Chem. Int. Ed.* **1977**, *16*, 264 and references therein.
[70] Ballini, R.; Astolfi, P. *Liebigs Ann.* **1996**, 1879.
[71] Koft, E. R.; Smith, A. B. *J. Am. Chem. Soc.* **1982**, *104*, 2659 and references therein.
[72] Salvá, J.; Faulkner, D. J. *J. Org. Chem.* **1990**, *55*, 1941.
[73] Ismail, K. A.; El-Tombary, A. A.; Aboulwafa, O. M.; Omar, A.-M. M. E.; El-Rewini, S. H. *Arch. Pharm.* **1996**, *329*, 433.
[74] Xu, K.; Fang, Y.; Yan, Z.; Zha, Z.; Wang, Z. *Org. Lett.* **2013**, *15*, 2148.
[75] Li, S.-Y.; Wang, X.-B.; Jiang, W.; Kong, L.-Y. *Eur. J. Org. Chem.* **2014**, 8035.
[76] Fischer, H. *Chem. Rev.* **2001**, *101*, 3581.
[77] Nair, R. N.; Bannister, T. D. *J. Org. Chem.* **2014**, *79*, 1467.
[78] Voigtritter, K.; Subir, G.; Lipshutz, B. H. *J. Org. Chem.* **2011**, *76*, 4697 and references therein.
[79] Chatterjee, A. K.; Choi, T.-L.; Sanders, D. P.; Grubbs, R. H. *J. Am. Chem. Soc.* **2003**, *125*, 11360 and references therein
[80] Runchie, K. A.; Taylor, R. J. K. *Chem. Commun.* **2002**, 974.
[81] Yu, J.-Q.; Corey, E. J. *J. Am. Chem. Soc.* **2003**, *125*, 3232.
[82] Bonete, P.; Nájera, C. *Tetrahedron* **1995**, *51*, 2763.
[83] Ronsheim, M. D.; Zercher, C. K. *J. Org. Chem.* **2003**, *68*, 4535.
[84] Bhogadhi, Y. N. D.; Zercher, C. K. *Org. Synth.* **2014**, *91*, 248.

[85] Jiang, Z.; Yang, Y.; Pan, Y.; Zhao, Y.; Liu, H.; Tan, C.-H. *Chem. Eur. J.* **2009**, *15*, 4925.
[86] Zhao, F.; Zhang, W.; Yang, Y.; Pan, Y.; Chen, W.; Liu, H.; Yan, L.; Tan, C.-H.; Jiang, Z. *Adv. Synth. Catal.* **2011**, *353*, 2624.
[87] Das, U.; Chen, Y.-R.; Tsai, Y.-L.; Lin, W. *Chem. Eur. J.* **2013**, *19*, 7713.
[88] Chen, Y.-Y.; Das, U.; Liu, M.-H.; Lin, W. *J. Org. Chem.* **2015**, *80*, 1985.
[89] Liao, Y.-H.; Liu, X.-L.; Wu, Z.-J.; Du, X.-L.; Zhang, X.-M.; Yuan, W.-C. *Chem. Eur. J.* **2012**, *18*, 6679.
[90] Ošeka, M.; Noole, A.; Žari, S.; Öeren, M.; Järving, I.; Lopp, M.; Kanger, T. *Eur. J. Org. Chem.* **2014**, 3599.
[91] Conant, J. B.; Lutz, R. E. *J. Am. Chem. Soc.* **1923**, *45*, 1303.
[92] Mc Murry, J. E.; Blaszczak, L. C. *J. Org. Chem.* **1974**, *39*, 2217.
[93] Padmaja, A.; Sudhakar Reddy, S.; Mohan, A. V. N.; Padmavathi, V. *Chem. Pharm. Bull.* **2008**, *56*, 647.
[94] Lippur, K.; Kaabel, S.; Järving, I.; Rissanen, K.; Kanger, T. *J. Org. Chem.* **2015**, *80*, 6336.
[95] Rao, H. S. P.; Senthilkumar, S. P. *J. Org. Chem.* **2004**, *69*, 2591.
[96] For examples of biological activity and chemistry of isatin derivatives see referenses in publications **II** and **III**.
[97] Liu, H.; Wu, H.; Luo, Z.; Shen, J.; Kang, G.; Liu, B.; Wan, Z.; Jiang, J. *Chem. Eur. J.* **2012**, *18*, 11899.
[98] Zhao, M.-X.; Chen, M.-X.; Tang, W.-H.; Wei, D.-K.; Dai, T.-L.; Shi, M. *Eur. J. Org. Chem.* **2012**, 3598.
[99] Dou, X.; Yao, W.; Jiang, C.; Lu, Y. *Chem. Comm.* **2014**, *50*, 11354.
[100] Kumar, S. B.; Ravinder, M.; Kishore, G.; Rao, V. J.; Yogeeswari, P.; Sriram, D. *Med. Chem. Res.* **2014**, *23*, 1934.
[101] Chu, W.; Rothfus, J.; Zhou, D.; Mach, R. H. *Bioorg. Med. Chem. Lett.* **2011**, *21*, 2192.
[102] Kester, R. F. Isatin and Oxindole Compounds as Glucokinase Activators and Their Preparation and Use in the Treatment of Diabetes. US 20120142705 A1, Jun 7, 2012.
[103] Porter, A. G.; Jänicke, R. U. *Cell Death Differ.* **1999**, *6*, 99.
[104] Chu, W.; Rothfuss, J.; Zhou, D.; Mach, R. H. *Bioorg. Med. Chem. Lett.* **2011**, *21*, 2192 and references therein.
[105] As most of the products were obtained with moderate enantioselectivity at rt, reactions were also conducted at 2 °C or -25 °C. See Supporting Information of the **Publication III** for full table and a short discussion concerning the reaction temperatures.
[106] See Supporting Information of the **Publication III** for the results obtained by running the reactions in toluene as well as comparison to the results obtained in 1,2-DCE.
[107] Prentice, G. M.; Pascu, S. I.; Filip, S. V.; West, K. R.; Pantoş, G. D. *Chem. Commun.* **2015**, *51*, 8265.
[108] For full details on the calculation see Supporting Information of **Publication II**.
[109] Foster, J. P.; Weinhold, F. *J. Am. Chem. Soc.* **1980**, *102*, 7211.
[110] Mulliken, R. S. *J. Chem. Phys.* **1955**, *23*, 1833.
[111] Peixoto, P. A.; Boulangé, A.; Leleu, S.; Franck, X. *Eur. J. Org. Chem.* **2013**, 3316.
[112] Floyd, M. B.; Du, M. T.; Fabio, P. F.; Jacob, L. A.; Johnson, B. D. *J. Org. Chem.* **1985**, *50*, 5022.
[113] Roush, W. R.; Myers, A. G. *J. Org. Chem.* **1981**, *46*, 1509.

Publication I

Žari, S.; Kailas, T.; Kudrjashova, M.; Öeren, M.; Järving, I.; Tamm, T.; Lopp, M.; Kanger, T. Organocatalytic Asymmetric Addition of Malonates to Unsaturated 1,4-Diketones. *Beilstein Journal of Organic Chemistry*, **2012**, *8*, 1452-1457.

Beilstein Journal
of Organic Chemistry

Organocatalytic asymmetric addition of malonates to unsaturated 1,4-diketones

Sergei Žari, Tiiu Kailas, Marina Kudrjashova, Mario Öeren, Ivar Järving, Toomas Tamm, Margus Lopp and Tõnis Kanger*

Full Research Paper

Open Access

Address:
Department of Chemistry, Tallinn University of Technology, Akadeemia tee 15, 12618 Tallinn, Estonia

Email:
Tõnis Kanger* - kanger@chemnet.ee

* Corresponding author

Keywords:
Michael addition; non-covalent catalysis; organocatalysis; squaramide; thiourea

Beilstein J. Org. Chem. **2012,** *8,* 1452–1457.
doi:10.3762/bjoc.8.165

Received: 24 May 2012
Accepted: 06 August 2012
Published: 04 September 2012

This article is part of the Thematic Series "Organocatalysis".

Guest Editor: B. List

Abstract

The organocatalytic Michael addition of malonates to symmetric unsaturated 1,4-diketones catalyzed by thiourea and squaramide derivatives with *Cinchona* alkaloids afforded the formation of a new C–C bond in high yields (up to 98%) and enantiomeric purities (up to 93%). The absolute configuration of the product was suggested from comparison of the experimental and calculated VCD spectra of the reaction product **3a**.

Introduction

The asymmetric 1,4-conjugated addition (Michael reaction) of C-nucleophiles to enones is a powerful tool for obtaining a significant variety of enantioenriched products through a carbon–carbon bond formation [1-5]. Recently, unsaturated 1,4-dicarbonyl compounds, such as 1,4-ketoesters [6-8], 1,4-diketones [9], 1,4-ketoamides [9,10] and dialkylfumarates [11], have been the substrates for this reaction. The reaction products can undergo further chemical transformations, allowing the possibility of cascade reactions, making the method attractive for the synthesis of several valuable compounds, such as drugs and natural products. Tan et al. performed the addition of 1,3-alkylthiomalonates to 1,4-dicarbonylbut-2-enes, catalyzed by chiral bicyclic guanidines [7,9,12]. Xiao et al. reported the addition of nitroalkanes to 4-oxo-enoates, using chiral urea derivatives [7]. Miura et al. achieved an asymmetric addition of α,α-disubstituted aldehydes to maleimides catalyzed by primary amine thiourea organocatalyst [13]. Wang et al. reported the addition of dialkylmalonates and nitromethane to 4-oxo-4-aryl-butenoates catalyzed by *N,N′*-dioxide-$Sc(OTf)_3$ complexes [8]. Despite these and other successful experimental results, the asymmetric addition of malonates to symmetric aromatic unsaturated 1,4-diketones has not been systematically studied. Products of that reaction can be used as precursors of biologically active compounds. Padmaja et al. have reported that racemic heterocyclic compounds derived from the Michael addition of malonates and malononitrile to unsaturated 1,4-diketones pos-

sess antimicrobial and antifungal properties [14,15]. Therefore, new asymmetric additions of C-nucleophiles to unsaturated 1,4-diketones are highly in demand.

The asymmetric desymmetrization of symmetric unsaturated 1,4-diketones is a very challenging target. *si*-Attack on one carbon atom of the double bond and *re*-attack on the other leads to the same enantiomer. From the synthetic point of view, the conjugate addition of the nucleophile is, at the same time, a formal umpolung reaction with respect to the other carbonyl group (Figure 1).

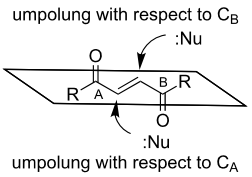

Figure 1: The conjugated addition to unsaturated 1,4-diketone **1**.

Results and Discussion

Catalyst screening

As a part of our ongoing studies in organocatalysis [16-19] we investigated the organocatalytic approach to the asymmetric desymmetrization of the title compounds with malonates. Three types of organocatalysts providing noncovalent interactions were used for this purpose: *Cinchona* alkaloids (**I**–**V**), thiourea derivatives (**VI**, **VII**) and squaramide derivatives (**VIII**, **IX**) (Figure 2). All of these screened catalysts are bifunctional compounds possessing hydrogen-bonding donor and acceptor moieties. Catalysts based on thiourea and squaramide differ from each other in their possible hydrogen-bond angles, rigidity of conformation, and pK_a values [20]. Although the two squaramide based catalysts **VIII** and **IX** are structurally similar, they have quite different properties. Catalyst **IX** is a self-association-free compound [21], while catalyst **VIII** forms associates, and the stereoselectivity of the reaction in its presence depends on the catalyst concentration [22].

The catalysts were screened in the reaction of phenyl disubstituted unsaturated 1,4-diketone **1a** with diethyl malonate (**2a**, Table 1). The reaction was run in DCE at room temperature in the presence of 10 mol % of catalyst with a five-fold excess of malonate. In all cases, the yields of the products were very high. *Cinchona* alkaloids (Table 1, entries 1–4) catalyzed the reaction with low stereoselectivity. There was a remarkable difference in their reaction rates. Quinine (**II**) and quinidine (**IV**, Table 1, entries 2 and 4) were more efficient than cinchonine (**I**) and cinchonidine (**III**, Table 1, entries 1 and 3). The reduction of the vinyl group in quinine afforded dihydroquinine **V**. Unfortunately, no changes in the stereoselectivity of the model reaction were observed (Table 1, entry 5). Both thiourea catalysts derived from *Cinchona* alkaloids (**VI**, **VII**) gave high yields with good selectivities (Table 1, entries 6 and 7). Squaramide

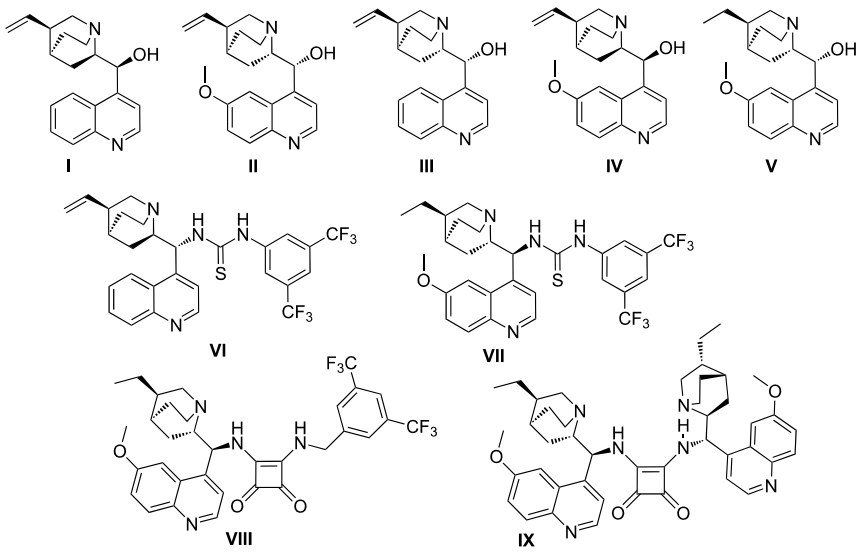

Figure 2: Organocatalysts screened.

Table 1: Screening of the catalysts for the asymmetric conjugated-addition reaction.

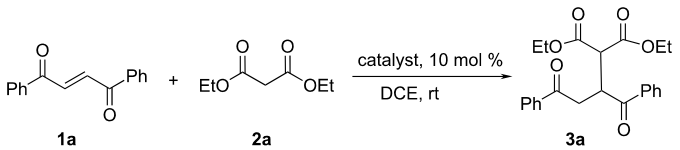

1a **2a** **3a**

entry	catalyst	time (h)	yield[a] (%)	ee[b] (%)	abs. conf.[c]
1	**I**	120	97	13	R
2	**II**	28	98	27	R
3	**III**	168	88	10	R
4	**IV**	24	>98	19	S
5	**V**	20	>98	18	R
6	**VI**	24	>98	74	S
7	**VII**	19	98	74	R
8	**VIII**	15	96	60	R
9	**IX**	96	96	39	R

[a]Isolated yield; [b]determined by chiral HPLC; [c]determined by a comparison of the experimental and calculated VCD spectra (see the following).

VIII and C_2-symmetric squaramide **IX** gave good yields but slightly lower selectivities (Table 1, entries 8 and 9). The catalyst **VII** was selected for further studies as being the most efficient. Also, considering the partially aromatic character of the cyclobutenedione system, which may possibly allow additional interactions with the aromatic substrates **1**, the catalyst **IX** was also chosen.

Scope of the reaction

Next, we studied the effect of the malonate structure on the stereoselectivity of the reaction (Table 2). Although, the ester moiety can be replaced by other functional groups in the course of further synthetic transformations its main role is to provide the addition products with high ee value. The conditions for the reaction remained the same as they were in the catalyst screening experiments, except that a smaller excess of malonate (3 equiv, unless stated otherwise) was used. This did not influence the reaction time or the enantioselectivity, but afforded easier purification of the crude product.

1,4-Diketone **1a** reacted smoothly with a variety of malonates **2a**–**2f**, affording the products **3a**–**3f** in high yields and with moderate to high stereoselectivities. In the case of the catalyst **VII**, the increase of steric hindrance of the malonate (Table 2, entries 1, 3, 5 and 7) led to a gradual drop in selectivity. Sterically more demanding malonates with branched alkyl or aryl groups (**2c–e**) gave products in much lower enantioselectivity (ee 37–69%) than the simple alkyl malonates (**2a, b)** (ee 73–74%). There was no clearly observed similar dependence with squaramide catalyst **IX**. Almost equally high ee values were obtained with methyl, phenyl or benzyl malonates (Table 2, entries 4, 10 and 12). A possible reason for the high selectivity with the phenyl-ring-containing esters could be the aromatic nature of the squaramide functional group in catalyst **IX**, allowing additional π–π-interactions.

The properties of the enone double bond of the substrate depend on the nature of the substituents in the phenyl ring. Therefore, the electronic effect of the *para*-substituent of unsaturated 1,4-diketone **1** on the reaction was investigated (Table 3). Electron-withdrawing groups, such as bromo and nitro, (Table 3, entries 10 and 13) as well as the electron-donating methoxy group (Table 3, entry 7) led to an increase in stereoselectivity, but the reaction time was also increased and the yields were lower with catalyst **VII**. A methyl substituent slightly decreased the enantioselectivity (Table 3, entry 4). This means that these dependencies cannot be clearly rationalized by the use of the electronic effects of the substituents in the phenyl ring. In the case of squaramide catalyst **IX**, all of the reactions became sluggish at room temperature (Table 3, entries 5, 8, 11 and 14). The reaction times were unreasonably long and the yields remained low. However, in the case of reactions with electron-withdrawing groups, the enantiomeric purity of the products was higher (Table 3, entries 11 and 14).

Increasing the temperature had a drastic positive effect on the reactions performed in the presence of catalyst **IX**. It was found that by raising the temperature to 80 °C it was possible to

Table 2: Enantioselective addition of malonates **2a-2f** to unsaturated 1,4-diketone **1a**.

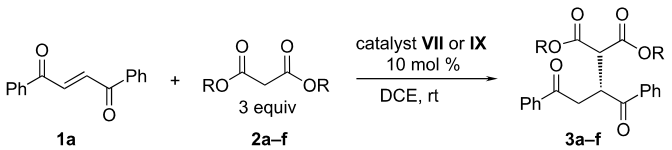

1a **2a–f** **3a–f**

entry	R	catalyst	time (h)	yield[c] (%)	ee[d] (%)
1	**a:** Et	**VII**	19	99	74
2	**a:** Et	**IX**	96	96	39
3	**b:** Me	**VII**	15	92	73
4	**b:** Me	**IX**	30	95	87
5	**c:** iPr	**VII**	36	96	69
6	**c:** iPr	**IX**	96	96	60
7[a]	**d:** *t*-Bu	**VII**	75	70	59
8[a]	**d:** *t*-Bu	**IX**	33	95	70
9[b]	**e:** Ph	**VII**	3	44	37
10[b]	**e:** Ph	**IX**	2	41	81
11	**f:** Bn	**VII**	6	95	68
12	**f:** Bn	**IX**	6	92	84

[a]Reaction at 80 °C, malonate/dione 2:1; [b]malonate/dione 1:1; [c]yields of isolated products; [d]determined by chiral HPLC.

Table 3: Enantioselective addition of diethylmalonate **2a** to substituted 1,4-diketones **1a, g–j**.

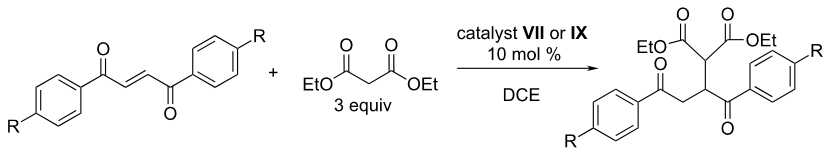

1a, g–j **2a** **3a, g–j**

entry	R	catalyst	temp. (°C)	time (h)	yield[b] (%)	ee[c] (%)
1	**a**: H	**VII**	rt	19	99	74
2	**a**: H	**IX**	rt	96	97	39
3	**a**: H	**IX**	80	10	97	82
4	**g**: Me	**VII**	rt	18	96	69
5	**g**: Me	**IX**	rt	213	25	18
6	**g**: Me	**IX**	80	22	76	66
7	**h**: MeO	**VII**	rt	88	90	79
8	**h**: MeO	**IX**	rt	48	—	—
9	**h**: MeO	**IX**	80	22	90	83
10[a]	**i**: Br	**VII**	rt	48	83	81
11[a]	**i**: Br	**IX**	rt	123	20	93
12[a]	**i**: Br	**IX**	80	6	86	91
13	**j**: NO_2	**VII**	rt	54	66	81
14	**j**: NO_2	**IX**	rt	94	44	89
15	**j**: NO_2	**IX**	80	6	98	89

[a]Dione/malonate 1.2:1; [b]yields of isolated products; [c]determined by chiral HPLC.

significantly decrease the reaction time and increase yields up to 98% with almost no negative effect on the stereoselectivity (ee 66–89%, Table 3, entries 6, 9, 12 and 15). Moreover, the compounds **3a** and **3g** were obtained in much higher enantioselectivities, and the reaction with the unsaturated 1,4-diketone containing the electron-donating substituent **1h**, which did not react at room temperature, also afforded the product in good yield and selectivity (Table 3, entry 9). As the squaramide-type catalyst **IX** is known to be self-association-free [21], the increase in enantioselectivity at higher temperatures can be attributed to the thermodynamic control of the conjugate addition. At the same time, the increase in temperature resulted in a small drop in stereoselectivity for the model reaction with catalyst **VII**.

The mechanism of the reaction is believed to be similar to that previously reported for 1,3-dicarbonyl compounds and acyl phosphonates [23]. Squaramide **IX** is a bifunctional catalyst that simultaneously coordinates electrophilic unsaturated 1,4-diketone via hydrogen bonding and activates the nucleophilic malonate via the tertiary amine of the quinuclidine moiety. Due to the symmetry of the substrate, there is no regioselectivity problem. A face selection is determined by the different access of the nucleophile to the tertiary amino group between the side chains of the catalysts. The *re*-face of the Michael acceptor is shielded by the flat quinoline unit and the *si*-attack of the malonate is preferred, affording *R*-selectivity (Figure 3).

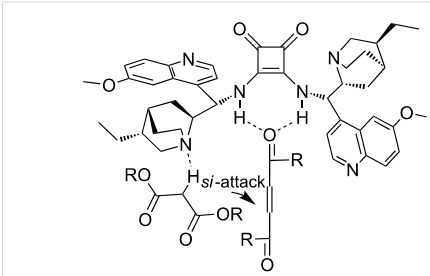

Figure 3: Proposed transition state.

Determination of the absolute configuration

The absolute configuration of the product **3a** was determined by a comparison of the experimental and calculated vibrational circular dichroism (VCD) spectra. DFT calculations (method B3PW91/6-311G**) of a series of conformers of compound **3a** with *R*-configuration were performed. Calculations of harmonic vibrational frequencies were carried out for all favored conformers to verify their stability. The Boltzmann distribution of the Gibbs energy showed that one conformation out of six is dominant (84%). The experimental and calculated IR spectra match well in the range 1500–1800 cm^{-1} (both experimental and calculated spectra are normalized to 100% by using the highest peak from that range, Figure 4A).

The most characteristic peaks of VCD spectra are in the same region (Figure 4B). The good agreement between calculated and experimental spectra directly allows for the assignment of the absolute configuration of **3a** as the *R*-enantiomer.

Conclusion

We have developed a highly enantioselective method for the desymmetrization of aromatic unsaturated 1,4-diketones through organocatalytic reactions with malonates. The reaction is catalyzed by thiourea and squaramide derivatives with *Cinchona* alkaloids and affords products in very high yields (up to 99%) and in high enantioselectivities (up to 93%). This enantioselective 1,4-addition to unsaturated 1,4-diketones affords valuable intermediates for further synthetic transformations.

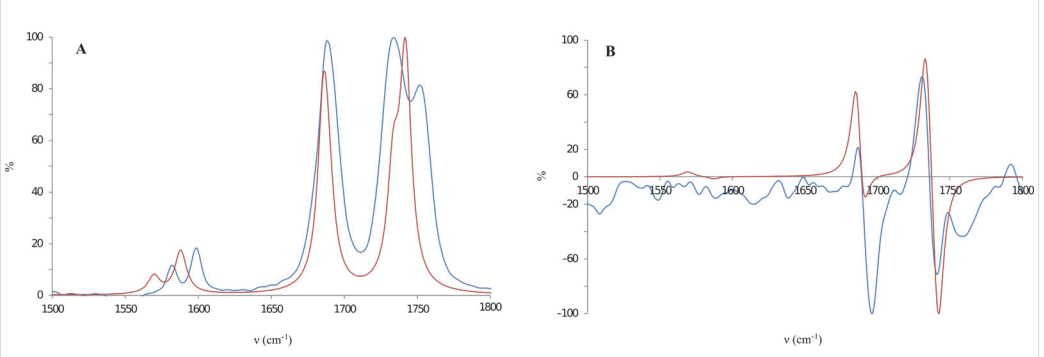

Figure 4: Calculated (red) and experimental (blue) IR (A) and VCD spectrum (B) of compound (*R*)-**3a**.

Supporting Information

Supporting Information File 1

Experimental procedures, compound characterization and computational data.
[http://www.beilstein-journals.org/bjoc/content/supplementary/1860-5397-8-165-S1.pdf]

Acknowledgements

The authors thank the Estonian Science Foundation (Grants No. 8289, 8255), the Ministry of Education and Research (Grant No. SF0140060s12), and the EU European Regional Development Fund (3.2.0101.08-0017) for financial support and COST Action CM0905 (ORCA, Organocatalysis).

References

1. Tsogoeva, S. B. *Eur. J. Org. Chem.* **2007,** 1701–1716. doi:10.1002/ejoc.200600653
2. Sulzer-Mossé, S.; Alexakis, A. *Chem. Commun.* **2007,** 3123–3135. doi:10.1039/B701216K
3. Ballini, R.; Bosica, G.; Fiorini, D.; Palmieri, A.; Petrini, M. *Chem. Rev.* **2005,** *105,* 933–972. doi:10.1021/cr040602r
4. Almaşi, D.; Alonso, D. A.; Nájera, C. *Tetrahedron: Asymmetry* **2007,** *18,* 299–365. doi:10.1016/j.tetasy.2007.01.023
5. Roca-Lopez, D.; Sadaba, D.; Delso, I.; Herrera, R. P.; Tejero, T.; Merino, P. *Tetrahedron: Asymmetry* **2010,** *21,* 2561–2601. doi:10.1016/j.tetasy.2010.11.001
6. Ye, W.; Leow, D.; Goh, S. L. M.; Tan, C.-T.; Chian, C.-H.; Tan, C.-H. *Tetrahedron Lett.* **2006,** *47,* 1007–1010. doi:10.1016/j.tetlet.2005.11.133
7. Lu, H. H.; Wang, X.-F.; Yao, C.; Zhang, J.; Wu, H.; Xiao, W.-J. *Chem. Commun.* **2009,** 4251–4253. doi:10.1039/b905033g
8. Wang, Z.; Chen, D.; Yang, Z.; Bai, S.; Liu, X.; Lin, L.; Feng, X. *Chem.–Eur. J.* **2010,** *16,* 10130–10136. doi:10.1002/chem.201001129
9. Jiang, Z.; Yang, Y.; Pan, Y.; Zhao, Y.; Liu, H.; Tan, C.-H. *Chem.–Eur. J.* **2009,** *15,* 4925–4930. doi:10.1002/chem.200802601
10. Zigterman, J. L.; Woo, J. C. S.; Walker, S. D.; Tedrow, J. S.; Borths, C. J.; Bunel, E. E.; Faul, M. M. *J. Org. Chem.* **2007,** *72,* 8870–8876. doi:10.1021/jo701682c
11. Shintani, R.; Ueyama, K.; Yamada, I.; Hayashi, T. *Org. Lett.* **2004,** *6,* 3425–3427. doi:10.1021/ol048421z
12. Ye, W.; Jiang, Z.; Zhao, Y.; Goh, S. L. M.; Leow, D.; Soh, Y.-T.; Tan, C.-H. *Adv. Synth. Catal.* **2007,** *349,* 2454–2458. doi:10.1002/adsc.200700326
13. Miura, T.; Masuda, A.; Ina, M.; Nakashima, K.; Nishida, S.; Tada, N.; Itoh, A. *Tetrahedron: Asymmetry* **2011,** *22,* 1605–1609. doi:10.1016/j.tetasy.2011.09.006
14. Padmaja, A.; Reddy, G. S.; Mohan, A. V. N.; Padmavathi, V. *Chem. Pharm. Bull.* **2008,** *56,* 647–653. doi:10.1248/cpb.56.647
15. Padmaja, A.; Payani, T.; Reddy, G. D.; Padmavathi, V. *Eur. J. Med. Chem.* **2009,** *44,* 4557–4566. doi:10.1016/j.ejmech.2009.06.024
16. Kanger, T.; Kriis, K.; Laars, M.; Kailas, T.; Müürisepp, A.-M.; Pehk, T.; Lopp, M. *J. Org. Chem.* **2007,** *72,* 5168–5173. doi:10.1021/jo070524i
17. Laars, M.; Ausmees, K.; Uudsemaa, M.; Tamm, T.; Kanger, T.; Lopp, M. *J. Org. Chem.* **2009,** *74,* 3772–3775. doi:10.1021/jo900322h
18. Noole, A.; Borissova, M.; Lopp, M.; Kanger, T. *J. Org. Chem.* **2011,** *76,* 1538–1545. doi:10.1021/jo200095e
19. Noole, A.; Pehk, T.; Järving, I.; Lopp, M.; Kanger, T. *Tetrahedron: Asymmetry* **2012,** *23,* 188–198. doi:10.1016/j.tetasy.2012.01.021
20. Alemán, J.; Parra, A.; Jiang, H.; Jørgensen, K. A. *Chem.–Eur. J.* **2011,** *17,* 6890–6899. doi:10.1002/chem.201003694
21. Lee, J. W.; Ryu, T. H.; Oh, J. S.; Bae, H. Y.; Jang, H. B.; Song, C. E. *Chem. Commun.* **2009,** 7224–7226. doi:10.1039/B917882A
22. Rho, H. S.; Oh, S. H.; Lee, J. W.; Lee, J. Y.; Chin, J.; Song, C. E. *Chem. Commun.* **2008,** 1208–1210. doi:10.1039/b719811f
23. Jiang, H.; Paixão, M. W.; Monge, D.; Jørgensen, K. A. *J. Am. Chem. Soc.* **2010,** *132,* 2775–2783. doi:10.1021/ja9097803

License and Terms

Publication II

Žari, S.; Kudrjashova, M.; Pehk, T.; Lopp, M.; Kanger, T. Remote Activation of the Nucleophilicity of Isatin, *Organic Letters*, **2014**, *16*, 1740-1743.

Organic LETTERS

Letter

pubs.acs.org/OrgLett

Remote Activation of the Nucleophilicity of Isatin

Sergei Žari,[†] Marina Kudrjashova,[†] Tõnis Pehk,[‡] Margus Lopp,[†] and Tõnis Kanger*[,†]

[†]Department of Chemistry, Tallinn University of Technology, Akadeemia tee 15, 12618 Tallinn, Estonia

[‡]National Institute of Chemical Physics and Biophysics, Akadeemia tee 23, 12618 Tallinn, Estonia

Supporting Information

ABSTRACT: The concept of the remote activation of reactivity was first applied in asymmetric organocatalysis. An isatin 3-phenylimine derivative acts as a donor in the thiourea catalyzed asymmetric addition to unsaturated 1,4-ketoesters, affording aza-Michael adducts in high enantiomeric purity and yield.

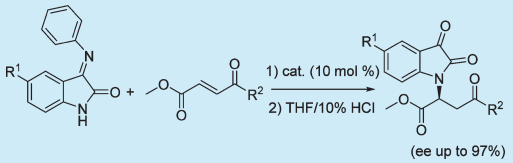

Isatin **1** is a well-known natural compound.[1] Its derivatives have been widely used as synthetic intermediates for the synthesis of spirocyclic compounds[2] and in multicomponent reactions.[3] Its core structure can be found in various biologically active compounds possessing, among others, anti-HIV,[4] anticancer,[5] antibacterial,[6] and antimalarian properties.[7] The combination of a phenyl ring, a γ-lactam moiety, and a carbonyl group in the isatin molecule gives rise to a variety of chemical transformations. Electrophilic substitution in an aromatic ring,[8] dipolar cycloaddition,[9] and especially the nucleophilic addition to the C3 carbonyl function of isatin are well-described.[10] Much less attention has been paid to the reactivity of the nucleophilic center at nitrogen. So far, reactions at the nitrogen atom are scarce[11] and have mainly been limited to alkylation or acylation to prevent side reactions. To the best of our knowledge, there are only a few references, by the same authors, where this reactivity has been described in a Michael reaction.[12] However, the conditions of these reactions were unconventional, using either solvent-free microwave irradiation or ionic liquids as solvents. No asymmetric version of an aza-Michael reaction of isatin has been described.[13]

Herein, we describe a novel reactivity of isatin-derived imine **2** in a thiourea-catalyzed asymmetric organocatalytic aza-Michael reaction. The key feature of the reaction is the remote activation of the nucleophilicity of the nitrogen atom by a 3-phenylimine moiety. Exploiting the nucleophilicity of the nitrogen atom and using it in reactions with electrophiles considerably broadens the synthetic utility of isatin and makes it possible to use it for the synthesis of more complex cyclic structures. The resulting imine can be easily hydrolyzed with an aqueous workup affording *N*-substituted isatins in a one-pot procedure. In connection with our ongoing studies of 1,4-unsaturated dicarbonyl compounds[14] and organocatalytic cascade reactions[15] we envisioned that the organocatalytic reaction between an enolizable unsaturated 1,4-dicarbonyl compound **3** and imine **2** derived from isatin would give a cascade of Mannich−Michael reactions in the presence of a thiourea catalyst (Scheme 1). To our surprise, no Mannich reaction was observed even in the presence of Pihko catalysts **I** and **III** which are known to be very efficient in promoting Mannich reactions.[16] Instead, aza-Michael product **4** was formed in good yield and high enantioselectivity. During the acidic workup the imine was hydrolyzed and isatin derivative **5** was formed.

Scheme 1. Expected and Actual Reactivity of Imine 2 Derived from Isatin 1

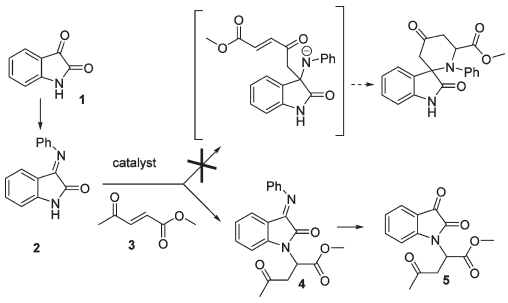

Based on that result, we decided to investigate the aza-Michael reaction in detail. The thiourea catalysts used are presented in Figure 1, and the results of the optimization are in Table 1.

All four catalysts screened resulted exclusively in aza-Michael product **4** with excellent enantioselectivity; however, the reaction rate strongly depended on the catalyst structure. Both catalysts **I** and **IV** showed good results, affording the product in high yield and selectivity in a reasonable time. It is worth mentioning that catalyst **I**, being a dual-activated analogue of **II**, was more efficient, while the reaction with **IV** proceeded much more smoothly than with its dual-activated analogue **III**. Considering the multistep synthesis of catalyst **I** together with its lower reactivity, catalyst **IV** was chosen for

Received: February 10, 2014
Published: March 10, 2014

   dx.doi.org/10.1021/ol500421k | *Org. Lett.* 2014, 16, 1740−1743

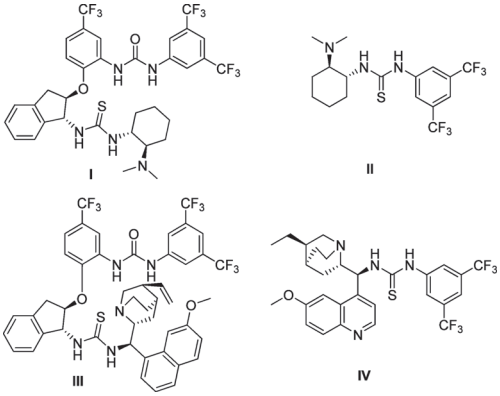

Figure 1. Screened chiral catalysts.

Table 1. Optimization of Reaction Conditions

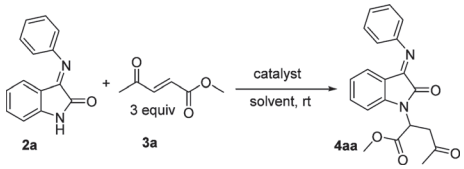

entry	catalyst (mol %)	solvent	time (h)	yield[a] (%)	ee (%)[b]
1	**I** (20)	toluene	48	99	95
2	**I** (10)	toluene	96	95	98
3	**I** (5)	toluene	216	51	99
4	**II** (10)	toluene	72	46	97
5	**III** (10)	toluene	72	29	97
6	**IV** (10)	toluene	72	95	96[c]
7	**IV** (10)	DCM	72	77	96[c]
8	**IV** (10)	THF	72	51	95[c]

[a]Isolated yield. [b]Determined by chiral HPLC. [c]Opposite enantiomer was in excess.

further investigations. The solvent screening revealed that toluene was the best solvent for the reaction.

With the optimal conditions in hand (10% of catalyst **IV**, toluene, room temperature), the reaction scope was investigated by using aliphatic or aromatic *para*-substituted unsaturated ketoesters **3a–g** (2 equiv) and 5-substituted isatin derivatives **2a–e** (Table 2).

In all cases, high or excellent enantioselectivities were obtained. Aliphatic ketoester **3a** was less reactive than aromatic ones (Table 2, entries 1 and 2–6). Compounds with electron-withdrawing substituents in the indolinone ring (**2d**, **2e**) increased the acidity of the N–H proton making deprotonation easier and the obtained conjugate base a better nucleophile, or alternatively, shifted the lactam–lactim equilibrium toward a more nucleophilic lactim. A shorter reaction time was needed to obtain a high yield for these compounds (Table 2, entries 10, 11). In contrast, isatin derivatives with electron-donating substituents (**2b**, **2c**) required a longer reaction time (Table 2, entries 8, 9). Michael acceptor **3** was, as expected, activated by electron-withdrawing groups at the aromatic ring of the phenyl-substituted ketoester (Table 2, entries 5, 7).

Table 2. Scope of the Reaction[a]

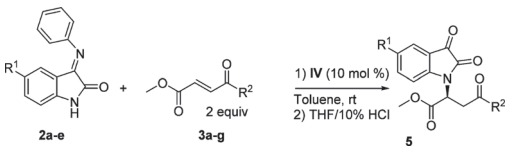

entry	2 R^1	3 R^2	5	time (h)	yield (%)[b]	ee (%)[c,d]
1	**2a**, H	**3a**, Me	**5aa**	72	80	97
2	**2a**, H	**3b**, Ph	**5ab**	18	95	94
3	**2a**, H	**3c**, *p*MePh	**5ac**	16	97	95
4	**2a**, H	**3d**, *p*MeOPh	**5ad**	16	95	96
5	**2a**, H	**3e**, *p*ClPh	**5ae**	5	95	93
6	**2a**, H	**3f**, *p*BrPh	**5af**	24	82	96
7[e]	**2a**, H	**3g**, *p*NO_2Ph	**5ag**	4	73	88
8	**2b**, Me	**3b**, Ph	**5bb**	20	83	90
9	**2c**, MeO	**3b**, Ph	**5cb**	96	75	95
10	**2d**, Br	**3b**, Ph	**5db**	3.5	91	91
11	**2e**, NO_2	**3b**, Ph	**5eb**	2.5	96	95

[a]For experimental conditions, see: Supporting Information. [b]Isolated yield. [c]Determined by HPLC with chiral stationary phase. [d]Absolute configuration (*S*) was determined by X-ray structure analysis[17] of **5ae** and presumed to be the same with the other substrates. [e]Ethyl ester was used.

Next, the role of the imine functional group was studied. Isatin **1** was much less effective in terms of yield, enantioselectivity, and reaction time than its imine derivative **2**. According to *ab initio* quantum chemistry calculations there is no significant difference in the charges of the amide N and H atoms of compounds **1** and **2a** (see Supporting Information). Therefore, we assumed that the interaction of imine derivative **2** with the catalyst was dependent on the substitution at the N-atom, and that plays a crucial role in the outcome of the reaction.

To check this assumption, various Schiff bases with different substituents (**2a**, **2f–i**) were prepared and tested in the reaction (Table 3). The results clearly illustrated that the difference in imine reactivity was based on its substituent. While using *N*-phenyl substituted imine **2a** resulted in nearly quantitative yield or product **5** within a reasonable reaction time (Table 3, entry 2), the other substituted imines **2f–i** were considerably less active.

Table 3. Effect of the Imine Substituent

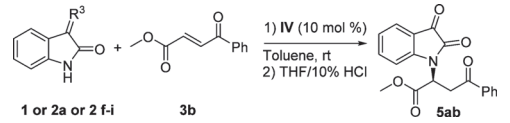

entry	R^3	time (h)	yield (%)[a]	ee (%)[b]
1[c]	(isatin **1**), O	48	59	62
2	**2a**, *N*-Ph	18	97	94
3	**2f**, *N*-H	144	12	75
4	**2g**, *N*-iPr	128	30	88
5	**2h**, *N*-*p*-MeOPh	72	62	98
6	**2i**, *N*-*p*-NO_2Ph	72	21	90

[a]Isolated yield. [b]Determined by HPLC with chiral stationary phase. [c]3 equiv of ketoester **3b** used.

dx.doi.org/10.1021/ol500421k | *Org. Lett.* 2014, 16, 1740–1743

Unsubstituted imine **2f** afforded the product in the lowest yield; however, the enantioselectivity of the reaction was higher than with isatin **1** (Table 3, entries 1, 3). Because **2f** was even less reactive than isatin, we concluded that replacing the carbonyl group with an unsubstituted imino group did not activate isatin. *N*-Alkyl substitution at the N atom (compound **2g**) exhibited slightly enhanced reactivity if compared with **2f**; however, the yield was still much lower than that for **2a** (Table 3, entries 2 and 4). The substitution at the *para* position of the aromatic ring of phenylimines (compounds **2h** and **2i**) also had a deleterious effect on the reactivity. Surprisingly, both the electron-donating methoxy group (compound **2h**) and electron-withdrawing nitro group (compound **2i**) had negative impacts on the reaction (Table 3, entries 5, 6). The low reactivity of nitro-substituted compound **2i** was probably caused by its poorer solubility if compared with the other investigated imines.

These experiments revealed the essential role of *N*-phenyl substitution at imine in making isatin derivative **2a** an active aza-Michael donor. An extra aromatic ring of imine **2a** (comparing with isatin **1**) let us assume that, in addition to the H-bonding interaction between the catalyst and oxindole derivative, $\pi-\pi$ interactions between aromatic rings could play some role. We assumed that the remote activation of isatin via complexation between imine **2** and catalyst **IV** by $\pi-\pi$ interactions of a quinoline fragment of the catalyst and imine's aromatic ring took place, increasing the nucleophilicity of the heterocyclic nitrogen. Simultaneously, the tertiary amino group from the quinuclidine fragment of **IV** could assist the deprotonation of the N−H proton of lactam and ketoester **3** could be activated by the hydrogen bonds from a thiourea moiety of the catalyst.

In order to obtain more evidence of the possible $\pi-\pi$ stacking between the catalyst **IV** and imines, the mixtures of these compounds were studied by NMR. A comparison of NMR spectra of imine **2a** (E/Z = 95:5) and the mixture of imine and catalyst **IV** showed differences in their chemical shifts (see Supporting Information). In the presence of the catalyst, the most significant differences occurred in the five-membered ring of isatin. The difference was biggest for the α-carbon to the nitrogen (0.5 ppm for ^{13}C). All signals of the protons of the six-membered ring of **2a** were shifted to a higher field pointing to the association with the aromatic ring(s) of the catalyst. The same can be concluded from the broadening of doublets of phenyl ring protons of imine. In the presence of catalyst **IV**, the NH signal of phenylimine **2a** at 135.0 ppm in ^{15}N NMR spectra ($CDCl_3$ solution at 296 K) was shifted 2.2 ppm to lower field. Imine nitrogen of **2a** which gave a signal at 356.7 ppm could not be detected on the addition of the catalyst due to the exchange broadening of *ortho* protons of the phenyl ring used for the detection of the ^{15}N resonance via the HMBC spectrum. In the case of imine **2g** (E/Z = 3:1) methyls of the isopropyl group became diastereotopic. It is only possible then that imine is in anisotropic environment, most likely due to binding to an enantiomerically pure catalyst.

In conclusion, the first highly enantioselective aza-Michael addition of isatin is reported. The reaction efficiency was greatly enhanced by derivatizing the isatin to a Schiff base that can be easily converted back by hydrolysis with no loss of yield and enantiomeric excess. This is the first example of remote activation of nucleophilicity in an organocatalytic reaction. The described reaction is efficient affording *N*-substituted isatins in high enantiomeric purity and high yield.

■ ASSOCIATED CONTENT

Supporting Information

Experimental details, characterization data for new compounds, copies of NMR spectra, HPLC chromatograms, X-ray structure, and computational data. This material is available free of charge via the Internet at http://pubs.acs.org.

■ AUTHOR INFORMATION

Corresponding Author

*E-mail: kanger@chemnet.ee.

Notes

The authors declare no competing financial interest.

■ ACKNOWLEDGMENTS

The authors thank the Estonian Ministry of Education and Research (Grant No. IUT 19-32) and EU European Regional Development Fund (3.2.0101.08-0017) for financial support. We thank Prof. Toomas Tamm for calculations, Dr. Ivar Järving for HRMS, Mrs. Kaja Ilmarinen for X-ray analysis, Dr. Aleksander-Mati Müürisepp for MS, and Ms. Tiina Aid for IR from Tallinn University of Technology.

■ REFERENCES

(1) Da Silva, J. F. M.; Garden, S. J.; Pinto, A. C. *J. Braz. Chem. Soc.* **2001**, *12*, 273−324.
(2) Singh, G. S.; Desta, Z. Y. *Chem. Rev.* **2012**, *112*, 6104−6155.
(3) Liu, Y.; Wang, H.; Wan, J. *Asian J. Org. Chem.* **2013**, *2*, 374−386.
(4) (a) Jiang, T.; Kuhen, K. L.; Wolff, K.; Yin, H.; Bieza, K.; Caldwell, J.; Bursulaya, B.; Wu, T. Y.-H.; He, Y. *Bioorg. Med. Chem. Lett.* **2006**, *16*, 2105−2108. (b) Pawar, V. S.; Lokwani, D. K.; Bhandari, S. V.; Bothara, K. G.; Chitre, T. S.; Devale, T. L.; Modhave, N. S.; Parikh, J. K. *Med. Chem. Res.* **2011**, *20*, 370−380.
(5) (a) Wee, X. K.; Yeo, W. K.; Zhang, B.; Tan, V. B. C.; Lim, K. M.; Tay, T. E.; Go, M.-L. *Bioorg. Med. Chem.* **2009**, *17*, 7562−7571. (b) Solomon, V. R.; Hu, C.; Lee, H. *Bioorg. Med. Chem.* **2009**, *17*, 7585−7592. (c) Matesic, L.; Locke, J. M.; Vine, K. L.; Ranson, M.; Bremner, J. B.; Skropeta, D. *Tetrahedron* **2012**, *68*, 6810−6819. (d) Romagnoli, R.; Baraldi, P. G.; Cruz-Lopez, O.; Preti, D.; Bermejo, J.; Estévez, F. *ChemMedChem* **2009**, *4*, 1668−1676.
(6) Kumari, G.; Singh, R. K. *Med. Chem. Res.* **2013**, *22*, 927−933.
(7) Rottmann, M.; McNamara, C.; Yeung, B. K. S.; Lee, M. C. S.; Zou, B.; Russell, B.; Seitz, P.; Plouffe, D. M.; Dharia, N. V.; Tan, J.; Cohen, S. B.; Spencer, K. R.; Gonzalez-Paez, G. E.; Lakshminarayana, S. B.; Suresh, B.; Goh, A.; Suwanarusk, R.; Jelga, T.; Schmitt, E. K.; Beck, H.-P.; Brun, R.; Nosten, F.; Renia, L.; Dartois, V.; Keller, T. H.; Fidock, D. A.; Winzeler, E. A.; Diagana, T. T. *Science* **2010**, *329*, 1175−1180.
(8) Tingare, Y. S.; Shen, M.-T.; Su, C.; Ho, S.-Y.; Tsai, S.-H.; Chen, B.-R.; Li, W.-R. *Org. Lett.* **2013**, *15*, 4292−4295.
(9) (a) Alimohammadi, K.; Sarrafi, Y.; Tajbakhsh, M.; Yeganegi, S.; Hamzehloueian, M. *Tetrahedron* **2011**, *67*, 1589−1597. (b) Schulz, V.; Davoust, M.; Lemarié, M.; Lohier, J.-F; Sopkova de Oliveira Santos, J.; Metzner, P.; Brière, J.-F. *Org. Lett.* **2007**, *9*, 1745−1748. (c) Lashgari, N.; Ziarani, G. M. *ARKIVOC* **2012**, 277−320.
(10) Selected examples: (a) Ball-Jones, N. R.; Badillo, J. J.; Franz, A. K. *Org. Biomol. Chem.* **2012**, *10*, 5165−5681. (b) Wang, G.-W.; Zhou, A.-X.; Wang, J.-J.; Hu, R.-B.; Yang, S.-D. *Org. Lett.* **2013**, *15*, 5270−5273. (c) Liu, H.; Wu, H.; Luo, Z.; Shen, J.; Kang, G.; Liu, B.; Wan, Z.; Jiang, J. *Chem.—Eur. J.* **2012**, *18*, 11899−11903.
(11) Zhao, M.-X.; Chen, M.-X.; Tang, W.-H.; Wei, D.-K.; Dai, T.-L.; Shi, M. *Eur. J. Org. Chem.* **2012**, 3598−3606.
(12) (a) Imanzadeh, G.; Aghaalizadeh, T.; Zamanloo, M.; Mansoori, Y. *J. Chil. Chem. Soc.* **2011**, *56*, 616 −620. (b) Imanzadeh, G. H.; Mollaei Tavana, M.; Zamanloo, M. R.; Mansoori, Y. *Chin. J. Chem.* **2009**, *27*, 389−396. (c) Imanzadeh, G.; Soltanizadeh, Z.; Khodayari,

A.; Zamanloo, M.; Mansoori, Y.; Salehzadeh, J. *Chin. J. Chem.* **2012**, *30*, 891−899.
(13) For recent reviews of aza-Michael reactions, see: (a) Enders, D.; Wang, C.; Liebich, J. X. *Chem.—Eur. J.* **2009**, *15*, 11058−11076. (b) Wang, J.; Li, P.; Choy, P. Y.; Chan, A. S. C.; Kwong, F. Y. *ChemCatChem* **2012**, *4*, 917−925. (c) Kotke, M.; Schreiner, P. R. In *Hydrogen Bonding in Organic Synthesis*, 1st ed.; Pihko, P. M., Ed.; Wiley-VCH: Weinheim, 2009; pp 141−351.
(14) Žari, S.; Kailas, T.; Kudrjashova, M.; Öeren, M.; Järving, I.; Tamm, T.; Lopp, M.; Kanger, T. *Beilstein J. Org. Chem.* **2012**, *8*, 1452−1457.
(15) (a) Noole, A.; Sucman, N. S.; Kabeshov, M. A.; Kanger, T.; Macaev, F. Z.; Malkov, A. V. *Chem.—Eur. J.* **2012**, *18*, 14929−14933. (b) Noole, A.; Järving, I.; Werner, F.; Lopp, M.; Malkov, A.; Kanger, T. *Org. Lett.* **2012**, *14*, 4922−4925. (c) Noole, A.; Ošeka, M.; Pehk, T.; Öeren, M.; Järving, I.; Elsegood, M. R. J.; Malkov, A. V.; Lopp, M.; Kanger, T. *Adv. Synth. Catal.* **2013**, *355*, 829−835. (d) Noole, A.; Ilmarinen, K.; Järving, I.; Lopp, M.; Kanger, T. *J. Org. Chem.* **2013**, *78*, 8117−8122.
(16) Probst, N.; Madarász, Á.; Valkonen, A.; Pápai, I.; Rissanen, K.; Neuvonen, A.; Pihko, P. M. *Angew. Chem., Int. Ed. Engl.* **2012**, *34*, 8495−8499. *Angew. Chem.* **2012**, *124*, 8623 −8627.
(17) The .cif file of **5ae** structure is available free of charge as a part of the Supporting Information.

dx.doi.org/10.1021/ol500421k | *Org. Lett.* 2014, 16, 1740−1743

Reprinted with permission from Thieme

Publication III

Žari, S. Metsala, A.; Kudrjashova, M.; Kaabel, S.; Järving, I.; Kanger, T. Asymmetric Organocatalytic Aza-Michael Reactions of Isatin Derivatives, *Synthesis*, **2015**, *47*, 875-886.

Synthesis S. Žari et al. Paper

Asymmetric Organocatalytic Aza-Michael Reactions of Isatin Derivatives

Sergei Žari
Andrus Metsala
Marina Kudrjashova
Sandra Kaabel
Ivar Järving
Tõnis Kanger*

Department of Chemistry, Tallinn University of Technology, Akadeemia tee 15, 12618 Tallinn, Estonia
tonis.kanger@ttu.ee

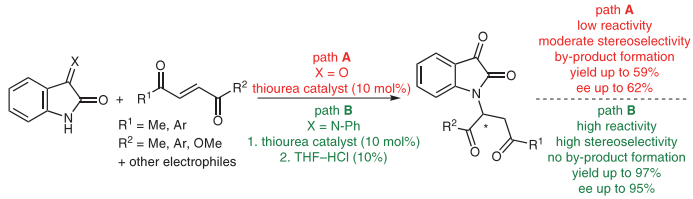

Received: 05.11.2014
Accepted after revision: 05.12.2014
Published online: 14.01.2015
DOI: 10.1055/s-0034-1379956; Art ID: ss-2014-t0676-op

Abstract Isatin was activated by derivatization to a Schiff base with aniline and used as an aza-Michael donor in organocatalytic asymmetric reactions with symmetric and nonsymmetric unsaturated 1,4-diketones. After hydrolysis (in situ), the N-substituted isatins were obtained in high yields (up to >95%) with high enantioselectivity (up to 95%).

Key words Michael addition, asymmetric catalysis, enantioselectivity, chemoselectivity, imines

Isatin (**1**) is a well-known natural indole derivative.[1] Because isatin derivatives display a broad spectrum of biological activities,[2] massive efforts have been made to access them via chemical synthesis.[3] The presence of the 1,2-disubstituted aromatic ring, carbonyl group, and γ-lactam moiety make isatin a versatile starting compound for a wide range of chemical transformations[4] including multicomponent reactions[5] and the synthesis of spirocyclic compounds.[6] The nucleophilicity of the nitrogen atom is mainly used for its alkylation,[7] acylation,[8] arylation,[9] or aza-Michael additions.[10] However, not much attention has been paid to the stereochemical aspects, as the obtained products are in most cases achiral or racemic. Medicinal chemistry studies have shown that N-substituted isatins,[11] including chiral ones in a racemic form,[12] possess different pharmaceutical properties. This makes a search for new asymmetric N-derivatization methods of isatin actual. So far, there have only been a few examples, where the N-substitution of isatin has been performed in an asymmetric manner. Shi et al. reported allylic amination of Morita–Baylis–Hillman carbonates with isatin in the presence of cinchona alkaloids.[13] Very recently, enantioselective prolinol-catalyzed N-alkylation of isatin acetals by enals was disclosed by Lu.[14] In our ongoing research on the asymmetric reactions of 1,4-dicarbonyl compounds[15] and oxindole derivatives,[16] we have previously applied the concept of remote activation of the nucleophilicty of isatin for the enantioselective aza-Michael addition.[17] (Scheme 1). It was found that derivatization of isatin (**1**) to Schiff base **2** was the crucial step for obtaining aza-Michael products **4** in high yields with high enantioselectivity (Scheme 1, path **A** vs path **B**), as well as reducing the reaction time and blocking possible by-product formation. The obtained N-alkylated products were easily converted back to isatins by acidic hydrolysis with no loss of yield or enantiomeric excess. The reactivity of the Schiff base strongly depended on the primary amine used. Imine derived from aniline (R^3 = Ph) was significantly more efficient than the others. NMR studies revealed strong interactions between isatin Schiff bases **2** and thiourea catalyst **I**, but the results could not explain the activation mechanism. In the current work, we focus on broadening of the scope of aza-Michael reactions with other electrophiles, including nonsymmetric unsaturated 1,4-diketones **5**, symmetric diketones **6**, and other typical Michael acceptors. Computational chemistry methods are used to rationalize this aza-Michael reaction.

In our previous work, keto esters were used as acceptors (Scheme 1, R^2 = OMe). Full regioselectivity was obtained and only one isomer derived from the attack on the α-position of the ester carbonyl was found. The transformation of isatin **1** to imine **2** is essential due to the nucleophilicity of the N-atom. Under thiourea catalysis, isatin itself reacts with enolizable carbonyl compounds (such as unsaturated diketones **5**) via aldol condensation at C3.[18] The reaction of imine **2** with nonsymmetric 1,4-diketone **5a** afforded, through an aza-Michael reaction, two regioisomers derived from either attack on the α-position of aliphatic (compound **7a**, major product) or aromatic carbonyl (compound **8a**, minor product) (Table 1).

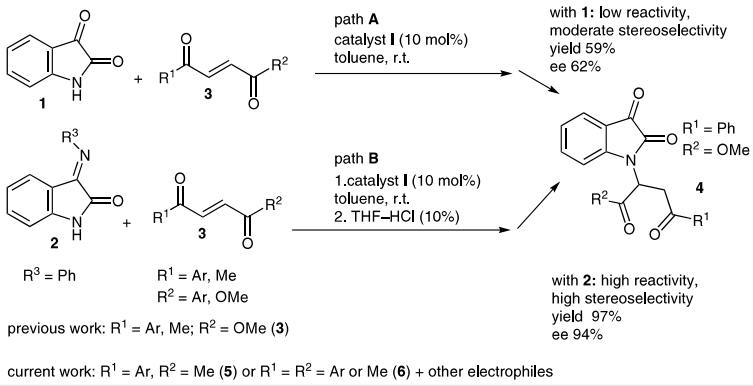

Scheme 1 Asymmetric aza-Michael addition of isatin (**1**) and isatin Schiff base **2** to unsaturated 1,4-dicarbonyl compounds

Table 1 Screening of Catalysts and Reaction Conditions[a]

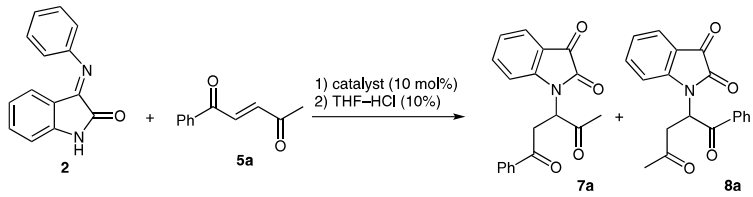

Entry	Catalyst	Time (h)	Yield (%)[b]	**7a**/**8a**[c]	**7a** ee (%)[d]
1	**I**	4	91	8:1	85 (*S*)
2[e]	**I**	20	85	6.5:1	88 (*S*)
3[f]	**I**	3.5	>95	5:1	87 (*S*)
4[g]	**I**	20	>95	9.5:1	86 (*S*)
5[h]	**I**	72	>95	12:1	92 (*S*)
6	**II**	7	>95	6:1	83 (*R*)
7	**III**	48	95	6:1	86 (*S*)
8	**IV**	20	95	11.5:1	80 (*R*)
9	**V**	20	95	3.3:1	67 (*R*)
10	**VI**	60	94	2.1:1	35 (*R*)
11	**VII**	96	traces	nd	nd
12[i]	**VIII**	96	traces	nd	nd
13[i]	**IX**	96	traces	nd	nd

[a] Reaction was conducted in toluene at r.t. (unless otherwise stated).
[b] Isolated yield.
[c] Determined by ^{1}H NMR spectroscopy.
[d] The absolute configuration was determined by an X-ray structure analysis of compound **9b** and is presumed to be the same. nd: not determined.
[e] The reaction was performed in THF.
[f] The reaction was performed in 1,2-DCE.
[g] Reaction at 2 °C.
[h] Reaction at –25 °C.
[i] Benzoic acid (10 mol%) was used as a co-catalyst.

We started the optimization of this model reaction by screening the catalyst and solvent (Table 1). Thioureas **I–III** (Figure 1) exhibited a similar stereoselectivity pattern in toluene (Table 1, entries 1, 6, 7). The reactions proceeded smoothly, affording the product **7a** in high yield with high enantioselectivity; the ratio of regioisomers varied from 8:1 to 6:1.

Takemoto catalyst **IV** gave the highest regioselectivity, but enantioselectivity was slightly lower (Table 1, entry 8). Pihko's catalysts **V** and **VI**,[19] squaramide **VII**, and catalysts with a primary amino group **VIII** and **IX** were not suitable for the reaction (entries 9–13). Catalyst **I** showed a better cumulative result (higher reactivity, allowing for further improvement of both enantio- and regioselectivity by running the reaction at a lower temperature). By lowering the temperature, the best regio-/enantioselectivity combination was achieved (entry 5), although the reaction became significantly slower. Changing toluene to 1,2-DCE resulted in a slightly faster reaction and better enantioselectivity at the expense of regioselectivity, while THF made the reaction sluggish, along with lowering regioselectivity.

With the optimal conditions in hand (10 mol% of catalyst **I** in toluene), we turned our attention to the scope of the reaction starting with a variety of nonsymmetric methyl aryl diketones **5** (Table 2). Decreasing the reaction temperature allowed us to obtain most of the products in >90% ee and in a high regioisomeric ratio. (As most of the products were obtained with moderate enantioselectivity at r.t., reactions were also conducted at 2 °C or –25 °C. The results obtained at room temperature and a short discussion are presented in a Table, see Supporting Information.) As expected, reaction rates and selectivities strongly depended on the substituent R of the diketone **5**. The major regioisomer was always formed by attack on the α-carbon of methyl ketone moiety. While electronegative or electron-withdrawing groups on the phenyl ring **5d**, **5e**, **5f** (entries 4–6) activated the substrate for the favorable regioisomer **7** formation, the electron-donating methoxy group in **5c** (entry 3) resulted in significantly lower regioselectivity. Replacing the phenyl ring with naphthyl did not change the result noticeably (entries 1 and 2). Diketones with ketones with heteroaromatic substituents **5g**, **5h** were less suitable for the reaction due to moderate enantioselectivity (entries 7, 8), while the reaction with 2-pyrrolyl substituted diketone **5i** afforded a racemic product in very low yield and regioselectivity (entry 9).

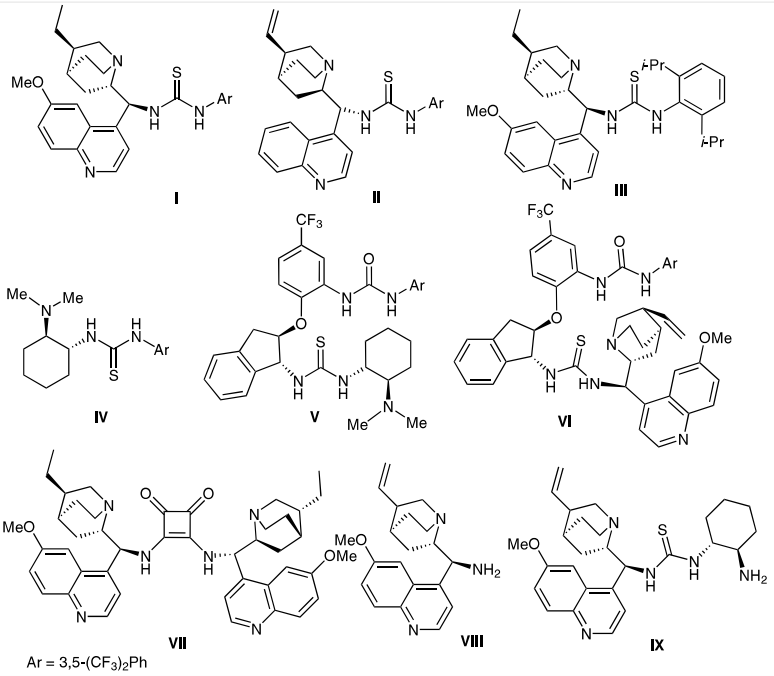

Figure 1 Catalysts screened

Table 2 Reactions of Isatin Schiff Base **2** with Unsaturated Nonsymmetric 1,4-Diketones **5a–i**

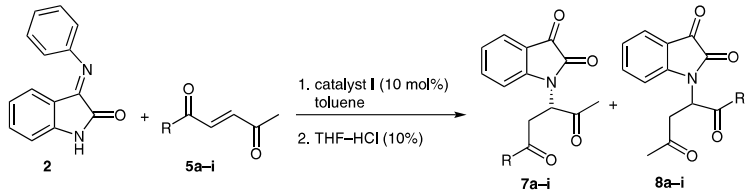

Entry	R	Temp (°C)	Time (h)	**7**/**8**[a]	Yield (%)[b]	ee of **7** (%)[c]
1	**a**, Ph	–25	72	12:1	>95	92
2	**b**, 2-naphthyl	2	24	8.5:1	>95	90
3	**c**, 4-$MeOC_6H_4$	2	24	4.5:1	>95	93
4	**d**, 4-ClC_6H_4	–25	72	15.5:1	>95	90
5	**e**, 4-BrC_6H_4	–25	72	15:1	>95	92
6	**f**, 4-$O_2NC_6H_4$	2	24	16.5:1	85	89
7	**g**, 2-thiophenyl	2	72	4:1	76	66
8	**h**, 2-furanyl	2	60	19.5:1	>95	74
9	**i**, 2-pyrrolyl	r.t.	72	4:1	10	*rac*

[a] Determined by ^{1}H NMR spectroscopy.
[b] Isolated yield.
[c] Determined by chiral HPLC.

Table 3 Reactions of Isatin Schiff Base **2** with Unsaturated Symmetric 1,4-Diketones **6a–g**

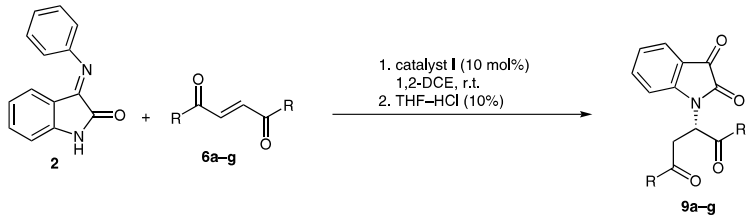

Entry	R	Time (h)	Yield (%)	ee (%)[a]
1[b]	**a**, Me	16	66	40
2[c]	**a**, Me	36	93	83
3	**b**, Ph	2	>95	95
4[d]	**b**, Ph	24	53	44
5	**c**, 4-MeC_6H_4	3.5	>95	95
6	**d**, 4-$MeOC_6H_4$	36	>95	84
7	**e**, 4-ClC_6H_4	30	>95	87
8[e]	**f**, 4-BrC_6H_4	228	72	64
9	**g**, 4-$O_2NC_6H_4$	4.5	74	nd[f]

[a] Determined by chiral HPLC; nd = not determined.
[b] The reaction was performed in toluene.
[c] The reaction was performed in toluene in the presence of 10 mol% of catalyst **IV**.
[d] The reaction was carried out in toluene with isatin (**1**) instead of Schiff base **2**.
[e] The reaction was carried out under more diluted conditions (0.2 M).
[f] Resolution of the enantiomers was not possible.

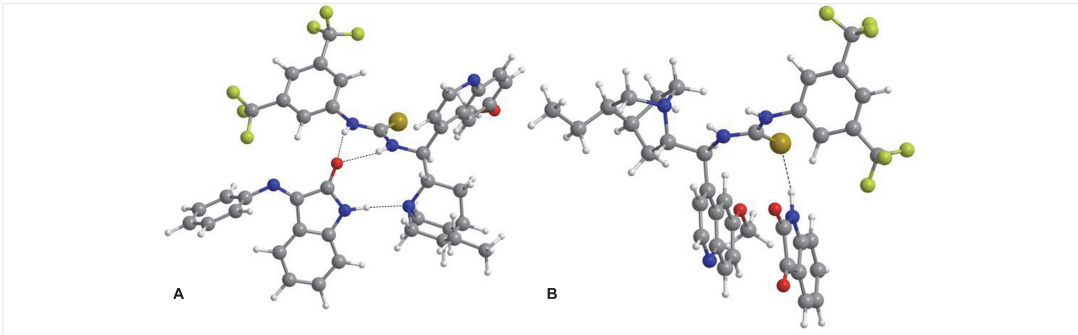

Figure 2 Two-component complexes between catalyst **I** and imine **2** (**A**) and isatin (**B**)

Next, the reaction with symmetric diketones **6a–g** was investigated. As in this case no regioisomers can be formed, 1,2-DCE was the optimal solvent. (A Table comparing the reactions in 1,2-DCE and toluene together with a short discussion is presented in Supporting Information.) The results are shown in Table 3.

Aliphatic diketone **6a** afforded product **9a** in low yield due to the formation of by-products (Table 3, entry 1). Replacing thiourea **I** with Takemoto catalyst **IV** resulted in obtaining a high yield of the product with acceptable enantioselectivity (Table 3, entry 2). Phenyl and tolyl-substituted aromatic diketones **6b** and **6c** reacted smoothly, affording the product in high yields and with excellent enantioselectivities (entries 3, 4). The reaction with a methoxy-substituted inactivated Michael acceptor diketone **6d** was considerably slower, but the product was also obtained in excellent yield and slightly lower enantioselectivity (entry 6). The diketones **6e** and **6f** substituted with 4-ClC_6H_4 and 4-BrC_6H_4 showed a substantial difference in reactivity: in the case of **6e** the reaction was complete in a reasonable time, while a longer reaction time was needed for the bromophenyl compound **6f**, most probably due to solubility issues (entries 7, 8). Nitro-substituted diketone **6g** reacted smoothly, but we were unable to determine its enantiomeric purity by chiral HPLC. An additional experiment showed that, as in the case of unsaturated 1,4-keto esters, derivatization of isatin (**1**) to a Schiff base **2** was essential for high yield and enantioselectivity (entry 3 vs 4). We next examined the reaction of isatin Schiff base **2** with other typical Michael acceptors (Scheme 2). Reactions with chalcone and its methyl analogue afforded the aza-Michael products **10**, **11** with high enantioselectivities; however, chalcone was less reactive, probably due to sterical hindrance near the stereogenic center. The symmetric unsaturated diester afforded the product **12** in low yield and with moderate enantioselectivity. For the reaction with alkylidenemalonate, a more reactive nitro analogue of Schiff base **2** was needed. Still, the product **13** was obtained in low yield with low enantiomeric purity. In the reactions with unsaturated 1,4-keto sulfone and β-nitro ester, only traces of products **14** and **15** were detected. In our previous work, we had shown that unsaturated keto esters were excellent Michael acceptors affording product **16**. To rationalize the reactivity of imines derived from isatin and the stereochemical outcome, this reaction was investigated by theoretical calculations. Pre-reaction states of imine or isatin with thiourea catalyst **I** were determined by molecular dynamics simulations using an AMBER99 force field. The formation of the hydrogen bonding between the catalyst and imine **2** versus isatin (**1**) was compared. The simulation results revealed that the imine was more involved in the hydrogen bonding network. The prevailing number of hydrogen bonds along the molecular dynamic trajectory for imine ranges from two to three, whereas for isatin this number is one (Table 4). In the case of imine there are two bonds between N–H atoms of the catalyst and the carbonyl group of oxindole ring together with the hydrogen bond between N–H (oxindole ring) and the tertiary amino group in the catalyst. For isatin only one bond is formed in the participation of the sulfur atom of the catalyst and N–H of the imine (Figure 2).

In the pre-reaction state, a well-defined complex with imine was formed whereas the complex with isatin had more conformational diversity. Adding the keto ester, methyl (*E*)-4-oxopent-2-enoate, to those two-component systems changed the hydrogen bondings network substantially. In the case of a three-component system (catalyst **I** + isatin + keto ester), the complex of sulfur hydrogen-bonded with isatin nitrogen disappeared, but very large numbers of different lowly populated hydrogen-bonded complexes appeared making these states very diverse. With imine **2** the lowest energy complexes were nonreactive. However, the complex where the nucleophilicity of the nitrogen atom was increased by a hydrogen bond between the tertiary amino group of the catalyst and between the carbonyl group and N–H atoms was also present (Figure 3).

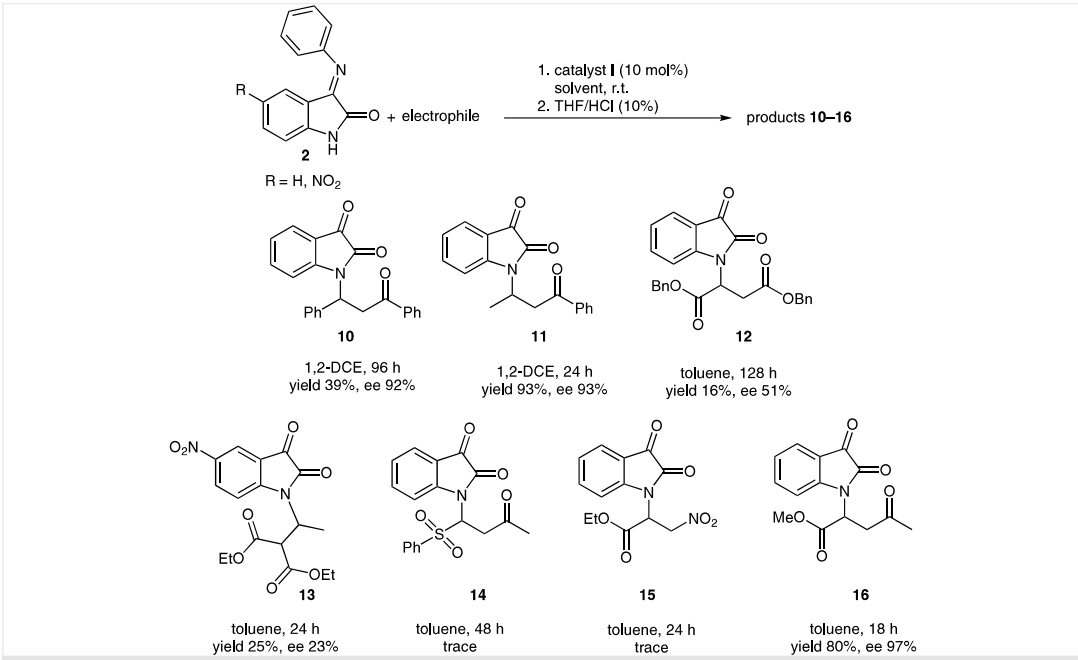

Scheme 2 Reactions with other electrophiles

Table 4 Comparison of the Population of H-Bonds between Catalyst **I** and Imine **2** or Isatin (**1**) During 270 ns of Simulation

Compound	Probability of number of H-bonds (%)					
	0	1	2	3	>3	sum
imine **2**	5.90	14.66	37.57	41.87	0	100
isatin (**1**)	2.46	97.47	0.06	0	0	100

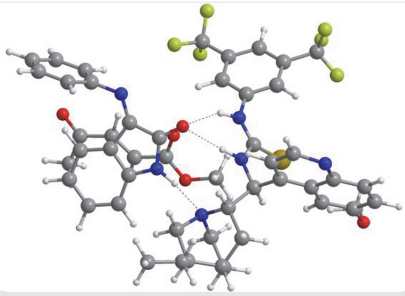

Figure 3 Three-component complex between catalyst **I**, imine **2** and methyl (*E*)-4-oxopent-2-enoate

In conclusion, we have demonstrated the organocatalytic enantioselective aza-Michael addition of isatin Schiff base **2** to both symmetric and nonsymmetric unsaturated 1,4-diketones and other electrophiles. The activation of isatin by derivatization to imine **2** is essential to reveal its aza-Michael donor properties. The high reactivity of imine **2** has been rationalized by molecular dynamics simulations.

Full assignment of ^{1}H and ^{13}C chemical shifts is based on the 1D and 2D FT NMR spectra measured on a Bruker Avance 400 MHz instrument. Residual solvent signals were used [$CDCl_3$ δ = 7.26 (^{1}H NMR), 77.16 (^{13}C NMR) or DMSO-d_6 δ = 2.54 (^{1}H NMR), 40.45 (^{13}C NMR)] as internal standards, unless otherwise indicated. Standard abbreviations were used to denote the peak multiplicities. High-resolution mass spectra were recorded on an Agilent Technologies 6540 UHD Accurate-Mass Q-TOF LC/MS spectrometer by using AJ-ESI ionization. MS spectra were measured on GC-MS spectrometer on a 70 eV EI. Optical rotations were obtained with an Anton Paar GWB Polarimeter MCP500. Chiral HPLC was performed using Chiralpak AD-H (250 × 4.6 mm), Chiralcel OD-H (250 × 4.6 mm), or Chiralpak AS-H (250 × 4.6 mm) columns. Precoated silica gel (Merck 60 F254) plates were used for TLC. Silica gel was used for column chromatography. The measured melting points are uncorrected. Commercial reagents were used as received. The solvents were freshly distilled using standard methods (CH_2Cl_2 and EtOAc over P_2O_5; benzene, toluene, and MeOH over Na). Commercial 1,2-DCE used for asymmetric reactions was distilled over CaH_2. The reactions were performed under air atmosphere

without additional moisture elimination, unless stated otherwise. Melting points and specific optical rotations for products **7**/**8** are reported for the ones with regioisomeric ratios >10:1.

Molecular Dynamics Simulations

The force field chosen was AMBER99[20] with a cutoff value of 7.86 Å for the Van der Waals forces; for the long range electrostatics the Particle Mesh Ewald approach (PME)[21] was used. The simulation was run under periodic boundary conditions, and at 298 K temperature and 1.0 atm of pressure. The NVT ensemble was simulated. Multiple timestep was used: 1.25 fs for intramolecular and 2.50 fs for intermolecular forces. After each 10 ps all the coordinates of the complex were saved as a snapshot. These MDS snapshots were prevailingly analyzed with the help of Yasara software; however, part of the trajectory analysis was performed with the VMD molecular visualization and analyze package. All the trajectory snapshots were analyzed in terms of hydrogen bond structure and dihedrical angle values. These values were sorted and the duplicate snapshots were removed from the analysis procedure. In such a way, the population analysis of all the unique structures were performed. In order to mimic the influence of solvent during subsequent MD runs, the simulation cell was 'filled' with toluene solvent in such a way that the solvent density fulfills the density values of 0.87 g/mL. In this way, 478 toluene molecules appear in the corresponding simulation cell. The cell had dimensions of 44 × 44 × 44 Å.

The above prepared complex was allowed to run an MD simulation within the time interval of 2000 ps for preliminary optimization of the solvated structure. After that initial relaxation and optimization step the actual simulation procedure was launched.

Chiral Catalysts

The catalysts **I**,[22] **II**,[22] **VIII**,[22], **III**,[16a] **IV**,[23] **V**,[19] **VI**,[19] **VII**,[24] and **IX**[25] were prepared by the corresponding literature procedures and the analytical data matched with those previously reported.

Isatin Schiff Bases

The compounds **2** were prepared by condensation on isatin and aniline in boiling MeOH with AcOH as a catalyst.[17]

Nonsymmetric Unsaturated 1,4-Diketones; General Procedure

All compounds were prepared by the in situ oxidation/Wittig reaction procedure, based on the method described in the literature.[26] The corresponding ylide (2.5 mmol, 1 equiv) was dissolved in CH_2Cl_2 (25 mL, 0.1 M), followed by the addition of 58% MnO_2 (2.2 g, 10 equiv) and hydroxyacetone (520 µL, 7.5 mmol, 3 equiv). The reaction mixture was stirred for 24 h at r.t., filtered through Celite, concentrated under reduced pressure, and the residue purified by column chromatography on silica gel using heptane–EtOAc mixtures as eluent.

(*E*)-1-(1*H*-Pyrrol-2-yl)pent-2-ene-2,4-dione (5i)

Yield: 269 mg (66%); yellow crystalline solid; mp >105 °C (dec.).

IR (KBr): 3271, 1670, 1642, 1592, 1543, 1405, 1253, 1145, 991, 765, 603, 567, 520 cm^{-1}.

^1H NMR (400 MHz, $CDCl_3$): δ = 9.99 (br s, 1 H), 7.52 (d, *J* = 15.7 Hz, 1 H), 7.19 (s, 1 H), 7.15 (d, *J* = 15.7 Hz, 1 H), 7.11 (s, 1 H), 6.42–6.33 (m, 1 H), 2.42 (s, 3 H).

^{13}C NMR (101 MHz, $CDCl_3$): δ = 198.2, 177.8, 136.8, 134.2, 132.9, 127.4, 118.7, 111.8, 29.2.

MS (70 eV): *m*/*z* = 163 [M^+], 148, 120, 94, 66, 43.

HRMS (ESI-QTOF): *m*/*z* [M + H]$^+$ calcd for $C_9H_9NO_2$: 164.0706; found: 164.0706.

Symmetric Diketones 6a–g; General Procedure

Diketones **6b**, **6c**, **6e**, and **6f** were prepared by Friedel–Crafts acylation of substituted benzenes with fumaryl chloride.[27] Compounds **6a** and **6d** were prepared by the same principle as the nonsymmetric diketones. Compound **6g** was prepared by a Wittig reaction with the corresponding α-ketoaldehyde.[15a]

Asymmetric Aza-Michael Reaction; General Procedure

Isatin Schiff base **2** (22.2 mg, 0.1 mmol), the corresponding electrophile (0.2 mmol), and catalyst **I** (6.0 mg, 0.01 mmol) were stirred in toluene or 1,2-DCE (0.3 mL) at the reported temperature for the appropriate time (Tables 2 and 3). In the case of the reactions carried out at 2 or –25 °C, the reaction vessel containing the reagents and the solvent were cooled prior to mixing together. The reactions were followed by TLC (CH_2Cl_2–EtOAc, 20:1). The hydrolysis was carried out in situ by adding a mixture of THF and 10% aq HCl (3:1, 1 mL) with vigorous stirring for 15–20 min. The reaction mixture was transferred to separatory funnel, diluted with H_2O (10 mL), and extracted with CH_2Cl_2 (3 × 10 mL). The combined extracts were dried ($MgSO_4$), concentrated, and the product was isolated by column chromatography.

The racemic standards were obtained by the same procedure using 1 equiv of K_2CO_3 as catalyst. After the completion of the reaction, the mixture was separated from K_2CO_3, hydrolyzed, and purified in the same manner.

(*S*)-1-(1,4-Dioxo-1-phenylpentan-3-yl)indoline-2,3-dione (7a)

Yield: 30.5 mg (95%); orange amorphous solid; $[\alpha]_D^{25}$ –136 (*c* 0.25, $CHCl_3$).

HPLC: Chiralpak AD-H column; 254 nm, 7:3 hexane–*i*-PrOH, 1 mL/min, 35 °C; t_R = 17.56 min (major isomer), t_R = 12.69 min (minor isomer); enantiomeric ratio 96:4, ee 92%, regioisomeric ratio 12:1.

IR (KBr): 1742, 1683, 1612, 1469, 1358, 754, 690 cm^{-1}.

^1H NMR (400 MHz, $CDCl_3$): δ = 7.97–7.92 (m, 2 H), 7.68–7.61 (m, 2 H), 7.61–7.55 (m, 1 H), 7.46 (t, *J* = 7.7 Hz, 2 H), 7.21–7.15 (m, 1 H), 7.12 (d, *J* = 8.0 Hz, 1 H), 5.46 (t, *J* = 6.3 Hz, 1 H), 4.13 (dd, *J* = 18.1, 6.4 Hz, 1 H), 3.50 (dd, *J* = 18.1, 6.3 Hz, 1 H), 2.26 (s, 3 H).

^{13}C NMR (101 MHz, $CDCl_3$): δ = 202.1, 196.2, 182.1, 158.3, 149.9, 138.9, 136.0, 134.0, 128.9, 128.3, 126.0, 124.5, 118.2, 111.2, 56.8, 36.4, 26.9.

MS (70 eV): *m*/*z* = 321 [M^+], 279, 250, 174, 159, 146, 119, 105, 92, 77, 43.

HRMS (ESI-QTOF): *m*/*z* [M + Na]$^+$ calcd for $C_{19}H_{15}NO_4$ + Na: 344.0893; found: 344.0897.

(*S*)-1-[1-(Naphthalen-2-yl)-1,4-dioxopentan-3-yl]indoline-2,3-dione (7b)

Yield: 37 mg (>95%); orange amorphous solid.

IR (KBr): 2923, 1741, 1678, 1611, 1469, 1358, 1179, 860, 820, 753, 475 cm^{-1}.

^1H NMR (400 MHz, $CDCl_3$): δ = 8.47 (s, 1 H), 7.96 (dd, *J* = 8.7, 1.7 Hz, 1 H), 7.93 (d, *J* = 8.0 Hz, 1 H), 7.88–7.83 (m, 2 H), 7.69–7.62 (m, 2 H), 7.62–7.57 (m, 1 H), 7.57–7.51 (m, 1 H), 7.21–7.14 (m, 2 H), 5.51 (t, *J* = 6.3 Hz, 1 H), 4.26 (dd, *J* = 18.0, 6.3 Hz, 1 H), 3.64 (dd, *J* = 18.0, 6.4 Hz, 1 H), 2.28 (s, 3 H).

^{13}C NMR (101 MHz, $CDCl_3$): δ = 202.2, 196.1, 182.1, 158.4, 149.9, 138.9, 135.9, 133.3, 132.5, 130.4, 129.8, 129.0, 128.8, 127.9, 127.1, 126.0, 124.5, 123.6, 118.2, 111.2, 56.9, 36.5, 26.8.

MS (70 eV): *m*/*z* = 371 [M$^+$], 329, 224, 181, 155, 127, 119, 105, 92, 77, 43.

HRMS (ESI-QTOF): *m*/*z* [M + Na]$^+$ calcd for $C_{23}H_{17}NO_4$ + Na: 394.1050; found: 394.1055.

(*S*,*E*)-1-(Naphthalen-2-yl)-3-[2-oxo-3-(phenylimino)indolin-1-yl]pentane-1,4-dione (7b imine)

Obtained by the general procedure without hydrolysis to determine the ee of **7b**; orange amorphous solid.

HPLC: Chiralpak AS-H column; 254 nm, 7:3 hexane–*i*-PrOH, 0.8 mL/min, 35 °C; t_R = 39.12 min (major isomer), t_R = 19.02 min (minor isomer); enantiomeric ratio 95:5.

IR (KBr): 1733, 1678, 1605, 1466, 1359, 1185, 1124, 862, 823, 751, 659 cm^{-1}.

^{1}H NMR (400 MHz, $CDCl_3$): δ = 8.50 (s, 1 H), 8.00 (dd, *J* = 8.7, 1.6 Hz, 1 H), 7.94 (d, *J* = 8.0 Hz, 1 H), 7.90–7.83 (m, 2 H), 7.63–7.51 (m, 2 H), 7.46–7.39 (m, 3 H), 7.27–7.22 (m, 1 H), 7.15 (d, *J* = 8.0 Hz, 1 H), 7.01–6.95 (m, 2 H), 6.81 (t, *J* = 7.6 Hz, 1 H), 6.69 (d, *J* = 7.7 Hz, 1 H), 5.59 (t, *J* = 5.9 Hz, 1 H), 4.32 (dd, *J* = 17.9, 6.3 Hz, 1 H), 3.68 (dd, *J* = 17.8, 6.2 Hz, 1 H), 2.32 (s, 3 H).

^{13}C NMR (101 MHz, $CDCl_3$): δ = 202.8, 196.5, 163.3, 153.3, 150.2, 146.3, 135.9, 134.5, 133.5, 132.5, 130.4, 129.8, 129.6, 128.9, 128.7, 127.9, 127.0, 126.7, 125.6, 123.7, 123.4, 117.7, 116.2, 110.5, 56.9, 36.6, 26.8.

MS (70 eV): *m*/*z* = 446 [M$^+$], 375, 355, 263, 222, 194, 155, 127, 77, 43.

HRMS (ESI-QTOF): *m*/*z* [M + H]$^+$ calcd for $C_{29}H_{22}N_2O_3$: 447.1703; found: 447.1717.

(*S*)-1-[1-(4-Methoxyphenyl)-1,4-dioxopentan-3-yl]indoline-2,3-dione (7c)

Yield: 35 mg (>95%); orange amorphous solid.

HPLC: Chiralpak AD-H column; 254 nm, 7:3 hexane–*i*-PrOH, 1 mL/min, 35 °C; t_R = 59.12 min (major isomer), t_R = 23.25 min (minor isomer); enantiomeric ratio 96.5:3.5, regioisomeric ratio 4.5:1.

IR (KBr): 2926, 1742, 1673, 1611, 1469, 1358, 1260, 1172, 1025, 834, 755 cm^{-1}.

^{1}H NMR (400 MHz, $CDCl_3$): δ = 7.93–7.87 (m, 2 H), 7.66–7.59 (m, 2 H), 7.19–7.10 (m, 2 H), 6.93–6.88 (m, 2 H), 5.43 (t, *J* = 6.3 Hz, 1 H), 4.05 (dd, *J* = 17.9, 6.2 Hz, 1 H), 3.85 (s, 3 H), 3.47 (dd, *J* = 17.9, 6.5 Hz, 1 H), 2.25 (s, 3 H).

^{13}C NMR (101 MHz, $CDCl_3$): δ = 202.2, 194.6, 182.2, 164.1, 158.3, 150.0, 138.8, 130.6, 129.0, 125.9, 124.4, 118.1, 114.0, 111.2, 56.9, 55.6, 36.0, 26.8.

MS (70 eV): *m*/*z* = 351 [M$^+$], 309, 204, 146, 135, 107, 92, 77, 43.

HRMS (ESI-QTOF): *m*/*z* [M + Na]$^+$ calcd for $C_{20}H_{17}NO_5$ + Na: 374.0999; found: 374.1003.

(*S*)-1-[1-(4-Chlorophenyl)-1,4-dioxopentan-3-yl]indoline-2,3-dione (7d)

Yield: 35 mg (>95%); orange crystals; mp 149–153 °C; $[\alpha]_D^{25}$ –123 (*c* 0.25, $CHCl_3$).

HPLC: Chiralpak AD-H column; 254 nm, 7:3 hexane–*i*-PrOH, 1 mL/min, 35 °C; t_R = 27.51 min (major isomer), t_R = 18.88 min (minor isomer); enantiomeric ratio 95:5, ee 90%, regioisomeric ratio 15.5:1.

IR (KBr): 1742, 1683, 1612, 1469, 1358, 1091, 996, 818, 754 cm^{-1}.

^{1}H NMR (400 MHz, $CDCl_3$): δ = 7.87 (d, *J* = 8.6 Hz, 2 H), 7.67–7.61 (m, 2 H), 7.42 (d, *J* = 8.6 Hz, 2 H), 7.18 (t, *J* = 7.6 Hz, 1 H), 7.10 (d, *J* = 8.2 Hz, 1 H), 5.43 (t, *J* = 6.3 Hz, 1 H), 4.09 (dd, *J* = 18.0, 6.5 Hz, 1 H), 3.42 (dd, *J* = 18.0, 6.2 Hz, 1 H), 2.25 (s, 3 H).

^{13}C NMR (101 MHz, $CDCl_3$): δ = 202.1, 195.1, 182.1, 158.3, 149.8, 140.4, 138.9, 134.3, 129.7, 129.2, 126.1, 124.6, 118.2, 111.1, 56.7, 36.3, 26.8.

MS (70 eV): *m*/*z* = 355 [M$^+$], 313, 284, 208, 193, 139, 119, 111, 92, 75, 43.

HRMS (ESI-QTOF): *m*/*z* [M + Na]$^+$ calcd for $C_{19}H_{14}ClNO_4$ + Na: 378.0504; found: 378.0508.

(*S*)-1-[1-(4-Bromophenyl)-1,4-dioxopentan-3-yl]indoline-2,3-dione (7e)

Yield: 39 mg (>95%); orange crystals; mp 159–161 °C; $[\alpha]_D^{25}$ –108 (*c* 0.25, $CHCl_3$).

HPLC: Chiralpak AD-H column; 254 nm, 7:3 hexane–*i*-PrOH, 1 mL/min, 35 °C; t_R = 34.11 min (major isomer), t_R = 21.16 min (minor isomer); enantiomeric ratio 96:4, ee 92%, regioisomeric ratio 15:1.

IR (KBr): 1742, 1684, 1612, 1469, 1358, 1178, 1071, 997, 817, 755 cm^{-1}.

^{1}H NMR (400 MHz, $CDCl_3$): δ = 7.81 (d, *J* = 8.5 Hz, 2 H), 8.68–8.62 (m, 2 H), 7.60 (d, *J* = 8.5 Hz, 2 H), 7.19 (t, *J* = 7.6 Hz, 1 H), 7.10 (d, *J* = 7.9 Hz, 1 H), 5.43 (t, *J* = 6.3 Hz, 1 H), 4.09 (dd, *J* = 18.0, 6.5 Hz, 1 H), 3.41 (dd, *J* = 18.0, 6.2 Hz, 1 H), 2.25 (s, 3 H).

^{13}C NMR (101 MHz, $CDCl_3$): δ = 202.1, 195.3, 182.0, 158.3, 149.8, 138.9, 134.7, 132.2, 129.8, 129.3, 126.1, 124.6, 118.2, 111.1, 56.7, 36.3, 26.8.

MS (70 eV): *m*/*z* = 401, 399 [M$^+$], 359, 357, 330, 328, 254, 252, 239, 237, 211, 209, 185, 183, 157, 155, 147, 119, 92, 76, 43.

HRMS (ESI-QTOF): *m*/*z* [M + Na]$^+$ calcd for $C_{19}H_{14}BrNO_4$ + Na: 421.9998; found: 421.9999.

(*S*)-1-[1-(4-Nitrophenyl)-1,4-dioxopentan-3-yl]indoline-2,3-dione (7f)

Yield: 31 mg (95%); orange crystalline solid; mp 149–152 °C; $[\alpha]_D^{25}$ –96 (*c* 0.25, $CHCl_3$).

HPLC: Chiralpak AD-H column; 254 nm, 7:3 hexane–*i*-PrOH, 1 mL/min, 35 °C; t_R = 41.01 min (major isomer), t_R = 44.16 min (minor isomer); enantiomeric ratio 94.5:5.5, ee 89%, regioisomeric ratio 16.5:1.

IR (KBr): 1742, 1693, 1612, 1525, 1470, 1347, 1178, 856, 757 cm^{-1}.

^{1}H NMR (400 MHz, $CDCl_3$): δ = 8.33–8.27 (m, 2 H), 8.16–8.09 (m, 2 H), 7.71–7.63 (m, *J* = 7.3, 4.1, 1.2 Hz, 2 H), 7.21 (t, *J* = 7.7 Hz, 1 H), 7.09 (d, *J* = 8.3 Hz, 1 H), 5.44 (t, *J* = 6.3 Hz, 1 H), 4.19 (dd, *J* = 18.1, 6.9 Hz, 1 H), 3.43 (dd, *J* = 18.1, 5.9 Hz, 1 H), 2.26 (s, 3 H).

^{13}C NMR (101 MHz, $CDCl_3$): δ = 202.0, 195.0, 181.8, 158.3, 150.8, 149.6, 140.4, 139.0, 129.5, 126.2, 124.8, 124.1, 118.2, 110.9, 56.7, 36.9, 26.7.

MS (70 eV): *m*/*z* = 366 [M$^+$], 324, 295, 219, 204, 177, 150, 119, 104, 92, 76, 43.

HRMS (ESI-QTOF): *m*/*z* [M + Na]$^+$ calcd for $C_{19}H_{14}N_2O_6$ + Na: 389.0744; found: 389.0747.

(*S*)-1-[1,4-Dioxo-1-(thiophen-2-yl)pentan-3-yl]indoline-2,3-dione (7g)

Yield: 25 mg (76%); orange amorphous solid.

HPLC: Chiralpak AD-H column; 254 nm, 7:3 hexane–*i*-PrOH, 1 mL/min, 35 °C; t_R = 17.40 min (major isomer), t_R = 15.35 min (minor isomer); enantiomeric ratio 83:17, regioisomeric ratio 4:1.

IR (KBr): 1741, 1659, 1611, 1525, 1469, 1415, 1358, 1180, 1098, 1054, 753 cm^{-1}.

^1H NMR (400 MHz, $CDCl_3$): δ = 7.76 (dd, *J* = 3.8, 1.1 Hz, 1 H), 7.67–7.61 (m, 3 H), 7.20–7.15 (m, 1 H), 7.14–7.10 (m, 2 H), 5.37 (t, *J* = 6.4 Hz, 1 H), 4.03 (dd, *J* = 17.7, 6.0 Hz, 1 H), 3.49 (dd, *J* = 17.7, 6.9 Hz, 1 H), 2.25 (s, 3 H).

^{13}C NMR (101 MHz, $CDCl_3$): δ = 201.9, 189.0, 182.1, 158.3, 149.9, 142.9, 138.9, 134.8, 133.0, 128.5, 126.0, 124.5, 118.2, 111.1, 56.8, 36.9, 26.7.

MS (70 eV): *m*/*z* = 327 [M^+], 299, 285, 256, 180, 146, 119, 111, 83.

HRMS (ESI-QTOF): *m*/*z* [M + Na]$^+$ calcd for $C_{17}H_{13}NO_4S$ + Na: 350.0457; found: 350.0463.

(*S*)-1-[1-(Furan-2-yl)-1,4-dioxopentan-3-yl]indoline-2,3-dione (7h)

Yield: 30 mg (>95%); orange amorphous solid; $[\alpha]_D^{25}$ –113 (*c* 0.25, $CHCl_3$).

HPLC: Chiralpak AD-H column; 254 nm, 7:3 hexane–*i*-PrOH, 1 mL/min, 35 °C; t_R = 16.57 min (major isomer), t_R = 13.78 min (minor isomer); enantiomeric ratio 87:13, ee 74%, regioisomeric ratio 19.5:1.

IR (KBr): 1742, 1672, 1611, 1468, 1415, 1358, 1158, 1018, 755 cm^{-1}.

^1H NMR (400 MHz, $CDCl_3$): δ = 7.67–7.60 (m, 2 H), 7.58 (dd, *J* = 1.6, 0.6 Hz, 1 H), 7.25–7.22 (m, 1 H), 7.20–7.14 (m, 1 H), 7.08 (d, *J* = 8.0 Hz, 1 H), 6.54 (dd, *J* = 3.6, 1.7 Hz, 1 H), 5.39 (t, *J* = 6.5 Hz, 1 H), 3.96 (dd, *J* = 17.8, 6.3 Hz, 1 H), 3.38 (dd, *J* = 17.8, 6.8 Hz, 1 H), 2.24 (s, 3 H).

^{13}C NMR (101 MHz, $CDCl_3$): δ = 201.9, 185.0, 182.1, 158.3, 151.9, 149.8, 147.1, 138.9, 126.0, 124.5, 118.3, 112.8, 111.1, 56.4, 36.1, 26.7.

MS (70 eV): *m*/*z* = 311 [M^+], 269, 240, 196, 146, 119, 95, 76, 67, 43.

HRMS (ESI-QTOF): *m*/*z* [M + Na]$^+$ calcd for $C_{17}H_{13}NO_5$ + Na: 334.0686; found: 334.0689.

(*S*)-1-[1,4-Dioxo-1-(1*H*-pyrrol-2-yl)pentan-3-yl]indoline-2,3-dione (7i)

Yield: 3 mg (10%); yellow amorphous solid.

HPLC: Chiralpak AD-H column; 254 nm, 7:3 hexane–*i*-PrOH, 1 mL/min, 35 °C; t_{R1} = 16.75 min, t_{R2} = 21.84 min; enantiomeric ratio ~50:50, regioisomeric ratio 4:1.

IR (KBr): 3307, 1741, 1643, 1612, 1545, 1469, 1406, 1359, 1113, 755 cm^{-1}.

^1H NMR (400 MHz, $CDCl_3$): δ = 9.28 (br s, 1 H), 7.67–7.59 (m, 2 H), 7.19–7.14 (m, 1 H), 7.05–7.01 (m, 2 H), 6.97–6.93 (m, 1 H), 6.30–6.23 (m, 1 H), 5.42 (dd, *J* = 7.12, 6.13 Hz, 1 H), 3.84 (dd, *J* = 17.1, 5.8 Hz, 1 H), 3.39 (dd, *J* = 17.1, 7.4 Hz, 1 H), 2.25 (s, 3 H).

^{13}C NMR (101 MHz, $CDCl_3$): δ = 202.3, 185.6, 182.1, 158.3, 149.9, 138.8, 131.1, 126.1, 125.5, 124.5, 118.2, 117.3, 111.4, 111.1, 57.0, 35.3, 26.9.

MS (70 eV): *m*/*z* = 310 [M^+], 292, 268, 197, 146, 119, 94, 66, 43.

HRMS (ESI-QTOF): *m*/*z* [M + Na]$^+$ calcd for $C_{17}H_{14}N_2O_4$ + Na: 333.0846; found: 333.0847.

(*R*)-1-(2,5-Dioxohexan-3-yl)indoline-2,3-dione (9a)

Yield: 24 mg (93%); orange crystals; mp 123–125 °C; $[\alpha]_D^{25}$ +129 (*c* 0.25, $CHCl_3$).

HPLC: Chiralcel OD-H column; 254 nm, 7:3 hexane–*i*-PrOH, 1 mL/min, 35 °C; t_R = 12.29 min (major isomer), t_R = 14.39 min (minor isomer); enantiomeric ratio 91.5:8.5, ee 83%.

IR (KBr): 1757, 1736, 1723, 1610, 1472, 1449, 1364, 1193, 1172, 768 cm^{-1}.

^1H NMR (400 MHz, $CDCl_3$): δ = 7.65 (dd, *J* = 7.5, 0.8 Hz, 1 H), 7.61 (td, *J* = 7.9, 1.4 Hz, 1 H), 7.18 (td, *J* = 7.6, 0.6 Hz, 1 H), 6.97 (d, *J* = 8.0 Hz, 1 H), 5.24 (t, *J* = 6.7 Hz, 1 H), 3.58 (dd, *J* = 18.0, 7.2 Hz, 1 H), 2.85 (dd, *J* = 18.0, 5.7 Hz, 1 H), 2.24 (s, 3 H), 2.19 (s, 3 H).

^{13}C NMR (101 MHz, $CDCl_3$): δ = 204.5, 202.2, 182.1, 158.2, 149.7, 138.9, 126.1, 124.6, 118.2, 111.0, 56.5, 40.8, 30.2, 26.7.

MS (70 eV): *m*/*z* = 259 [M^+], 217, 188, 175, 146, 119, 90, 43.

HRMS (ESI-QTOF): *m*/*z* [M + Na]$^+$ calcd for $C_{14}H_{13}NO_4$ + Na: 282.0737; found: 282.0736.

(*S*)-1-(1,4-Dioxo-1,4-diphenylbutan-2-yl)indoline-2,3-dione (9b)

Yield: 37 mg (>95%); yellow crystals; mp 74–76 °C; $[\alpha]_D^{25}$ –228 (*c* 0.25, $CHCl_3$).

HPLC: Chiralpak AD-H column; 254 nm, 7:3 hexane–*i*-PrOH, 1 mL/min, 35 °C; t_R = 20.60 min (major isomer), t_R = 19.11 min (minor isomer); enantiomeric ratio 97.5:2.5, ee 95%.

IR (KBr): 1740, 1682, 1611, 1469, 1449, 1348, 1221, 1179, 1001, 756, 690 cm^{-1}.

^1H NMR (400 MHz, $CDCl_3$): δ = 8.04–7.93 (m, 4 H), 7.63–7.53 (m, 4 H), 7.51–7.39 (m, 4 H), 7.19 (d, *J* = 8.1 Hz, 1 H), 7.14–7.08 (m, 1 H), 6.55 (dd, *J* = 8.3, 5.0 Hz, 1 H), 4.36 (dd, *J* = 17.7, 8.4 Hz, 1 H), 3.46 (dd, *J* = 17.6, 5.0 Hz, 1 H).

^{13}C NMR (101 MHz, $CDCl_3$): δ = 196.1, 194.6, 181.9, 157.6, 149.5, 138.8, 136.1, 134.4, 134.3, 133.9, 129.2, 128.9, 128.7, 128.3, 125.9, 124.3, 118.2, 111.9, 51.7, 36.6.

MS (70 eV): *m*/*z* = 383 [M^+], 355, 278, 236, 208, 147, 119,105, 77, 69.

HRMS (ESI-QTOF): *m*/*z* [M + Na]$^+$ calcd for $C_{24}H_{17}NO_4$ + Na: 406.1050; found: 406.1053.

(*S*)-1-[1,4-Dioxo-1,4-di(-*p*-tolyl)butan-2-yl]indoline-2,3-dione (9c)

Yield: 40 mg (>95%); yellow needles; mp 115–117 °C; $[\alpha]_D^{25}$ –204 (*c* 0.25, $CHCl_3$).

HPLC: Chiralpak AD-H column; 254 nm, 7:3 hexane–*i*-PrOH, 1 mL/min, 35 °C; t_R = 26.58 min (major isomer); t_R = 33.55 min (minor isomer); enantiomeric ratio 97.5:2.5, ee 95%.

IR (KBr): 2922, 1740, 1679, 1610, 1469, 1348, 1182, 1004, 817, 755 cm^{-1}.

^1H NMR (400 MHz, $CDCl_3$): δ = 7.90 (d, *J* = 8.2 Hz, 2 H), 7.86 (d, *J* = 8.2 Hz, 2 H), 7.60–7.51 (m, 2 H), 7.25–7.16 (m, 4 H), 7.09 (t, *J* = 7.5 Hz, 1 H), 6.52 (dd, *J* = 8.2, 5.1 Hz, 1 H), 4.30 (dd, *J* = 17.6, 8.3 Hz, 1 H), 3.43 (dd, *J* = 17.6, 5.1 Hz, 1 H), 2.40 (s, 3 H), 2.36 (s, 3 H).

^{13}C NMR (101 MHz, $CDCl_3$): δ = 195.7, 194.2, 182.1, 157.6, 149.6, 145.4, 144.8, 138.7, 133.7, 131.8, 129.8, 129.5, 128.85, 128.4, 125.8, 124.2, 118.2, 112.0, 51.7, 36.4, 21.84, 21.82.

MS (70 eV): *m*/*z* = 411 [M^+], 383, 386, 319, 264, 147, 119, 91, 65, 43.

HRMS (ESI-QTOF): *m*/*z* [M + Na]$^+$ calcd for $C_{26}H_{21}NO_4$ + Na: 434.1363; found: 434.1361.

(*S*)-1-[1,4-Bis(4-methoxyphenyl)-1,4-dioxobutan-2-yl]indoline-2,3-dione (9d)

Yield: 44 mg (>95%); yellow crystals; mp 172–174 °C; $[\alpha]_D^{25}$ –197 (*c* 0.25, $CHCl_3$).

HPLC: Chiralpak AD-H column; 254 nm, 7:3 hexane–*i*-PrOH, 1 mL/min, 35 °C; t_R = 72.59 min (major isomer), t_R = 93.09 min (minor isomer); enantiomeric ratio 92:8, ee 84%.

IR (KBr): 2932, 1741, 1673, 1600, 1512, 1468, 1348, 1262, 1171, 1028, 837, 757 cm^{-1}.

^1H NMR (400 MHz, $CDCl_3$): δ = 8.06–7.97 (m, 2 H), 7.99–7.90 (m, 2 H), 7.61–7.49 (m, 2 H), 7.20 (d, *J* = 7.9 Hz, 1 H), 7.10 (t, *J* = 7.8 Hz, 1 H), 6.97–6.84 (m, 4 H), 6.54 (dd, *J* = 8.4, 5.0 Hz, 1 H), 4.29 (dd, *J* = 17.4, 8.5 Hz, 1 H), 3.86 (s, 3 H), 3.83 (s, 3 H), 3.39 (dd, *J* = 17.4, 5.0 Hz, 1 H).

^{13}C NMR (101 MHz, $CDCl_3$): δ = 194.5, 192.9, 182.2, 164.5, 164.1, 157.6, 149.7, 138.7, 131.3, 130.6, 129.3, 127.2, 125.8, 124.2, 118.2, 114.4, 114.0, 112.3, 55.7, 55.7, 51.4, 36.1.

MS (70 eV): *m*/*z* = 443 [M^+], 411, 374, 296, 253, 161, 147, 135, 119, 107, 92, 77, 64, 43.

HRMS (ESI-QTOF): *m*/*z* [M + Na]$^+$ calcd for $C_{26}H_{21}NO_6$ + Na: 466.1261; found: 466.1264.

(*S*)-1-[1,4-Bis(4-chlorophenyl)-1,4-dioxobutan-2-yl]indoline-2,3-dione (9e)

Yield: 44 mg (>95%); yellow crystals; mp 189–191 °C; $[\alpha]_D^{25}$ –171 (*c* 0.25, $CHCl_3$).

HPLC: Chiralpak AS-H column; 254 nm, 95:5 hexane–*i*-PrOH, 1.0 mL/min, 35 °C; t_R = 89.06 min (major isomer), t_R = 75.87 min (minor isomer); enantiomeric ratio 93.5:6.5, ee 87%.

IR (KBr): 1741, 1685, 1612, 1469, 1357, 1219, 1093, 831, 755 cm^{-1}.

^1H NMR (400 MHz, $CDCl_3$): δ = 7.97–7.86 (m, 4 H), 7.62–7.55 (m, 2 H), 7.47–7.43 (m, 2 H), 7.40 (d, *J* = 8.6 Hz, 2 H), 7.17–7.10 (m, 2 H), 6.47 (dd, *J* = 8.7, 4.5 Hz, 1 H), 4.34 (dd, *J* = 17.6, 8.8 Hz, 1 H), 3.36 (dd, *J* = 17.6, 4.6 Hz, 1 H).

^{13}C NMR (101 MHz, $CDCl_3$): δ = 194.9, 193.4, 181.7, 157.6, 149.2, 141.1, 140.5, 138.8, 134.3, 132.5, 130.1, 129.7, 129.6, 129.3, 126.1, 124.6, 118.2, 111.8, 51.5, 36.5.

MS (70 eV): *m*/*z* = 451 [M^+], 339, 304, 269, 193, 165, 139, 119, 111, 92, 75, 64.

HRMS (ESI-QTOF): *m*/*z* [M + Na]$^+$ calcd for $C_{24}H_{15}Cl_2NO_4$ + Na: 474.0270; found: 474.1287.

(*S*)-1-[1,4-Bis(4-bromophenyl)-1,4-dioxobutan-2-yl]indoline-2,3-dione (9f)

Yield: 39 mg (72%); orange needles; mp 184–186 °C; $[\alpha]_D^{25}$ –112 (*c* 0.25, $CHCl_3$).

HPLC: Chiralpak AD-H column; 254 nm, 7:3 hexane–*i*-PrOH, 1 mL/min, 35 °C; t_R = 39.27 min (major isomer), t_R = 45.82 min (minor isomer); enantiomeric ratio 82:18, ee 64%.

IR (KBr): 1740, 1682, 1612, 1585, 1469, 1348, 1179, 1071, 1005, 820, 754 cm^{-1}.

^1H NMR (400 MHz, $CDCl_3$): δ = 7.91–7.76 (m, 4 H), 7.66–7.50 (m, 6 H), 7.20–7.05 (m, 2 H), 6.45 (dd, *J* = 8.7, 4.6 Hz, 1 H), 4.33 (dd, *J* = 17.7, 8.8 Hz, 1 H), 3.35 (dd, *J* = 17.6, 4.6 Hz, 1 H).

^{13}C NMR (101 MHz, $CDCl_3$): δ = 195.1, 193.7, 181.6, 157.6, 149.1, 138.8, 134.7, 132.9, 132.5, 132.3, 130.1, 129.9, 129.8, 129.3, 126.1, 124.6, 118.2, 111.8, 51.5, 36.4.

MS (70 eV): *m*/*z* = 541 [M^+], 394, 392, 317, 315, 287, 285, 211, 209, 185, 183, 157, 155, 147, 119, 92, 76, 64.

HRMS (ESI-QTOF): *m*/*z* [M + H]$^+$ calcd for $C_{24}H_{15}Br_2NO_4$: 539.9441; found: 539.9443.

(*S*)-1-[1,4-Bis(4-nitrophenyl)-1,4-dioxobutan-2-yl]indoline-2,3-dione (9g)

Yield: 35 mg (74%); yellow crystalline solid; mp 255–258 °C; $[\alpha]_D^{25}$ –105 (*c* 0.125, DMSO).

IR (KBr): 1743, 1689, 1612, 1525, 1468, 1346, 1280, 1108, 1008, 855, 755 cm^{-1}.

^1H NMR (400 MHz, $CDCl_3$): δ = 8.38–8.33 (m, 2 H), 8.32–8.26 (m, 2 H), 8.19–8.10 (m, 4 H), 7.70–7.59 (m, 2 H), 7.20 (t, *J* = 7.6 Hz, 1 H), 7.17 (d, *J* = 7.9 Hz, 1 H), 6.49 (dd, *J* = 8.7, 4.1 Hz, 1 H), 4.47 (dd, *J* = 17.8, 8.9 Hz, 1 H), 3.40 (dd, *J* = 17.8, 4.3 Hz, 1 H).

^{13}C NMR (101 MHz, $CDCl_3$): δ = 194.6, 193.4, 181.1, 157.6, 151.1, 151.0, 148.6, 140.1, 139.0, 138.8, 129.7, 129.5, 126.5, 125.1, 124.4, 124.3, 118.3, 111.4, 52.0, 37.1.

MS (70 eV): *m*/*z* = 351, 326, 298, 176, 150, 119, 104, 92, 76, 64.

HRMS (ESI-QTOF): *m*/*z* [M + Na]$^+$ calcd for $C_{24}H_{15}N_3O_8$ + Na: 496.0751; found: 496.0752.

1-(3-Oxo-1,3-diphenylpropyl)indoline-2,3-dione (10)

Yield: 23 mg (39%); orange crystals; mp 146–149 °C; $[\alpha]_D^{25}$ +14 (*c* 0.25, $CHCl_3$).

HPLC: Chiralpak AD-H column; 254 nm, 7:3 hexane–*i*-PrOH, 1 mL/min, 35 °C; t_R = 14.85 min major isomer, t_R = 16.22 min (minor isomer); enantiomeric ratio 96:4, ee 92%.

IR (KBr): 1734, 1679, 1611, 1468, 1350, 1211, 1020, 750, 693 cm^{-1}.

^1H NMR (400 MHz, $CDCl_3$): δ = 8.01–7.94 (m, 2 H), 7.61–7.49 (m, 5 H), 7.49–7.41 (m, 2 H), 7.41–7.29 (m, 3 H), 7.15–7.06 (m, 2 H), 5.75 (dd, *J* = 9.1, 4.9 Hz, 1 H), 4.76 (dd, *J* = 18.1, 9.2 Hz, 1 H), 3.72 (dd, *J* = 18.1, 4.9 Hz, 1 H).

^{13}C NMR (101 MHz, $CDCl_3$): δ = 196.9, 183.2, 158.8, 151.6, 138.5, 138.4, 136.3, 133.8, 129.3, 128.9, 128.6, 128.4, 127.3, 125.5, 123.8, 117.9, 111.3, 54.0, 41.4.

MS (70 eV): *m*/*z* = 355 [M^+], 250, 208, 179, 146, 119, 105, 92, 77.

HRMS (ESI-QTOF): *m*/*z* [M + Na]$^+$ calcd for $C_{23}H_{17}NO_3$ + Na: 378.1101; found: 378.1104.

1-(4-Oxo-4-phenylbutan-2-yl)indoline-2,3-dione (11)

Yield: 27 mg (92%); reddish crystals; mp 116–118 °C; $[\alpha]_D^{25}$ +9 (*c* 0.25, $CHCl_3$).

HPLC: Chiralcel OJ-H column; 254 nm, 7:3 hexane–*i*-PrOH, 1 mL/min, 35 °C; t_R = 22.00 min (major isomer), t_R = 27.22 min (minor isomer); enantiomeric ratio 96.5:3.5, ee 93%.

IR (KBr): 2980, 1731, 1683, 1613, 1470, 1353, 1219, 1311, 1220, 1003, 755, 691 cm^{-1}.

^1H NMR (400 MHz, $CDCl_3$): δ = 7.97–7.89 (m, 2 H), 7.62 (td, *J* = 7.9, 1.4 Hz, 1 H), 7.59–7.53 (m, 2 H), 7.44 (t, *J* = 7.7 Hz, 2 H), 7.19 (d, *J* = 8.1 Hz, 1 H), 7.12–7.05 (m, 1 H), 4.81–4.70 (m, 1 H), 4.12 (dd, *J* = 18.0, 7.9 Hz, 1 H), 3.43 (dd, *J* = 18.0, 5.5 Hz, 1 H), 1.61 (d, *J* = 7.0 Hz, 3 H).

^{13}C NMR (101 MHz, $CDCl_3$): δ = 197.6, 183.5, 158.6, 151.4, 138.5, 136.4, 133.7, 128.9, 128.3, 125.6, 123.5, 117.8, 110.9, 45.9, 41.9, 18.0.

MS (70 eV): *m*/*z* = 293 [M^+], 236, 160, 146, 105, 90, 77.

HRMS (ESI-QTOF): *m*/*z* [M + Na]$^+$ calcd for $C_{18}H_{15}NO_3$ + Na: 316.0944; found: 316.0949.

Dibenzyl 2-(2,3-Dioxoindolin-1-yl)succinate (12)

Yield: 7 mg (16%); yellow needles; mp 99–101 °C; $[\alpha]_D^{25}$ –9 (*c* 0.25, $CHCl_3$).

HPLC: Chiralpak AD-H column; 254 nm, 7:3 hexane–*i*-PrOH, 1 mL/min, 35 °C; t_R = 27.84 min (major isomer), t_R = 14.63 min (minor isomer); enantiomeric ratio 75.5:24.5, ee 51%.

IR (KBr): 3034, 1739, 1613, 1471, 1361, 1310, 1218, 1169, 910, 753, 698 cm^{-1}.

^{1}H NMR (400 MHz, $CDCl_3$/TMS): δ = 7.60–7.57 (m, 1 H), 7.48 (td, *J* = 7.9, 1.3 Hz, 1 H), 7.34–7.24 (m, 8 H), 7.24–7.18 (m, 2 H), 7.10 (t, *J* = 7.5 Hz, 1 H), 6.83 (d, *J* = 8.0 Hz, 1 H), 5.36 (dd, *J* = 8.5, 6.0 Hz, 1 H), 5.18 (d, *J* = 12.2 Hz, 1 H), 5.15 (d, *J* = 12.2 Hz, 1 H), 5.10 (d, *J* = 12.2 Hz, 1 H), 5.07 (d, *J* = 12.2 Hz, 1 H), 3.43 (dd, *J* = 16.9, 6.0 Hz, 1 H), 3.14 (dd, *J* = 16.9, 8.5 Hz, 1 H).

^{13}C NMR (101 MHz, $CDCl_3$): δ = 182.1, 169.8, 167.8, 158.1, 149.8, 138.5, 135.2, 134.7, 128.8, 128.7 (4C), 128.6, 128.5 (4C), 125.8, 124.1, 118.0, 110.8, 68.4, 67.3, 51.0, 33.9.

MS (70 eV): *m*/*z* = 443 [M$^+$], 352, 280, 266, 236, 172, 146, 117, 107, 91, 77.

HRMS (ESI-QTOF): *m*/*z* [M + Na]$^+$ calcd for $C_{26}H_{21}NO_6$ + Na: 466.1261; found: 466.1269.

Diethyl 2-[1-(5-Nitro-2,3-dioxoindolin-1-yl)ethyl]malonate (13)

Yield: 9 mg (25%); yellow viscous oil.

HPLC: Chiralpak AD-H column; 254 nm, 7:3 hexane–*i*-PrOH, 1 mL/min, 35 °C; t_R = 18.56 min (major isomer), t_R = 34.31 min (minor isomer); enantiomeric ratio 61.5:38.5.

IR (KBr): 2985, 1754, 1615, 1528, 1473, 1343, 1280, 1223, 1020, 839, 748 cm^{-1}.

^{1}H NMR (400 MHz, $CDCl_3$): δ = 8.54 (dd, *J* = 8.8, 2.4 Hz, 1 H), 8.44 (d, *J* = 2.3 Hz, 1 H), 7.32 (d, *J* = 8.9 Hz, 1 H), 4.73 (dq, *J* = 13.7, 6.8 Hz, 1 H), 4.45 (d, *J* = 11.0 Hz, 1 H), 4.29 (q, *J* = 7.1 Hz, 2 H), 4.04 (qq, *J* = 10.8, 7.1 Hz, 2 H), 1.59 (d, *J* = 6.9 Hz, 3 H), 1.32 (t, *J* = 7.1 Hz, 3 H), 1.11 (t, *J* = 7.1 Hz, 3 H).

^{13}C NMR (101 MHz, $CDCl_3$): δ = 180.9, 167.1, 166.9, 158.1, 155.2, 144.1, 133.6, 121.1, 117.4, 111.7, 62.5, 62.4, 54.2, 49.7, 16.1, 14.2, 14.0.

MS (70 eV): *m*/*z* = 378 [M$^+$], 332, 286, 219, 191, 164, 141, 113, 85, 69.

HRMS (ESI-QTOF): *m*/*z* [M + Na]$^+$ calcd for $C_{17}H_{18}N_2O_8$ + Na: 401.0955; found: 401.0956.

Acknowledgment

The authors thank the Estonian Ministry of Education and Research (Grant Nos. IUT 19-32, IUT19-9, and B25) and the EU European Regional Development Fund (3.2.0101.08-0017) for financial support. We thank Dr. Aleksander-Mati Müürisepp and Ms. Tiina Aid from the Tallinn University of Technology for assistance with MS and IR measurements, respectively. We thank Mr. Dmitri Trubicyn for the synthesis of the starting compounds and preliminary asymmetric experiments.

Supporting Information

Supporting information for this article is available online at http://dx.doi.org/10.1055/s-0034-1379956.

References

(1) Da Silva, J. F. M.; Garden, S. J.; Pinto, A. C. *J. Braz. Chem. Soc.* **2001**, *12*, 273.
(2) (a) Bhrigu, B.; Pathak, D.; Siddiqui, N.; Alam, M. S.; Ahsan, W. *Int. J. Pharm. Sci. Drug Res.* **2010**, *2*, 229. (b) Vine, K. L.; Matesic, L.; Locke, J.; Skropeta, D. *Anti-Cancer Agents Med. Chem.* **2013**, *2*, 254. (c) Pawar, V. S.; Lokwani, D. K.; Bhandari, S. V.; Bothara, K. G.; Chitre, T. S.; Devale, T. L.; Modhave, N. S.; Parikh, J. K. *Med. Chem. Res.* **2011**, *20*, 370. (d) Kumari, G.; Singh, R. K. *Med. Chem. Res.* **2013**, *22*, 927. (e) Zahid, H. C.; Humajun, P.; Rauf, A.; Khalid, M. K.; Claudiu, H. S. *J. Enzyme Inhib. Med. Chem.* **2004**, *19*, 417.
(3) For recent reviews, see: (a) Liu, Y.-C.; Zhang, R.; Wu, Q.-Y.; Chen, Q.; Yang, G.-F. *Org. Prep. Proced. Int.* **2014**, *46*, 317. (b) Borad, M. A.; Bhoi, M. N.; Prajapati, N. P.; Patel, H. D. *Synth. Commun.* **2014**, *44*, 1043. (c) Borad, M. A.; Bhoi, M. N.; Prajapati, N. P.; Patel, H. D. *Synth. Commun.* **2014**, *44*, 897. (d) Xia, M.; Ma, R.-Z. *J. Heterocycl. Chem.* **2014**, *51*, 539. (e) Mohammadi, S.; Heiran, R.; Herrera, R. P.; Marqués-López, E. *ChemCatChem* **2013**, *5*, 2131.
(4) Silva, B. F. *J. Braz. Chem. Soc.* **2013**, *24*, 707.
(5) Liu, Y.; Wang, H.; Wan, J. *Asian J. Org. Chem.* **2013**, *112*, 6104.
(6) Singh, G. S.; Desta, Z. Y. *Chem. Rev.* **2012**, *112*, 6104.
(7) Schmidt, M. S.; Reverdito, A. M.; Kremenchuzky, L.; Perillo, I. A.; Blanco, M. M. *Molecules* **2008**, *13*, 831.
(8) Yang, W.; Du, D.-M. *Chem. Commun.* **2013**, *49*, 8842.
(9) Coppola, G. M. *J. Heterocycl. Chem.* **1987**, *24*, 1249.
(10) (a) Imanzadeh, G.; Aghaalizadeh, T.; Zamanloo, M.; Mansoori, Y. *J. Chil. Chem. Soc.* **2011**, *56*, 616; *Chem. Abstr.* **2011**, *155*, 661939. (b) Imanzadeh, G. H.; Mollaei Tavana, M.; Zamanloo, M. R.; Mansoori, Y. *Chin. J. Chem.* **2009**, *27*, 389; *Chem. Abstr.* **2009**, *151*, 510383. (c) Imanzadeh, G.; Soltanizadeh, Z.; Khodayari, A.; Zamanloo, M.; Mansoori, Y.; Salehzadeh, J. *Chin. J. Chem.* **2012**, *30*, 891; *Chem. Abstr.* **2012**, *157*, 550775.
(11) (a) Kumar, S. B.; Ravinder, M.; Kishore, G.; Rao, V. J.; Yogeeswari, P.; Sriram, D. *Med. Chem. Res.* **2014**, *23*, 1934. (b) Xie, C.; Tang, M.-L.; Li, F.-N.; Guan, L.-P.; Pan, C.-Y.; Wang, S.-H. *Med. Chem. Res.* **2014**, *23*, 2161. (c) Chu, W.; Rothfus, J.; Zhou, D.; Mach, R. H. *Bioorg. Med. Chem. Lett.* **2011**, *21*, 2192.
(12) Kester, R. F. US Patent 20120142705 A1, **2012**; *Chem. Abstr.* **2012**, *157*, 814268.
(13) Zhao, M.-X.; Chen, M.-X.; Tang, W.-H.; Wei, D.-K.; Dai, T.-L.; Shi, M. *Eur. J. Org. Chem.* **2012**, 3598.
(14) Dou, X.; Yao, W.; Jiang, C.; Lu, Y. *Chem. Commun.* **2014**, *50*, 11354.
(15) (a) Žari, S.; Kailas, T.; Kudrjashova, M.; Öeren, M.; Järving, I.; Tamm, T.; Lopp, M.; Kanger, T. *Beilstein J. Org. Chem.* **2012**, *8*, 1452. (b) Ošeka, M.; Noole, A.; Žari, S.; Öeren, M.; Järving, I.; Lopp, M.; Kanger, T. *Eur. J. Org. Chem.* **2014**, 3599.
(16) (a) Noole, A.; Sucman, N. S.; Kabeshov, M. A.; Kanger, T.; Macaev, F. Z.; Malkov, A. V. *Chem. Eur. J.* **2012**, *18*, 14929. (b) Noole, A.; Järving, I.; Werner, F.; Lopp, M.; Malkov, A.; Kanger, T. *Org. Lett.* **2012**, *14*, 4922. (c) Noole, A.; Ošeka, M.; Pehk, T.; Öeren, M.; Järving, I.; Elsegood, M. R. J.; Malkov, A. V.; Lopp, M.; Kanger, T. *Adv. Synth. Catal.* **2013**, *355*, 829. (d) Noole, A.; Ilmarinen, K.; Järving, I.; Lopp, M.; Kanger, T. *J. Org. Chem.* **2013**, *78*, 8117.

(17) Žari, S.; Kudrjashova, M.; Pehk, T.; Lopp, M.; Kanger, T. *Org. Lett.* **2014**, *16*, 1740.
(18) Liu, H.; Wu, H.; Luo, Z.; Shen, J.; Kang, G.; Liu, B.; Wan, Z.; Jiang, J. *Chem. Eur. J.* **2012**, *18*, 11899.
(19) Probst, N.; Madarász, Á.; Valkonen, A.; Pápai, I.; Rissanen, K.; Neuvonen, A.; Pihko, P. M. *Angew. Chem. Int. Ed.* **2012**, *34*, 8495; *Angew. Chem.* **2012**, *124*, 8623.
(20) Wang, J.; Cieplak, P.; Kollman, P. A. *J. Comput. Chem.* **2000**, *21*, 1049.
(21) Darden, T.; York, D.; Pedersen, L. *J. Chem. Phys.* **1993**, *98*, 10089.
(22) Vakulya, B.; Varga, S.; Csámpai, A.; Soós, T. *Org. Lett.* **2005**, *7*, 1967.
(23) Tomotaka, O.; Hoashi, Y.; Takemoto, Y. *J. Am. Chem. Soc.* **2003**, *125*, 12672.
(24) Lee, J. W.; Ryu, T. H.; Oh, J. S.; Bae, H. Y.; Janga, H. B.; Song, C. E. *Chem. Commun.* **2009**, 7224.
(25) Li, P.; Wang, Y.; Liang, X.; Ye, J. *Chem. Commun.* **2008**, 3302.
(26) Runcie, K. A.; Taylor, R. J. K. *Chem. Commun.* **2002**, 974.
(27) Conant, J. B.; Lutz, R. E. *J. Am. Chem. Soc.* **1923**, *45*, 1301.

Acknowledgments

This work was conducted in the Department of Chemistry of the Faculty of Science at Tallinn University of Technology. The work was financially supported by the Estonian Ministry of Education and Research (grants IUT 19-32 and SF0140060s12), the Estonian Science Foundation (grant ETF8289), the EU Regional Development Fund (3.2.0101.08-0017) and the Graduate School of Functional Materials and Technologies (FMTDK). We acknowledge COST action CM0905 (ORCA) for networking and collaboration possibilities.

First of all, I would like to thank my supervisor, Professor Tõnis Kanger, for guiding me through my master's and PhD studies, helping me to develop a true scientific attitude and keeping me on the right track while still allowing me to check all my ideas. I thank Dr. Kadri Kriis for teaching me the basics of working in the organic chemistry lab during my bachelor's studies. I am grateful to Professor Margus Lopp for valuable advice and discussions during lab seminars, as well as for delivering splendid lectures. I thank my co-workers, especially Artur, Kristin, Maksim and Kärt, for creating a positive work atmosphere and adding positive emotions to my studies. My thanks to Dr. Marina Kudrjashova, Dr. Tõnis Pehk and Dr. Andrus Metsala for productive co-operative work and broadening my scientific interests. I thank Professor Toomas Tamm and Mario Öeren for help with computational chemistry. I am grateful to all of the people who helped me with all kinds of analyses over the years. Also, I would like to thank Professor Henk Hiemstra and Dr. Jan van Maarseveen and all of the others in the Synthetic Organic Chemistry group of the University of Amsterdam for memorable experiences during my PhD internship. Finally, I thank my family for all of their support during my studies.

"A person who never made a mistake never tried anything new" – *Albert Einstein*

Abstract

H-bond-mediated catalysis has developed into a powerful and versatile tool for asymmetric synthesis. Although a lot of analytical and computational studies of the reaction mechanisms have been conducted, a full understanding of the catalytic processes has not been achieved so far. The structural features of the unsaturated 1,4-dicarbonyl compounds make them excellent targets for asymmetric transformations, affording chiral products possessing different functional groups.

Thiourea **33-** and squaramide **29-**mediated asymmetric desymmetrization of aromatic unsaturated 1,4-diketones with malonates **94** was studied. The Michael products were obtained in excellent yields and high enantioselectivites. In the case of squaramide **29**, running the reaction at 80 °C instead of room temperature made it possible to significantly improve the outcome of the reaction. When β-ketoesters **96** were used as nucleophiles, the diastereoselectivity was low in the case of both catalysts, although both enantiomers were obtained in high enantioselectivity.

Derivatizing isatin **100** into its aniline Schiff base **103a** afforded an excellent nucleophile for a highly stereoselective thiourea **33-**catalyzed aza-Michael addition to unsaturated 1,4-ketoesters **91**, and symmetric and non-symmetric diketones (**89** and **90**). However, using other electrophiles was limited under the same conditions. In order to explain the remote activation of isatin, several techniques were used.

Screening the Schiff bases **103** with different substituents showed that reactivity greatly depended on the nitrogen substituent, with phenyl being the best.

NMR studies of Schiff base/catalyst complexes revealed that in the presence of the catalyst **33** or **4**, changes in chemical shift and the shapes of peaks occurred. The significant changes in the signals corresponding to the nitrogen substituents showed strong interactions between the catalyst and imine.

Molecular dynamics calculations confirmed this assumption, showing three H-bonds between **33** and **103a**, while only one H-bond formed with unsubstituted isatin. Simulation of the addition reaction to aliphatic ketoester further revealed that Shiff base **103a** was far superior to isatin **100**.

Kokkuvõte

Katalüüs H-sideme kaudu on arenenud efektiivseks ja universaalseks asümmeetrilise sünteesi meetodiks. Vaatamata mitmetele analüütilistele ja arvutuskeemia uuringutele, pole katalüütiliste protsesside mehhanism alati selge. Küllastumata 1,4-dikarbonüülühendite struktuuri iseärasused teevad neist suurepärased asümmeetrilise sünteesi sihtmärgid, võimaldades sünteesida polüfunktsionaalseid kiraalseid produkte.

Uuriti tiokarbamiidi **33** ja skvaaramiidi **29** poolt katalüüsitud aromaatsete küllastumata 1,4-diketoonide **90** desümmetriseerimist malonaatidega. Michaeli liitumise produktid saadi väga heade saagiste (kuni 99%) ja kõrgete enantioselektiivsustega (kuni 93%). Skvaaramiidi **29** puhul tõi temperatuuri tõstmine 80 °C-ni kaasa positiivse mõju reaktsioonide tulemustele (suurenes nii kiirus, saagis kui ka enantioselektiivsus). β-ketoestrite kasutamise korral oli tekkinud diastereomeeride suhe madal (kuni 66:34), kuid mõlema diastereomeeri enantiomeersed puhtused olid kõrged (*ee* kuni 90%).

Isatiini **100** derivatiseerimisel aniliiniga saadi Schiffi alus **103a**, milles suurenes oluliselt tsüklis paikneva lämmastikuaatomi nukleofiilsus. Saadi suurepärased nukleofiilid organokatalüütiliseks stereoselektiivseks aza-Michaeli liitumiseks küllastumata 1,4-ketoestritele, sümmeetrilistele ja mittesümmeetrilistele diketoonidele. Teiste elektrofiilide kasutamine samade tingimuste juures on piiratud. Isatiini aktiveerimise mehhanismi uurimiseks kasutati nii sünteetilisi, spektroskoopilisi kui ka arvutuskeemia meetodeid.

Varieerides erinevaid Schiffi aluseid **103** leiti, et derivaadi reaktiivsus sõltub oluliselt imiinist, olles maksimaalne fenüülasendaja korral.

Katalüsaator/imiin komplekside TMR analüüsid näitasid, et katalüsaatori **33** või **4** juuresolekul muutuvad spektris imiinide süsiniku- ja vesinikuaatomite signaalide keemilised nihked ja piikide kuju. Olulised lämmastiku asendaja signaalide muutused viitavad tugevatele interaktsioonidele imiini ja katalüsaatori vahel.

Samuti toetavad seda molekulaardünaamilised arvutused, näidates kolme H-sidet imiini **103a** ja katalüsaatori **33** vahel, samal ajal kui asendamata isatiiniga **100** moodustub ainult üks H-side.

Elulookirjeldus

1. Isikuandmed
Ees- ja perekonnanimi: Sergei Žari
Sünniaeg ja koht: 19.01.1987, Tallinn
Kodakondsus: Eesti

2. Kontaktandmed

Aadress: Keemiainstituut, TTÜ, Akadeemia tee 15, Tallinn 12618
Telefon: +37255522727
E-posti aadress: sergei.zari@ttu.ee

3. Haridus

Tallinna Tehnikaülikool	2011	Loodusteaduste magister, *cum laude*
Tallinna Tehnikaülikool	2009	Loodusteaduste bakalaureus
Tallinna Humanitaargümnaasium	2005	keskharidus

4. Teenistuskäik

1.09.11-31.12.13	TTÜ Keemiainstituut	insener

5. Juhendatud lõputööd

2011-2014	Dmitri Trubitsõni bakalaureusetöö, kaitstud TTÜ-s

6. Teadustöö

Asümmeetriline süntees/katalüüs ja selle rakendamine, uute reaktsioonide väljatöötamine, reaktsioonide mehhanismide uurimine

7. Tunnustused

Tallinna Tehkikaülikooli Teadusosakonna doktoriõppe stipendium **2015**

Curriculum Vitae

1. Personal data

Name: Sergei Žari
Date and place of birth: 19.01.1987, Tallinn
Citizenship: Estonian

2. Contact information

Aadress: Department of Chemistry, TUT, Akadeemia tee 15, Tallinn 12618
Phone: +37255522727
e-mail: sergei.zari@ttu.ee

3. Education

Tallinn University of Technology	2011	*MSc*, *cum laude*
Tallinn University of Technology	2009	*BSc*
Tallinn High School of Humanities	2005	Secondary education

4. Professional appointments

1.09.11-31.12.13	Department of Chemistry, TUT	engineer

5. Supervised theses

2011-2014 Dmitri Trubitsõn's *BSc* thesis, defended at TUT

6. Scientific interests

Asymmetric synthesis/catalysis and its application, development of new reactions, research on reaction mechanisms

7. Awards

TUT Research Administration Office Scholarship **2015**

8. Original publications

1) Žari, S.; Kailas, T.; Kudrjashova, M.; Öeren, M.; Järving, I.; Tamm, T.; Lopp, M.; Kanger, T. Organocatalytic Asymmetric Addition of Malonates to Unsaturated 1,4-Diketones. *Beilstein Journal of Organic Chemistry*, **2012**, *8*, 1452-1457.

2) Žari, S.; Kudrjashova, M.; Pehk, T.; Lopp, M.; Kanger, T. Remote Activation of the Nucleophilicity of Isatin. *Organic Letters*, **2014**, *16*, 1740-1743.

3) Ošeka, M.; Noole, A.; Žari, S.; Öeren, M.; Järving, I.; Lopp, M.; Kanger, T. Asymmetric Diastereoselective Synthesis of Spirocyclopropane Derivatives of Oxindole. *European Journal of Organic Chemistry*, **2014**, 3599-3606.

4) Žari, S. Metsala, A.; Kudrjashova, M.; Kaabel, S.; Järving, I.; Kanger, T. Asymmetric Organocatalytic Aza-Michael Reactions of Isatin Derivatives. *Synthesis*, **2015**, *47*, 875-886.

DISSERTATIONS DEFENDED AT
TALLINN UNIVERSITY OF TECHNOLOGY ON
NATURAL AND EXACT SCIENCES

1. **Olav Kongas**. Nonlinear Dynamics in Modeling Cardiac Arrhytmias. 1998.
2. **Kalju Vanatalu**. Optimization of Processes of Microbial Biosynthesis of Isotopically Labeled Biomolecules and Their Complexes. 1999.
3. **Ahto Buldas**. An Algebraic Approach to the Structure of Graphs. 1999.
4. **Monika Drews**. A Metabolic Study of Insect Cells in Batch and Continuous Culture: Application of Chemostat and Turbidostat to the Production of Recombinant Proteins. 1999.
5. **Eola Valdre**. Endothelial-Specific Regulation of Vessel Formation: Role of Receptor Tyrosine Kinases. 2000.
6. **Kalju Lott**. Doping and Defect Thermodynamic Equilibrium in ZnS. 2000.
7. **Reet Koljak**. Novel Fatty Acid Dioxygenases from the Corals *Plexaura homomalla* and *Gersemia fruticosa.* 2001.
8. **Anne Paju**. Asymmetric oxidation of Prochiral and Racemic Ketones by Using Sharpless Catalyst. 2001.
9. **Marko Vendelin**. Cardiac Mechanoenergetics *in silico*. 2001.
10. **Pearu Peterson**. Multi-Soliton Interactions and the Inverse Problem of Wave Crest. 2001.
11. **Anne Menert**. Microcalorimetry of Anaerobic Digestion. 2001.
12. **Toomas Tiivel**. The Role of the Mitochondrial Outer Membrane in *in vivo* Regulation of Respiration in Normal Heart and Skeletal Muscle Cell. 2002.
13. **Olle Hints**. Ordovician Scolecodonts of Estonia and Neighbouring Areas: Taxonomy, Distribution, Palaeoecology, and Application. 2002.
14. **Jaak Nõlvak**. Chitinozoan Biostratigrapy in the Ordovician of Baltoscandia. 2002.
15. **Liivi Kluge**. On Algebraic Structure of Pre-Operad. 2002.
16. **Jaanus Lass**. Biosignal Interpretation: Study of Cardiac Arrhytmias and Electromagnetic Field Effects on Human Nervous System. 2002.
17. **Janek Peterson**. Synthesis, Structural Characterization and Modification of PAMAM Dendrimers. 2002.
18. **Merike Vaher**. Room Temperature Ionic Liquids as Background Electrolyte Additives in Capillary Electrophoresis. 2002.
19. **Valdek Mikli**. Electron Microscopy and Image Analysis Study of Powdered Hardmetal Materials and Optoelectronic Thin Films. 2003.
20. **Mart Viljus**. The Microstructure and Properties of Fine-Grained Cermets. 2003.
21. **Signe Kask**. Identification and Characterization of Dairy-Related *Lactobacillus.* 2003
22. **Tiiu-Mai Laht**. Influence of Microstructure of the Curd on Enzymatic and Microbiological Processes in Swiss-Type Cheese. 2003.
23. **Anne Kuusksalu**. 2–5A Synthetase in the Marine Sponge *Geodia cydonium*. 2003.

24. **Sergei Bereznev**. Solar Cells Based on Polycristalline Copper-Indium Chalcogenides and Conductive Polymers. 2003.
25. **Kadri Kriis**. Asymmetric Synthesis of C_2-Symmetric Bimorpholines and Their Application as Chiral Ligands in the Transfer Hydrogenation of Aromatic Ketones. 2004.
26. **Jekaterina Reut**. Polypyrrole Coatings on Conducting and Insulating Substracts. 2004.
27. **Sven Nõmm**. Realization and Identification of Discrete-Time Nonlinear Systems. 2004.
28. **Olga Kijatkina**. Deposition of Copper Indium Disulphide Films by Chemical Spray Pyrolysis. 2004.
29. **Gert Tamberg**. On Sampling Operators Defined by Rogosinski, Hann and Blackman Windows. 2004.
30. **Monika Übner**. Interaction of Humic Substances with Metal Cations. 2004.
31. **Kaarel Adamberg**. Growth Characteristics of Non-Starter Lactic Acid Bacteria from Cheese. 2004.
32. **Imre Vallikivi**. Lipase-Catalysed Reactions of Prostaglandins. 2004.
33. **Merike Peld**. Substituted Apatites as Sorbents for Heavy Metals. 2005.
34. **Vitali Syritski**. Study of Synthesis and Redox Switching of Polypyrrole and Poly(3,4-ethylenedioxythiophene) by Using *in-situ* Techniques. 2004.
35. **Lee Põllumaa**. Evaluation of Ecotoxicological Effects Related to Oil Shale Industry. 2004.
36. **Riina Aav**. Synthesis of 9,11-Secosterols Intermediates. 2005.
37. **Andres Braunbrück**. Wave Interaction in Weakly Inhomogeneous Materials. 2005.
38. **Robert Kitt**. Generalised Scale-Invariance in Financial Time Series. 2005.
39. **Juss Pavelson**. Mesoscale Physical Processes and the Related Impact on the Summer Nutrient Fields and Phytoplankton Blooms in the Western Gulf of Finland. 2005.
40. **Olari Ilison**. Solitons and Solitary Waves in Media with Higher Order Dispersive and Nonlinear Effects. 2005.
41. **Maksim Säkki**. Intermittency and Long-Range Structurization of Heart Rate. 2005.
42. **Enli Kiipli**. Modelling Seawater Chemistry of the East Baltic Basin in the Late Ordovician–Early Silurian. 2005.
43. **Igor Golovtsov**. Modification of Conductive Properties and Processability of Polyparaphenylene, Polypyrrole and polyaniline. 2005.
44. **Katrin Laos**. Interaction Between Furcellaran and the Globular Proteins (Bovine Serum Albumin β-Lactoglobulin). 2005.
45. **Arvo Mere**. Structural and Electrical Properties of Spray Deposited Copper Indium Disulphide Films for Solar Cells. 2006.
46. **Sille Ehala**. Development and Application of Various On- and Off-Line Analytical Methods for the Analysis of Bioactive Compounds. 2006.
47. **Maria Kulp**. Capillary Electrophoretic Monitoring of Biochemical Reaction Kinetics. 2006.

48. **Anu Aaspõllu.** Proteinases from *Vipera lebetina* Snake Venom Affecting Hemostasis. 2006.
49. **Lyudmila Chekulayeva**. Photosensitized Inactivation of Tumor Cells by Porphyrins and Chlorins. 2006.
50. **Merle Uudsemaa**. Quantum-Chemical Modeling of Solvated First Row Transition Metal Ions. 2006.
51. **Tagli Pitsi**. Nutrition Situation of Pre-School Children in Estonia from 1995 to 2004. 2006.
52. **Angela Ivask**. Luminescent Recombinant Sensor Bacteria for the Analysis of Bioavailable Heavy Metals. 2006.
53. **Tiina Lõugas**. Study on Physico-Chemical Properties and Some Bioactive Compounds of Sea Buckthorn (*Hippophae rhamnoides* L.). 2006.
54. **Kaja Kasemets**. Effect of Changing Environmental Conditions on the Fermentative Growth of *Saccharomyces cerevisae* S288C: Auxo-accelerostat Study. 2006.
55. **Ildar Nisamedtinov**. Application of ^{13}C and Fluorescence Labeling in Metabolic Studies of *Saccharomyces* spp. 2006.
56. **Alar Leibak**. On Additive Generalisation of Voronoï's Theory of Perfect Forms over Algebraic Number Fields. 2006.
57. **Andri Jagomägi**. Photoluminescence of Chalcopyrite Tellurides. 2006.
58. **Tõnu Martma**. Application of Carbon Isotopes to the Study of the Ordovician and Silurian of the Baltic. 2006.
59. **Marit Kauk**. Chemical Composition of $CuInSe_2$ Monograin Powders for Solar Cell Application. 2006.
60. **Julia Kois**. Electrochemical Deposition of $CuInSe_2$ Thin Films for Photovoltaic Applications. 2006.
61. **Ilona Oja Açik**. Sol-Gel Deposition of Titanium Dioxide Films. 2007.
62. **Tiia Anmann**. Integrated and Organized Cellular Bioenergetic Systems in Heart and Brain. 2007.
63. **Katrin Trummal**. Purification, Characterization and Specificity Studies of Metalloproteinases from *Vipera lebetina* Snake Venom. 2007.
64. **Gennadi Lessin**. Biochemical Definition of Coastal Zone Using Numerical Modeling and Measurement Data. 2007.
65. **Enno Pais**. Inverse problems to determine non-homogeneous degenerate memory kernels in heat flow. 2007.
66. **Maria Borissova**. Capillary Electrophoresis on Alkylimidazolium Salts. 2007.
67. **Karin Valmsen**. Prostaglandin Synthesis in the Coral *Plexaura homomalla*: Control of Prostaglandin Stereochemistry at Carbon 15 by Cyclooxygenases. 2007.
68. **Kristjan Piirimäe**. Long-Term Changes of Nutrient Fluxes in the Drainage Basin of the Gulf of Finland – Application of the PolFlow Model. 2007.
69. **Tatjana Dedova**. Chemical Spray Pyrolysis Deposition of Zinc Sulfide Thin Films and Zinc Oxide Nanostructured Layers. 2007.
70. **Katrin Tomson**. Production of Labelled Recombinant Proteins in Fed-Batch Systems in *Escherichia coli*. 2007.
71. **Cecilia Sarmiento**. Suppressors of RNA Silencing in Plants. 2008.

72. **Vilja Mardla**. Inhibition of Platelet Aggregation with Combination of Antiplatelet Agents. 2008.
73. **Maie Bachmann**. Effect of Modulated Microwave Radiation on Human Resting Electroencephalographic Signal. 2008.
74. **Dan Hüvonen**. Terahertz Spectroscopy of Low-Dimensional Spin Systems. 2008.
75. **Ly Villo**. Stereoselective Chemoenzymatic Synthesis of Deoxy Sugar Esters Involving *Candida antarctica* Lipase B. 2008.
76. **Johan Anton**. Technology of Integrated Photoelasticity for Residual Stress Measurement in Glass Articles of Axisymmetric Shape. 2008.
77. **Olga Volobujeva**. SEM Study of Selenization of Different Thin Metallic Films. 2008.
78. **Artur Jõgi**. Synthesis of 4'-Substituted 2,3'-dideoxynucleoside Analogues. 2008.
79. **Mario Kadastik**. Doubly Charged Higgs Boson Decays and Implications on Neutrino Physics. 2008.
80. **Fernando Pérez-Caballero**. Carbon Aerogels from 5-Methylresorcinol-Formaldehyde Gels. 2008.
81. **Sirje Vaask**. The Comparability, Reproducibility and Validity of Estonian Food Consumption Surveys. 2008.
82. **Anna Menaker**. Electrosynthesized Conducting Polymers, Polypyrrole and Poly(3,4-ethylenedioxythiophene), for Molecular Imprinting. 2009.
83. **Lauri Ilison**. Solitons and Solitary Waves in Hierarchical Korteweg-de Vries Type Systems. 2009.
84. **Kaia Ernits**. Study of In_2S_3 and ZnS Thin Films Deposited by Ultrasonic Spray Pyrolysis and Chemical Deposition. 2009.
85. **Veljo Sinivee**. Portable Spectrometer for Ionizing Radiation "Gammamapper". 2009.
86. **Jüri Virkepu**. On Lagrange Formalism for Lie Theory and Operadic Harmonic Oscillator in Low Dimensions. 2009.
87. **Marko Piirsoo**. Deciphering Molecular Basis of Schwann Cell Development. 2009.
88. **Kati Helmja**. Determination of Phenolic Compounds and Their Antioxidative Capability in Plant Extracts. 2010.
89. **Merike Sõmera**. Sobemoviruses: Genomic Organization, Potential for Recombination and Necessity of P1 in Systemic Infection. 2010.
90. **Kristjan Laes**. Preparation and Impedance Spectroscopy of Hybrid Structures Based on $CuIn_3Se_5$ Photoabsorber. 2010.
91. **Kristin Lippur**. Asymmetric Synthesis of 2,2'-Bimorpholine and its 5,5'-Substituted Derivatives. 2010.
92. **Merike Luman**. Dialysis Dose and Nutrition Assessment by an Optical Method. 2010.
93. **Mihhail Berezovski**. Numerical Simulation of Wave Propagation in Heterogeneous and Microstructured Materials. 2010.
94. **Tamara Aid-Pavlidis**. Structure and Regulation of BDNF Gene. 2010.

95. **Olga Bragina**. The Role of Sonic Hedgehog Pathway in Neuro- and Tumorigenesis. 2010.
96. **Merle Randrüüt**. Wave Propagation in Microstructured Solids: Solitary and Periodic Waves. 2010.
97. **Marju Laars**. Asymmetric Organocatalytic Michael and Aldol Reactions Mediated by Cyclic Amines. 2010.
98. **Maarja Grossberg**. Optical Properties of Multinary Semiconductor Compounds for Photovoltaic Applications. 2010.
99. **Alla Maloverjan**. Vertebrate Homologues of Drosophila Fused Kinase and Their Role in Sonic Hedgehog Signalling Pathway. 2010.
100. **Priit Pruunsild**. Neuronal Activity-Dependent Transcription Factors and Regulation of Human *BDNF* Gene. 2010.
101. **Tatjana Knjazeva**. New Approaches in Capillary Electrophoresis for Separation and Study of Proteins. 2011.
102. **Atanas Katerski**. Chemical Composition of Sprayed Copper Indium Disulfide Films for Nanostructured Solar Cells. 2011.
103. **Kristi Timmo.** Formation of Properties of $CuInSe_2$ and $Cu_2ZnSn(S,Se)_4$ Monograin Powders Synthesized in Molten KI. 2011.
104. **Kert Tamm**. Wave Propagation and Interaction in Mindlin-Type Microstructured Solids: Numerical Simulation. 2011.
105. **Adrian Popp**. Ordovician Proetid Trilobites in Baltoscandia and Germany. 2011.
106. **Ove Pärn**. Sea Ice Deformation Events in the Gulf of Finland and This Impact on Shipping. 2011.
107. **Germo Väli**. Numerical Experiments on Matter Transport in the Baltic Sea. 2011.
108. **Andrus Seiman**. Point-of-Care Analyser Based on Capillary Electrophoresis. 2011.
109. **Olga Katargina**. Tick-Borne Pathogens Circulating in Estonia (Tick-Borne Encephalitis Virus, *Anaplasma phagocytophilum*, *Babesia* Species): Their Prevalence and Genetic Characterization. 2011.
110. **Ingrid Sumeri**. The Study of Probiotic Bacteria in Human Gastrointestinal Tract Simulator. 2011.
111. **Kairit Zovo**. Functional Characterization of Cellular Copper Proteome. 2011.
112. **Natalja Makarytsheva**. Analysis of Organic Species in Sediments and Soil by High Performance Separation Methods. 2011.
113. **Monika Mortimer**. Evaluation of the Biological Effects of Engineered Nanoparticles on Unicellular Pro- and Eukaryotic Organisms. 2011.
114. **Kersti Tepp**. Molecular System Bioenergetics of Cardiac Cells: Quantitative Analysis of Structure-Function Relationship. 2011.
115. **Anna-Liisa Peikolainen**. Organic Aerogels Based on 5-Methylresorcinol. 2011.
116. **Leeli Amon**. Palaeoecological Reconstruction of Late-Glacial Vegetation Dynamics in Eastern Baltic Area: A View Based on Plant Macrofossil Analysis. 2011.

117. **Tanel Peets**. Dispersion Analysis of Wave Motion in Microstructured Solids. 2011.
118. **Liina Kaupmees**. Selenization of Molybdenum as Contact Material in Solar Cells. 2011.
119. **Allan Olspert**. Properties of VPg and Coat Protein of Sobemoviruses. 2011.
120. **Kadri Koppel**. Food Category Appraisal Using Sensory Methods. 2011.
121. **Jelena Gorbatšova**. Development of Methods for CE Analysis of Plant Phenolics and Vitamins. 2011.
122. **Karin Viipsi**. Impact of EDTA and Humic Substances on the Removal of Cd and Zn from Aqueous Solutions by Apatite. 2012.
123. **David Schryer**. Metabolic Flux Analysis of Compartmentalized Systems Using Dynamic Isotopologue Modeling. 2012.
124. **Ardo Illaste**. Analysis of Molecular Movements in Cardiac Myocytes. 2012.
125. **Indrek Reile**. 3-Alkylcyclopentane-1,2-Diones in Asymmetric Oxidation and Alkylation Reactions. 2012.
126. **Tatjana Tamberg**. Some Classes of Finite 2-Groups and Their Endomorphism Semigroups. 2012.
127. **Taavi Liblik**. Variability of Thermohaline Structure in the Gulf of Finland in Summer. 2012.
128. **Priidik Lagemaa**. Operational Forecasting in Estonian Marine Waters. 2012.
129. **Andrei Errapart**. Photoelastic Tomography in Linear and Non-linear Approximation. 2012.
130. **Külliki Krabbi**. Biochemical Diagnosis of Classical Galactosemia and Mucopolysaccharidoses in Estonia. 2012.
131. **Kristel Kaseleht**. Identification of Aroma Compounds in Food using SPME-GC/MS and GC-Olfactometry. 2012.
132. **Kristel Kodar**. Immunoglobulin G Glycosylation Profiling in Patients with Gastric Cancer. 2012.
133. **Kai Rosin**. Solar Radiation and Wind as Agents of the Formation of the Radiation Regime in Water Bodies. 2012.
134. **Ann Tiiman**. Interactions of Alzheimer's Amyloid-Beta Peptides with Zn(II) and Cu(II) Ions. 2012.
135. **Olga Gavrilova**. Application and Elaboration of Accounting Approaches for Sustainable Development. 2012.
136. **Olesja Bondarenko**. Development of Bacterial Biosensors and Human Stem Cell-Based *In Vitro* Assays for the Toxicological Profiling of Synthetic Nanoparticles. 2012.
137. **Katri Muska**. Study of Composition and Thermal Treatments of Quaternary Compounds for Monograin Layer Solar Cells. 2012.
138. **Ranno Nahku**. Validation of Critical Factors for the Quantitative Characterization of Bacterial Physiology in Accelerostat Cultures. 2012.
139. **Petri-Jaan Lahtvee**. Quantitative Omics-level Analysis of Growth Rate Dependent Energy Metabolism in *Lactococcus lactis*. 2012.
140. **Kerti Orumets**. Molecular Mechanisms Controlling Intracellular Glutathione Levels in Baker's Yeast *Saccharomyces cerevisiae* and its Random Mutagenized Glutathione Over-Accumulating Isolate. 2012.

141. **Loreida Timberg**. Spice-Cured Sprats Ripening, Sensory Parameters Development, and Quality Indicators. 2012.
142. **Anna Mihhalevski**. Rye Sourdough Fermentation and Bread Stability. 2012.
143. **Liisa Arike**. Quantitative Proteomics of *Escherichia coli*: From Relative to Absolute Scale. 2012.
144. **Kairi Otto**. Deposition of In_2S_3 Thin Films by Chemical Spray Pyrolysis. 2012.
145. **Mari Sepp**. Functions of the Basic Helix-Loop-Helix Transcription Factor TCF4 in Health and Disease. 2012.
146. **Anna Suhhova**. Detection of the Effect of Weak Stressors on Human Resting Electroencephalographic Signal. 2012.
147. **Aram Kazarjan**. Development and Production of Extruded Food and Feed Products Containing Probiotic Microorganisms. 2012.
148. **Rivo Uiboupin**. Application of Remote Sensing Methods for the Investigation of Spatio-Temporal Variability of Sea Surface Temperature and Chlorophyll Fields in the Gulf of Finland. 2013.
149. **Tiina Kriščiunaite**. A Study of Milk Coagulability. 2013.
150. **Tuuli Levandi**. Comparative Study of Cereal Varieties by Analytical Separation Methods and Chemometrics. 2013.
151. **Natalja Kabanova**. Development of a Microcalorimetric Method for the Study of Fermentation Processes. 2013.
152. **Himani Khanduri**. Magnetic Properties of Functional Oxides. 2013.
153. **Julia Smirnova**. Investigation of Properties and Reaction Mechanisms of Redox-Active Proteins by ESI MS. 2013.
154. **Mervi Sepp**. Estimation of Diffusion Restrictions in Cardiomyocytes Using Kinetic Measurements. 2013.
155. **Kersti Jääger**. Differentiation and Heterogeneity of Mesenchymal Stem Cells. 2013.
156. **Victor Alari**. Multi-Scale Wind Wave Modeling in the Baltic Sea. 2013.
157. **Taavi Päll**. Studies of CD44 Hyaluronan Binding Domain as Novel Angiogenesis Inhibitor. 2013.
158. **Allan Niidu**. Synthesis of Cyclopentane and Tetrahydrofuran Derivatives. 2013.
159. **Julia Geller**. Detection and Genetic Characterization of *Borrelia* Species Circulating in Tick Population in Estonia. 2013.
160. **Irina Stulova**. The Effects of Milk Composition and Treatment on the Growth of Lactic Acid Bacteria. 2013.
161. **Jana Holmar**. Optical Method for Uric Acid Removal Assessment During Dialysis. 2013.
162. **Kerti Ausmees**. Synthesis of Heterobicyclo[3.2.0]heptane Derivatives *via* Multicomponent Cascade Reaction. 2013.
163. **Minna Varikmaa**. Structural and Functional Studies of Mitochondrial Respiration Regulation in Muscle Cells. 2013.
164. **Indrek Koppel**. Transcriptional Mechanisms of BDNF Gene Regulation. 2014.
165. **Kristjan Pilt**. Optical Pulse Wave Signal Analysis for Determination of Early Arterial Ageing in Diabetic Patients. 2014.

166. **Andres Anier**. Estimation of the Complexity of the Electroencephalogram for Brain Monitoring in Intensive Care. 2014.
167. **Toivo Kallaste**. Pyroclastic Sanidine in the Lower Palaeozoic Bentonites – A Tool for Regional Geological Correlations. 2014.
168. **Erki Kärber**. Properties of ZnO-nanorod/In_2S_3/$CuInS_2$ Solar Cell and the Constituent Layers Deposited by Chemical Spray Method. 2014.
169. **Julia Lehner**. Formation of Cu_2ZnSnS_4 and $Cu_2ZnSnSe_4$ by Chalcogenisation of Electrochemically Deposited Precursor Layers. 2014.
170. **Peep Pitk**. Protein- and Lipid-rich Solid Slaughterhouse Waste Anaerobic Co-digestion: Resource Analysis and Process Optimization. 2014.
171. **Kaspar Valgepea**. Absolute Quantitative Multi-omics Characterization of Specific Growth Rate-dependent Metabolism of *Escherichia coli*. 2014.
172. **Artur Noole**. Asymmetric Organocatalytic Synthesis of 3,3'-Disubstituted Oxindoles. 2014.
173. **Robert Tsanev**. Identification and Structure-Functional Characterisation of the Gene Transcriptional Repressor Domain of Human Gli Proteins. 2014.
174. **Dmitri Kartofelev**. Nonlinear Sound Generation Mechanisms in Musical Acoustic. 2014.
175. **Sigrid Hade**. GIS Applications in the Studies of the Palaeozoic Graptolite Argillite and Landscape Change. 2014.
176. **Agne Velthut-Meikas**. Ovarian Follicle as the Environment of Oocyte Maturation: The Role of Granulosa Cells and Follicular Fluid at Pre-Ovulatory Development. 2014.
177. **Kristel Hälvin**. Determination of B-group Vitamins in Food Using an LC-MS Stable Isotope Dilution Assay. 2014.
178. **Mailis Päri**. Characterization of the Oligoadenylate Synthetase Subgroup from Phylum Porifera. 2014.
179. **Jekaterina Kazantseva**. Alternative Splicing of *TAF4*: A Dynamic Switch between Distinct Cell Functions. 2014.
180. **Jaanus Suurväli**. Regulator of G Protein Signalling 16 (RGS16): Functions in Immunity and Genomic Location in an Ancient MHC-Related Evolutionarily Conserved Synteny Group. 2014.
181. **Ene Viiard**. Diversity and Stability of Lactic Acid Bacteria During Rye Sourdough Propagation. 2014.
182. **Kristella Hansen**. Prostaglandin Synthesis in Marine Arthropods and Red Algae. 2014.
183. **Helike Lõhelaid**. Allene Oxide Synthase-lipoxygenase Pathway in Coral Stress Response. 2015.
184. **Normunds Stivrinš**. Postglacial Environmental Conditions, Vegetation Succession and Human Impact in Latvia. 2015.
185. **Mary-Liis Kütt**. Identification and Characterization of Bioactive Peptides with Antimicrobial and Immunoregulating Properties Derived from Bovine Colostrum and Milk. 2015.
186. **Kazbulat Šogenov**. Petrophysical Models of the CO_2 Plume at Prospective Storage Sites in the Baltic Basin. 2015.

187. **Taavi Raadik**. Application of Modulation Spectroscopy Methods in Photovoltaic Materials Research. 2015.
188. **Reio Põder**. Study of Oxygen Vacancy Dynamics in Sc-doped Ceria with NMR Techniques. 2015.
189. **Sven Siir**. Internal Geochemical Stratification of Bentonites (Altered Volcanic Ash Beds) and its Interpretation. 2015.
190. **Kaur Jaanson**. Novel Transgenic Models Based on Bacterial Artificial Chromosomes for Studying BDNF Gene Regulation. 2015.